EVALUATION OF METAKAOLINS FOR USE AS SUPPLEMENTARY CEMENTITIOUS MATERIALS

A Thesis
Presented to
The Academic Faculty

by

Joy M. Justice

In Partial Fulfillment
Of the Requirements for the Degree
Master of Science in Materials Science and Engineering

Georgia Institute of Technology
April, 2005

EVALUATION OF METAKAOLINS FOR USE AS SUPPLEMENTARY CEMENTITIOUS MATERIALS

Approved by:

Dr. Kimberly E. Kurtis, advisor
School of Civil and Environmental Engineering
Georgia Institute of Technology

Dr. Joe K. Cochran, Jr.
School of Materials Science and Engineering
Georgia Institute of Technology

Dr. Thomas H. Sanders, Jr.
School of Materials Science and Engineering
Georgia Institute of Technology

Date Approved: April 1, 2005

Acknowledgements

This research would not have been possible without the support of many people. First and foremost, I would like to thank my advisor, Dr. Kimberly Kurtis. She provided guidance, offered many creative insights, and always did so with a smile. I am also grateful to Z.Z. Zhang and Billy Wiggins at Thiele Kaolin Company for providing this great research opportunity.

Coming from a materials science background, I had a lot of civil engineering and cement chemistry questions when I joined this group in early 2004. I am forever grateful to Ben Mohr for his technical expertise and endless patience. I am appreciative of the many students who donated their time to this project: Staci Beckwith, Anthony Fisher, Luke Kennison, Lauren McCormick, and Matt Sellers (and Ben, too!). I am grateful to my committee, Dr. Cochran and Dr. Sanders, for their helpful suggestions and to Dr. Hill and Dr. Thadhani for the use of their thermal analysis equipment. Thanks also to my officemate, Jeff, and my roommate, Morgan, who, in her spare time, happens to be a craft genius, a medical doctor, a Nobel laureate, and the co-founder of our fan club (which currently has two members). Thanks for all the laughs!

Finally, I would like to thank my family -- my parents Mike and Bev Justice, sister Amy Justice, and boyfriend Tony Stickel -- for their continuous love, unending support, and constant encouragement. You guys rock! I love you dearly.

Table of Contents

List of Tables

List of Figures

Summary

Two metakaolins will be evaluated for use as supplementary cementitious materials in cement-based systems. The metakaolins vary in their surface area (11.1 v. 25.4 m^2/g), but are quite similar in mineralogical composition. Performance of metakaolin mixtures will be compared to control mixtures and to mixtures incorporating silica fume as partial replacement for cement at water-to-cementitious materials ratios of 0.40, 0.50, and 0.60. In this study, the early age properties of fresh concrete and the mechanical and durability properties of hardened concrete will be examined. Early age evaluations will aim to determine the reactivity of metakaolin (heat of hydration) and its effect on mixture workability (slump, setting time, unit weight). In addition, three types of shrinkage will be monitored in metakaolin-cement systems: chemical, autogenous, and free. Compressive, tensile and flexural strength and elastic modulus will be measured at various concrete ages. The influence of metakaolin addition on durability will be assessed through accelerated testing for sulfate resistance, expansion due to alkali-silica reaction, and through rapid chloride permeability measurements.

To further quantify the underlying mechanisms of metakaolin's action, the microstructure of pastes will be examined. Calcium hydroxide (CH) content will be determined using thermogravimetric analysis and verified using differential thermal analysis. Surface area and pore size distribution will be evaluated via nitrogen

adsorption. These analyses should yield information about the pozzolanic reactivity of metakaolin, associated CH consumption and pore structure refinement, and resulting improvements in mechanical performance and durability of metakaolin-concretes.

Chapter I

Introduction

Concrete is one of most extensively used construction materials in the world, with two billion tons placed worldwide each year [Mindess, 2003]. It is attractive in many applications because it offers considerable strength at a relatively low cost. Concrete can generally be produced of locally available constituents, can be cast into a wide variety of structural configurations, and requires minimal maintenance during service. However, environmental concerns, stemming from the high energy expense and CO_2 emission associated with cement manufacture, have brought about pressures to reduce cement consumption through the use of supplementary materials [Mindess, 2003; Sabir, 2001].

Supplementary cementitious materials (SCMs) are finely ground solid materials that are used to replace part of the cement in a concrete mixture. These materials react chemically with hydrating cement to form a modified paste microstructure. In addition to their positive environmental impact, SCMs may improve concrete workability, mechanical properties, and durability. SCMs may possess pozzolanic or latent hydraulic reactivity or a combination of these. The term pozzolan refers to a silecious material, which, in finely divided form and in the presence of water, will react chemically with calcium hydroxide (CH[1]) to form cementitious compounds. Pozzolans can be of natural

[1] Cement chemistry notation:
A = Al_2O_3 C = CaO F = Fe_2O_3 H = H_2O S = SiO_2 Š = SO_3

or industrial origin. Natural pozzolans include volcanic ash and diatomaceous earth, although pozzolans from industrial by-products are more commonly used today. Fly ash (FA), the most extensively used SCM, is the inorganic, noncombustible residue of powdered coal after burning in power plants. Silica fume (SF) is harvested from the effluent gases produced in the manufacture of silicon metal and alloys. Latent hydraulic SCMs, like slag, react directly with water to form cementitious compounds. Slags used in concrete come from the blast furnace production of iron from ore [Mindess, 2003; Sabir, 2001].

Metakaolin (MK) is an SCM that conforms to ASTM C 618, Class N pozzolan specifications. MK is unique in that it is not the by-product of an industrial process nor is it entirely natural; it is derived from a naturally occurring mineral and is manufactured specifically for cementing applications. Unlike by-product pozzolans, which can have variable composition, MK is produced under carefully controlled conditions to refine its color, remove inert impurities, and tailor particle size [Brooks, 2001; Ding, 2002]. As such, a much higher degree of purity and pozzolanic reactivity can be obtained. MK has great promise as an SCM, as it can improve many properties of concrete while also reducing cement consumption.

This research evaluates the potential of two Georgia-produced metakaolins for use as supplementary cementitious materials. The influence of metakaolin fineness is investigated and the performance of these particular metakaolins is compared to a commercial silica fume. Measurements of early age properties of fresh concrete, including slump, unit weight, and setting time, are examined, as well as three types of shrinkage. Mechanical performance (compressive strength, splitting tensile strength,

flexural strength, elastic modulus) and durability (chloride permeability, sulfate resistance, alkali reactivity) are also evaluated. In addition, the evolution of hydration products over time is examined by thermal analysis. Chapter II consists of a literature review of metakaolin replacement and its effect on concrete properties. Mixture designs, testing program, and other experimental procedures are discussed in Chapter III. Chapter IV contains the results and discussion of all data from testing. Finally, Chapter V presents conclusions, recommendations for use of these MKs, and suggestions for future testing.

Chapter II

Literature Review

2.1 General Information

2.1.1 History

Metakaolin is produced by heat-treating kaolin, one of the most abundant natural minerals. Kaolin is a fine, white clay that has traditionally been used in the manufacture of porcelain and as a coating for paper. The term kaolin is derived from the name of the Chinese town *Kao-ling*, which translates loosely to "high ridge" and is home to the mountain that yielded the first kaolins to be sent to Europe [High Reactivity Metakaolin: Engineered Mineral Admixture for Use with Portland Cement, 2004].

The vast majority of clay refined in the United States comes from Georgia, and the state is recognized as a world leader in the mining, production, processing, and application of kaolin products [Schroeder, 2003]. During the Cretaceous and Tertiary geological periods, the Atlantic Ocean covered much of the southern half of Georgia. The Piedmont Plateau met the ocean at the "Fall Line," which extended northeast across the state from Columbus to Augusta and is now commonly referred to as the "kaolin belt" (Figure 2.1). As weathered granitic rocks deteriorated, they were carried seaward and formed large sedimentary deposits in this region. These deposits, buried beneath 50-100 meters of earth, contain a large volume of kaolin, as well as quartz, mica, limonite, and

anatase. At present, more than eight million metric tons of kaolin are mined from Georgia each year, with an estimated value of over $1 billion [China Clay Producers Association, 2002].

Figure 2.1. "Kaolin belt" across central Georgia
[China Clay Producers Association, 2002].

The first documented use of MK was in 1962, when it was incorporated in the concrete used in the Jupia Dam in Brazil. It has been commercially available since the mid-1990s and currently costs approximately $500/ton [Zhang, 2004]. MK typically contains 50-55% SiO_2 and 40-45% Al_2O_3 [Poon, 2001]. Other oxides present in small amounts include Fe_2O_3, TiO_2, CaO, and MgO. MK particles are generally one-half to five microns in diameter -- an order of magnitude smaller than cement grains and an order of magnitude larger than silica fume particles. MK is white in color (whereas silica fume is typically dark grey or black), making it particularly attractive in color matching and other architectural applications. Due to the controlled nature of the processing, MK powders are very consistent in appearance and performance [Ding, 2002]. Physical characteristics of commonly used pozzolans are shown in Table 2.1.

Table 2.1. Physical characteristics of selected pozzolans [Mindess, 2003].

Material	Mean Size (10^{-6} m)	Surface Area (m^2/g)	Particle Shape	Specific Gravity
Portland Cement	10-15	< 1	angular, irregular	3.2
Fly Ash	10-15	1-2	mostly spherical	2.2-2.4
Silica Fume	0.1-0.3	15-25	spherical	2.2
Metakaolin	1-2	15	platey	2.4

2.1.2 Production

Kaolin is a phyllosilicate, consisting of alternate layers of silica and alumina in tetrahedral and octahedral coordination, respectively (Figures 2.2 and 2.3). This electrically neutral crystalline layer structure, which is a common characteristic of clay minerals, leads to a fine particle size and platelike morphology and allows the particles to move readily over one another, giving rise to physical properties such as softness, soapy feel, and easy cleavage [Kingery, 1976]. Kaolinite is the mineralogical term for hydrated aluminum disilicate, $Al_2Si_2O_5(OH)_4$, the primary constituent of kaolin (40-70%). Other minerals comprising kaolin include quartz, muscovite-like micas, and rutile [Moulin, 2001].

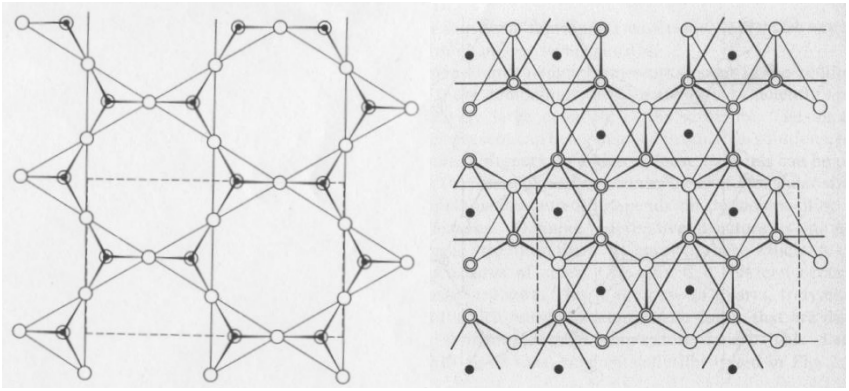

(a) (b)

Figure 2.2. Atomic arrangements of (a) Si_2O_5 and (b) $AlO(OH)_2$ layers --

• Si (a) or Al (b); ○ Oxygen; ◘ Hydroxyl [Brinkley, 1958].

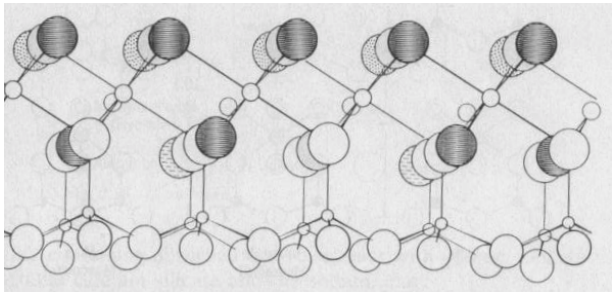

Figure 2.3. Perspective drawing of kaolinite with Si-O tetrahedrons on the bottom half and Al-O, OH octahedrons on the top half of the layer [Brinkley, 1958].

Under normal environmental conditions, kaolin is quite stable. However, when heated to temperatures of 650-900 °C, kaolin loses 14% of its mass in bound hydroxyl ions. This heat treatment, or calcination, breaks down the structure of kaolin such that the alumina and silica layers become puckered and lose their long-range order. Resulting from this dehydroxylation and disorder is MK, a highly reactive transition phase. MK is an amorphous pozzolan, with some latent hydraulic properties, that is well-suited for use as an SCM [Bensted, 2002].

The calcining temperature plays a central role in the reactivity of the resulting MK product. Ambroise *et al.* [Ambroise, 1985] studied the effects of calcining temperature on the strength development of MK-lime pastes. These authors found 700 °C to be optimal and later showed that calcination below this temperature results in a less reactive material containing more residual kaolinite. Above 850 °C, they reported, recrystallization began and reactivity declined, as kaolin had begun to convert to relatively inert ceramic materials, such as spinel, silica, and mullite [Bensted, 2002]. The heating process, illustrated by differential thermal analysis (DTA), is shown in Figure 2.4.

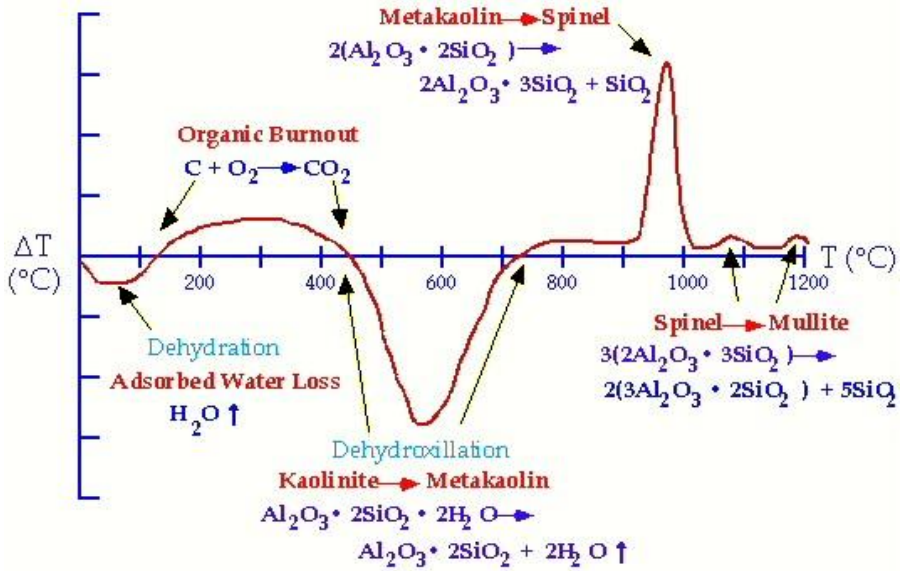

Figure 2.4. DTA thermogram of kaolin [DTA and TGA of Ball Clay and Kaolin, 1998].

Calcining is traditionally carried out in rotary kilns and takes several hours. The use of a fluidized bed process may reduce calcining time to minutes, although both of these methods require grinding of the agglomerated products. Flash-calcining, which consists of rapid heating, often to 1000 °C, followed by rapid cooling, may reduce the processing time further -- from minutes to several tenths of a second. Additionally, there is no grinding step required, as the starting material is finely powdered kaolin suspended in a gas [Salvador, 1995]. The MKs examined in this study were produced using vertical hearth fluid bed calciners, into which the clay was fed at the top and the product collected from the bottom.

While prolonged soak-calcining at lower temperatures is generally quite effective at removing hydroxyl groups, Salvador [Salvador, 1995] showed that the calcining rate does influence the pozzolanic reactivity of MK. In his study, flash-calcined kaolins had higher water absorption capacities, and thus required more water to achieve suitable

workability, suggesting these had a higher initial reactivity than soak-calcined kaolins. Further, at the same water-to-cementitious materials ratio (w/cm), cylinders made with flash-calcined kaolins always performed better in compression than those made with soak-calcined kaolins.

2.1.3 Pozzolanic Reaction and CH Consumption

Regardless of the reactivity of an SCM, if it is extremely fine, it will generally impart some benefit to mortars and concrete. Small particles, which can fit between cement grains, allow for more efficient paste packing, which in turn reduces bleeding, lowers the mean size of capillary pores, and may reduce water requirements due to a ball-bearing effect (if the particles are round) [Mindess, 2003]. Improved particle packing at the aggregate/paste interface results in a thinner transition zone with a denser, more homogeneous microstructure [Wild, 1996]. In addition, acting together, many small particles have a large total surface area, leading to an increase in reactivity.

Another important factor to consider when using SCMs is dilution. When used as a replacement for cement, concrete mixtures will experience some effect of the removal of cement from the reacting system. As such, unless the SCM begins reacting immediately, there will generally be a reduction in the rate of heat evolution and strength gain in proportion to the amount of cement being replaced. Fly ash, especially, and even silica fume to a lesser extent, do not show beneficial effects until later in the hydration process [Curcio, 1998; Poon, 2001]. MK, however, because it is very small and possesses some latent hydraulic reactivity, may overcome the dilution effect, contributing to both heat and strength evolution at very early ages.

The presence of MK has an immense effect on the hydration of portland cement (PC). When portland cement alone hydrates, typically 20-30% of the resulting paste mass is CH. However, when MK is introduced, it reacts rapidly with these newly forming CH compounds to produce supplementary calcium silicate hydrate (C-S-H). Recalling cement chemistry notation from p. 1, the basic hydration reactions are as follows:

$$2C_32 + 11H \rightarrow C_3S_2H_8 + 3CH$$
$$\text{(C-S-H)} \quad \text{(CH)}$$
$$2C_2S + 9H \rightarrow C_3S_2H_8 + CH$$

$$C_3A + 3C\check{S}H_2 + 26H \rightarrow C_6A\check{S}_3H_{32}$$
$$\text{(gypsum)} \qquad \text{(ettringite)}$$
$$2C_3A + C_6A\check{S}_3H_{32} + 4H \rightarrow 3C_4A\check{S}H_{12}$$
$$\text{(monosulfate)}$$
$$C_4A\check{S}H_{12} + 2C\check{S}H_2 + 16H \rightarrow C6A\check{S}3H_{32}$$

$$MK\ [Al_2Si_2O_7] + CH + H \rightarrow C\text{-}S\text{-}H,\ C_4AH_{13},\ C_3AH_6,\ C_2ASH_8$$

In general, SCMs with higher alumina contents, such as MK, tend to have higher pozzolanic capacities because formation of C-A-H has a high CH demand. This is critical, as CH does not make a significant contribution to concrete strength and can be detrimental to durability. Its elimination or reduction by secondary reaction with MK can greatly enhance concrete performance [Mindess, 2003; Poon, 2002].

Determination of the degree of pozzolanic reaction completed can be accomplished via a selective dissolution procedure, like that developed by Oshawa *et al.* [Oshawa, 1985] and Li *et al.* [Li, 1985]. The procedure is based on the assumption that the majority of the unreacted pozzolan is acid insoluble. In a blended cement paste, the pozzolan reacts with CH to form acid soluble hydration products. Thus, it is possible to dissolve the unreacted cement and the hydration products of both the cement and the

pozzolan, leaving behind the insoluble residue of the unreacted pozzolan. The degree of pozzolanic reaction completed is defined as the percentage of unreacted pozzolan remaining relative to the initial amount of pozzolan present in the cement paste.

Results from such selective dissolution evaluations, carried out by Poon *et al.* [Poon, 2001], showed that the degree of pozzolanic reaction was higher at a replacement level of 5% MK than at replacement levels of 10% and 20% for all ages. Similar results were observed with silica fume, though the 5% silica fume values were never as high as the 5% MK values. This higher rate of pozzolanic reaction in pastes with a lower replacement level could likely be attributed to the greater amount of cement, and thus higher concentration of CH, available for reaction with the pozzolan.

Because MK reacts with and consumes free CH, another method for determining the extent of pozzolanic reaction completed is to measure the remaining CH content in a paste, mortar, or concrete sample. As part of the same study, Poon *et al.* [Poon, 2001] also determined total CH content of paste samples, both based on the ignited weight and the weight of cement, using differential scanning calorimetry. This was performed in air atmosphere at a heating rate of 10 ˚C/min. The CH content was calculated from the weight loss between 425 ˚C and 550 ˚C. In either case, cements blended with 20% MK showed the least total CH at all ages. MK mixtures showed steadily decreasing CH contents up to 90 days, as illustrated in Figure 2.5.

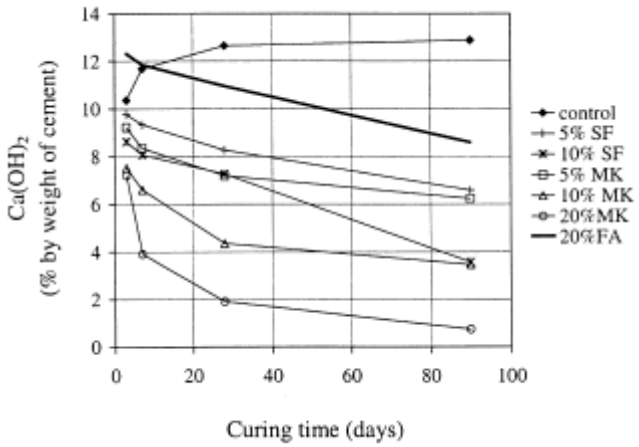

Figure 2.5. CH content calculated based on cement weight [Poon, 2001].

Wild and Khatib [Wild, 1997] performed a similar experiment, measuring CH consumption in MK-PC pastes and mortars, which were cured in water at 20 °C. Results from these thermogravimetric analyses (TGA) are shown in Figure 2.6. The CH, expressed as a percentage of cement weight, showed a minimum at about 14 days of curing. This was attributed to a peak in pozzolanic activity for which more CH was being removed from the paste by reaction with MK than was being generated by the cement hydration. Interestingly, the peak in relative compressive strength (the ratio of strength at a given age to the strength of the control at the same age) coincided with the maximum in pozzolanic activity -- at 14 days of age. Increases in CH content and a lag in strength gain beyond 14 days were attributed to the formation of an inhibiting layer of reaction product on the surface of the MK particles.

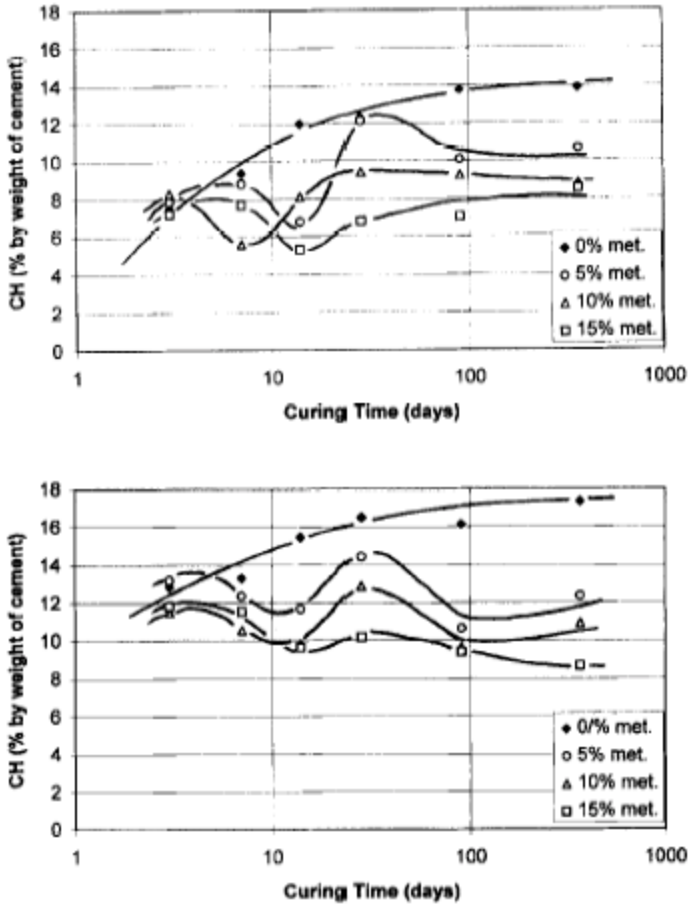

Figure 2.6. Change in CH content versus curing time, as measured by TGA, for metakaolin (a) mortar and (b) paste [Wild, 1997].

Frías and Cabrera [Frías, 2000] evaluated CH content of MK pastes via DTA and TGA. These analyses were conducted in nitrogen atmosphere and at a heating rate of 20 °C/min. CH contents of MK-PC specimens were found to increase with age until 3-7 days. Subsequently, as with the Wild and Khatib [Wild, 1997] study, CH contents began decreasing in proportion to the percentage of MK added. Interestingly, the 10% and 15% MK curves showed an inflection point around 90 days of age, after which CH content again began to rise, however slightly (Figure 2.7). This point could represent the end of the pozzolanic reaction due to the total consumption of MK.

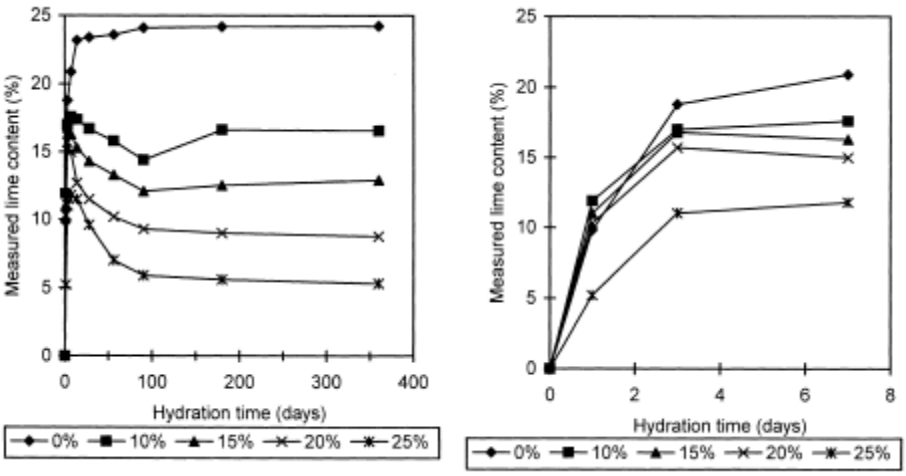

Figure 2.7. Evolution of CH with hydration time [Frías, 2000].

Oriol and Pera [Oriol, 1995] utilized DTA and Fourier transform infrared spectrometry to follow lime consumption in MK blended cements under microwave treatment. This treatment was intended to accelerate hydration like traditional thermal curing methods. These authors reported that total elimination of CH was achievable in binders containing 15% MK given sufficient hydration time. To fully eliminate CH in binders with a w/cm of 0.5 in just 28 days, between 30% and 40% MK was required.

2.1.4 Porosity Evolution

In most cases, mortars and concrete containing pozzolanic SCMs have total porosity values equal to or less than that of PC concrete. However, it is not so much the total porosity as it is the pore size distribution and the permeability that are critical to the performance and durability of concrete. The evolution of porosity depends on certain characteristics of the SCM, such as particle size, chemical composition, mineralogy, and loss on ignition. Because of its fineness and high pozzolanic reactivity, MK has great potential to decrease concrete porosity.

Frías and Cabrera [Frías, 2000] evaluated the evolution of total, capillary, and gel porosity with hydration time via mercury intrusion porosimetry (MIP). Capillary pores were considered to fall within 0.01-5.00 μm, while gel pores were smaller than 0.01 μm. Five pastes were prepared at a w/cm of 0.55 and were tested nine times over the course of one year. To stop hydration, samples were either vacuum oven-dried at 1 bar and 50 ˚C (for MIP) or microwaved (for DTA and TGA). Unfortunately, these authors did not compare the two techniques to determine if microwave drying damaged the paste pore structure or altered its composition.

There was a reduction in total porosity observed up to 28 days, after which it remained fairly constant. Mixtures containing MK actually showed higher total porosities than controls (approximately 16%), likely due to the high water content, although the MK pastes had fewer pores in the 0.01-5.00 μm range and more pores smaller than 0.01 μm, indicating refinement. Additionally, with longer hydration times, there was no significant difference in the capillary porosity of pastes made with 15, 20, or 25% MK, indicating that 15% replacement may be sufficient.

Khatib and Wild [Khatib, 1996], like the previous authors, examined pastes with a w/cm of 0.55 using MIP. MK incorporation led to pore structure refinement, with the proportion of pores having radii smaller than 20 nm increasing significantly as the replacement level increased (Figure 2.8). At 14 days, pastes with 15% MK had nearly 60% of their total pore volume in sub-20 nm pores, while the control paste had only about 30%. This represents the age at which the percentage of fine pores is the highest and also where strength enhancement by MK reaches a maximum, confirming that the major part of the pore refinement process occurs at a very early age [Khatib, 1998]. The

authors attributed this to an inhibiting layer of reaction product around the metakaolin particles, thus terminating their reaction with CH and preventing further pore refinement beyond 14 days. It should be noted, however, that MK does not have much influence on total intruded pore volume, which increased slightly relative to controls in these evaluations. The authors suspect that this may be the result of a phase transformation of MK/CH reaction products leading to a decrease in solid volume and an increase in porosity.

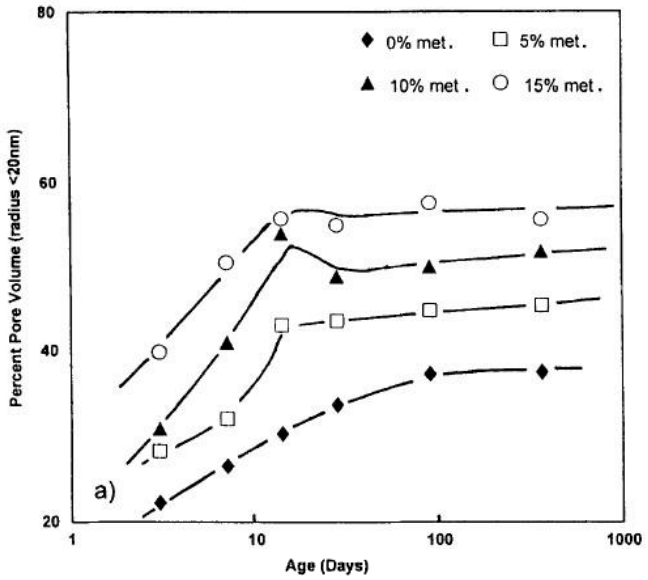

Figure 2.8. Pore size distribution (radii < 20 nm) versus curing time for pastes containing 0-15% MK [Khatib, 1996].

Poon *et al.* [Poon, 2001] also utilized MIP to evaluate porosity and pore size distribution of MK pastes. These pastes had lower porosity and smaller average pore diameters than the control and the silica fume pastes at all ages tested (3, 7, 28, and 90 days). This indicates that MK is more effective than silica fume in the refinement of pore structure. These results are different than those reported by both Frías and Cabrera

[Frías, 2000] and Khatib and Wild [Khatib, 1996], who both found MK pastes to have 16% greater porosity than controls at 28 days. However, these previous studies were conducted at a w/cm of 0.55, while the Poon *et al.* study was conducted with pastes prepared at a w/cm of 0.30. Ambroise *et al.* [Ambroise, 1994] found similar results to Poon *et al.*, although unfortunately did not examine MK-PC and plain PC pastes with the same water contents. They found that a 20% MK paste with a w/cm of 0.34 had nearly the same porosity as a control paste with a w/cm of 0.25. This implies that the porosity of an MK paste at a w/cm of 0.25 would be lower than the control, and supports the conclusion that MK makes a significant contribution to pore structure refinement. While these results are interesting, there is some disagreement as to whether MIP is a reliable technique; many believe that the high pressures it requires can actually cause the pore structure to collapse, yielding inaccurate results [Diamond, 2000].

Khatib and Clay [Khatib, 2003] investigated the water absorption by capillary rise and total immersion of concrete containing MK. Five concrete mixtures, containing 0-20% MK, were examined. After the required curing period, cubes were sliced into sections and dried in an oven at 100 ˚C for 48 h. Capillary rise was measured by placing dried slices on supports in a shallow tray, adding water until the level was approximately 1.5 mm above the base of the sample, and measuring sample mass at regular intervals. Total water absorption was measured by comparing the dry mass to the saturated mass achieved after 48 h of immersion at 20 ˚C.

Increasing MK content resulted in a decrease in the slope of the linear portion of the absorption-time curve, indicating that the presence of MK decreases absorption by capillary rise. This slope, which was termed the water absorption coefficient (WAC),

was then plotted against curing time (Figure 2.9). For all mixtures, the WAC decreased sharply up to 14 days curing. Then, while the control mixture continued slowly decreasing, the MK mixtures increased up to 28 days and ultimately leveled off. Despite this increase, the WAC for all MK mixtures was lower than for the control specimen. Further, Khatib and Clay [Khatib, 2003] reported that upon visual examination at the end of the capillary test, control specimens had water on their top surfaces. As the percentage of MK increased, the appearance of water was greatly reduced, and the 15% and 20% MK samples had no visible water on their top surfaces [Khatib, 2003].

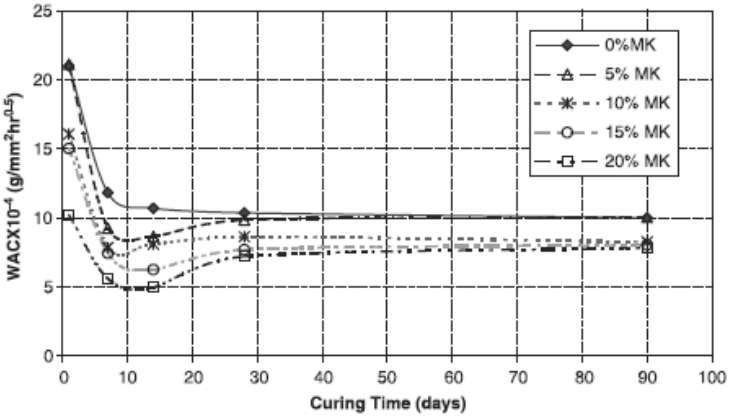

Figure 2.9. Variation of water absorption coefficient with curing time for concrete containing MK [Khatib, 2003].

In terms of total water absorption, MK specimens actually showed a slight increase over controls. That is, after 48 h of immersion in water at 20 °C, samples containing metakaolin had higher saturated masses than controls. There was a systematic increase in water absorption with increasing MK content. Although unique, such immersion techniques seem somewhat rudimentary and should have been verified by

more quantitative methods. However, the results are in accord with those of Frías and Cabrera [Frías, 2000] and Khatib and Wild [Khatib, 1996]: water absorption during full immersion seems to be related to total pore volume, which has been shown to increase with MK usage. Conversely, water penetration into concrete by capillary action has been shown to decrease when MK is used, suggesting a discontinuity of pores [Khatib, 2003].

2.2 Early Age Properties

2.2.1 Slump

Early age properties measure the workability and setting behavior of fresh concrete. These generally include slump, unit weight, setting time, and heat of hydration. The properties of fresh concrete are important because they affect the choice of equipment needed for handling and consolidation and because they may affect the properties of hardened concrete [Mindess, 2003].

Slump is by far the oldest and most widely used test of workability. This test involves filling a cone mold with fresh concrete in three layers of equal volume, rodding each layer 25 times, lifting the mold away vertically, and measuring the height difference between the cone mold and the concrete. Metakaolin has been shown to produce smaller slumps than control mixtures, although its effect relative to mixtures containing silica fume is not agreed upon. Ding and Li [Ding, 2002] reported that MK offered much better workability than did silica fume for the same mixture proportions. These mixtures contained 5, 10, or 15% replacement with either MK or silica fume, and a w/cm of 0.35. Additionally, they found that at 5% and 10% replacement, MK mixtures had a slightly higher slump than the control mixture. At 15% replacement with MK, slump decreased

approximately 10% from the control value. In contrast, slump decreased almost linearly with increasing silica fume replacement, indicating that MK concrete mixtures should require less superplasticizer than corresponding silica fume mixtures to achieve similar workability at the same w/cm.

Fresh properties of Dubey and Banthia's [Dubey, 1998] eight mixtures are shown in Table 2.2. These mixtures all contained 161.35 kg/m^3 of water and 350 mL of superplasticizer per 100 kg of cement. Slump values for the various mixtures demonstrate that the reduction in workability due to replacement with 10% silica fume was more pronounced than that obtained with an equal amount of MK replacement. This indicates that, in order to achieve a given workability, MK concrete should require a lower dose of water-reducing chemical admixture than silica fume concrete. Dubey and Banthia propose that this may be due to the larger particle size of MK relative to silica fume (1.5 μm v. 0.1 μm) in their study.

Table 2.2. Fresh and hardened properties of various concrete mixtures [Dubey, 1998].

Mix	Mix description	Slump, mm	Air content, percent	Unit weight, kg/m^3	Compressive strength, MPa	
					7 day	28 day
C	Control 100 percent cement	140	1.4	2437.0	53.6	66.0
S	Control + 10 percent silica fume	60	1.5	2440.0	53.8	68.4
M	Control + 10 percent HRM	120	1.6	2468.0	58.0	72.0
SM	Control + 5 percent silica fume + 5 percent HRM	60	1.4	2448.0	55.4	70.3
CF	Control + 1.0 percent fibers	120	1.5	2511.0	54.3	68.0
SF	Control + 10 percent silica fume + 1.0 percent fibers	70	1.7	2533.0	55.5	70.1
MF	Control + 10 percent HRM + 1.0 percent fibers	100	1.5	2546.0	59.2	72.2
SMF	Control + 5 percent silica fume + 5 percent HRM + 1.0 percent fibers	80	1.6	2532.0	57.0	71.4

The above results were supported by those of Caldarone *et al.* [Caldarone, 1994], but the opposite phenomenon was observed by Bai *et al.* [Bai, 1999], who found workability to be substantially reduced for mixtures containing MK. Khatib and Clay [Khatib, 2003] reported that the dosage of superplasticizer required, in their study, increased with increasing MK content, to compensate for losses in workability. Qian *et al.* [Qian, 2001] also found slump to progressively decrease with MK content in concrete mixtures containing 1% naphthalene sulfonate-based powder superplasticizer. However, by increasing the superplasticizer dose to 1.2%, the slump showed only minor variation with increasing MK content.

2.2.2 Setting Time

The setting of concrete is generally understood as the onset of solidification and hardening (strength gain) of a fresh concrete mixture. Initial setting time (initial set) is defined as the time elapsed between the addition of water and the point when paste ceases to be fluid and plastic. This is the limit for handling concrete -- it should be placed before initial set. Final set indicates the onset of the development of mechanical strength. Many factors influence setting time, including the w/cm, casting and curing temperature, admixture type, source, and dosage, and cement content, fineness, and composition [Brooks, 2000].

Knowledge of setting behavior is extremely important in the field of concrete construction. This information is helpful in scheduling the various stages of construction operations, such as transporting, placing, compacting, finishing, and demoulding of concrete, and is a necessity when deciding whether set-accelerating or set-retarding

admixtures will be necessary. Further, measurements of autogenous shrinkage, an important property of high-strength (HSC) and high-performance concrete (HPC), should commence at the time of initial set. Previous researchers have found MK incorporation to have varying effects on the setting behavior of mortars and pastes.

Brooks *et al.* [Brooks, 2000] examined the effect of silica fume, MK, FA, and slag on setting time of high strength concrete via ASTM C 403. This method involves passing freshly mixed concrete through a 5 mm sieve, and measuring the force required for a needle to penetrate 25 mm into the collected mortar. An optimum w/cm of 0.28 was obtained for the control mixture using the Cabrera Vibrating Slump test, developed by Cabrera and Lee [Cabrera, 1985], and was used for all concrete mixtures. A sulfonated vinyl copolymer superplasticizer was added as necessary to achieve similar workability between mixtures.

Initial and final setting times are defined as the times at which the penetration resistance in mortar reaches values of 3.5 MPa (500 psi) and 27.6 MPa (4000 psi), respectively (ASTM C 403). Brooks *et al.* found that all SCMs tended to retard setting time, and that increasing the levels of silica fume, FA, and slag resulted in greater retardation of the set. For HSC containing MK, there was a progressive increase in the retarding effect up to 10% replacement, but a reduction at higher replacement levels.

Similar results were reported by Batis *et al.* [Batis, 2004], who examined both a local Greek kaolin heat-treated in their own lab and a commercially available MK product. These authors found all MK mixtures to have significantly longer setting times than control pastes. The mixture slowest to set was incorporated with 20% MK, requiring 205 minutes for initial set versus 105 minutes for the control. This could be

due, in part, to the high water demand of MK pastes. While controls required a w/c of 0.275 to achieve "normal consistency," 20% MK mixtures required a w/cm of 0.41.

Vu *et al.* [Vu, 2001] reported that higher blending percentages resulted in a higher water demand to reach normal consistency. For the particular Vietnamese kaolin used in this study, setting times of pastes in the lower replacement range (10-20% MK) were not significantly affected by blending. Beyond this range, the initial and final setting times increased by 15% and 10%, respectively, likely due to the lower cement and higher water contents involved.

Conversely, in a 2001 study, Moulin *et al.* [Moulin, 2001] found pastes made from MK blended cements to have a much shorter setting time compared to control pastes. These results were obtained using a Vicat needle apparatus according to ASTM C 191 and were conducted at a w/cm on 0.40. Moulin also examined the rheology of the same pastes using a shear vane rheometer to characterize yield stress. He found that the presence of MK significantly increased both the five and 90 minute yield stress when compared to reference pastes. This confirmed that MK blending results in a higher water demand and leads to thixotropic behavior, and Moulin *et al.* explained these to be the result of the accelerating effect of MK on PC hydration.

Caldarone *et al.* [Caldarone, 1994] also found MK to shorten setting time, as compared to control samples. In this study, initial set of MK mixtures was reported as 4.1 h, while SF and control mixtures did not achieve initial set until 4.2 h and 4.8 h, respectively. However, these authors, who were careful to note when ASTM standards were followed, do not indicate how initial set was determined. Since the remainder of the

evaluations were performed on concrete, we are left to assume that initial set was determined by visual inspection of concrete specimens, which is arbitrary.

2.2.3 Heat of Hydration

The use of MK increases the heat evolved during hydration. This has been attributed both to the accelerating effect of MK on PC hydration and the high reactivity of MK with CH. Enhanced temperature rise becomes critical in larger members and slabs, as it may lead to thermal stress cracking. However, in cold weather concreting or where faster set is required, this property can be desirable.

According to Zhang and Malhotra [Zhang, 1995], whereas FA incorporation decreased the overall heat evolved, 10% replacement with MK actually caused a 7 °C increase over PC-concrete [Zhang, 1995]. Ambroise *et al.* [Ambroise, 1994] reported temperature rises of 8 °C, 6 °C, and 1 °C over controls, for 10%, 20%, and 30% replacement, respectively, in mortars. The smaller temperature increases at higher replacement levels are likely due to the dilution effect of removing such a large mass of cement from the system. In comparison, replacement with 10% silica fume produced a temperature rise of only 0.5 °C.

Frías *et al.* [Frías, 2000] compared FA, silica fume, and MK in terms of heat evolution using a Langavant calorimeter. This semi-adiabatic method, described in the Spanish standard UNE 80 118, measures the heat generated during cement hydration using a thermally isolated Dewar flask. Heat is defined as the temperature difference between the hydrating mortar and an inert mortar (at least three months old). Blended

cement pastes contained 10% or 30% SCM and were used to produce mortars with a sand-to-cement ratio of 3:1 and a w/cm of 0.50.

The total heat evolved (up to 120 h) was found to decrease significantly with increasing FA substitution, increase slightly on substitution with 10% silica fume, and essentially stay the same for increasing levels of MK substitution. However, these authors also measured the temperature rise, or the peak height relative to controls, for these hydrating mortars. FA mortars exhibited a continual reduction in temperature rise with increase in substitution level, silica fume incorporation resulted in a decrease of 1.5-3.0 °C, and MK caused an increase in temperature peak of 6-7 °C. From this, it is clear that reducing the cement content of a mixture will reduce the heat output from cement hydration, but will not necessarily reduce the initial rate of heat evolution or the maximum temperature reached.

Bai *et al.* [Bai, 2002] looked specifically at the effects of FA and MK on heat evolved using embedded thermocouples. Mortar mixtures were placed in 150 mm plywood cube molds and thermally isolated by encasement in 100 mm thick expanded polystyrene and another layer of plywood. With increasing replacement levels, the temperature rise in FA systems was found to decrease, while the temperature rise in MK systems was found to increase substantially. Numeric peak temperature values were as follows: 29 °C, 27 °C, and 31 °C for the control, 10% FA, and 10% MK mixtures, respectively. Bai *et al.* further investigated the use of FA and MK in ternary blends at total PC replacement levels of up to 40%. These appeared to have a compensatory effect on temperature rise: the temperature rise for a 10% FA-10% MK blend was exactly the same as that of the control (Figure 2.10).

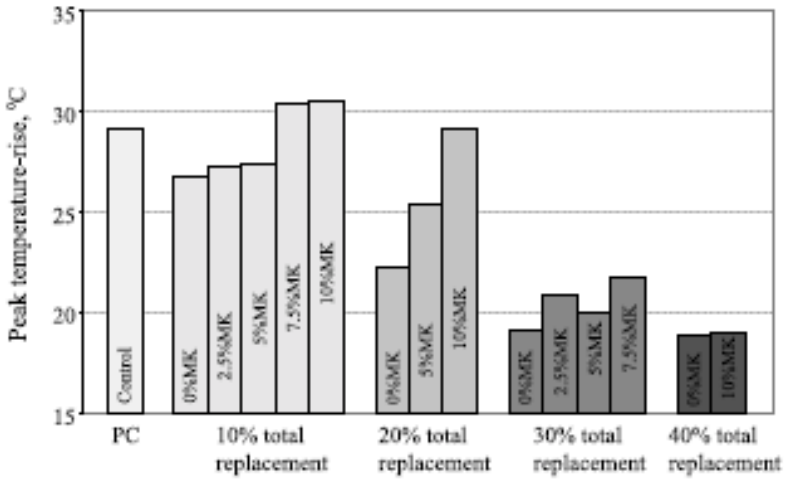

Figure 2.10. Peak temperature rise for MK-FA-PC blended mortars [Bai, 2002].

2.3 Shrinkage

The effect of MK on shrinkage properties is not well understood or agreed upon. In general, however, MK is expected to increase shrinkage in cementitious systems. Its inclusion offers many performance enhancements, including increases in strength and decreases in permeability. Both are likely due to refinements in pore structure, which generally causes greater shrinkage.

Chemical shrinkage is a result of the volume difference between reactants and products in a hydrating cement system. As hydration proceeds, the volume occupied by the products is smaller than that of the reactants. Thus, unless water is supplied from an external source, this volume discrepancy, or chemical shrinkage, will result in the formation of empty pores within the cement paste microstructure. This empty porosity then leads to a reduction in paste internal relative humidity and a measurable autogenous shrinkage of the material [Bentz, 1999]. Free, or drying, shrinkage is the contraction that results as a paste, mortar, or concrete loses water to the environment.

Brooks *et al.* [Brooks, 2001] found MK replacement to decrease very early age autogenous shrinkage of concrete, likely the most critical kind. The materials used in this investigation were portland cement, natural river sand, quartzitic gravel with a maximum size of 10 mm, metakaolin (BET specific surface area=15 m^2/g), and sulfonated vinyl copolymer superplasticizer. During the first 24 h of curing, autogenous shrinkage was measured inside cylindrical molds with PTFE linings and embedded strain gauges, and was found to decrease with increasing MK content. Concrete made using 15% MK replacement for cement showed a 65% reduction in autogenous shrinkage as compared to controls at 24 h of age. These results are shown in Figure 2.11a.

After 24 h, concrete samples were demoulded and sealed with aluminum waterproofing tape. This sealing method was effective, as specimens showed minimal mass loss over the duration of testing. Continuing to measure autogenous shrinkage from the age of 24 h, the authors found that all MK samples experienced greater shrinkage than control samples. During the first two weeks, samples containing higher MK contents shrank more; however, from approximately five weeks on, mixtures containing less MK showed more shrinkage. Relative to controls, the 200-day autogenous shrinkage increased by 91%, 80%, and 56%, for concrete replaced with 5%, 10%, and 15% MK, respectively (Figure 2.11b).

Brooks *et al.* [Brooks, 2001] went on to calculate total shrinkage by combining the 24 h autogenous shrinkage with drying shrinkage of the same specimens, which were held in an environmental chamber at 21 °C and 65% relative humidity after demolding (Figure 2.11c). This total shrinkage was intended to mimic field conditions, sealed in forms for the first 24 h and exposed to the environment thereafter. When combined as

such, the overall effect of the MK was to reduce total shrinkage of specimens. All MK mixtures showed less total shrinkage than controls, with higher replacement levels having a more pronounced shrinkage-reducing effect.

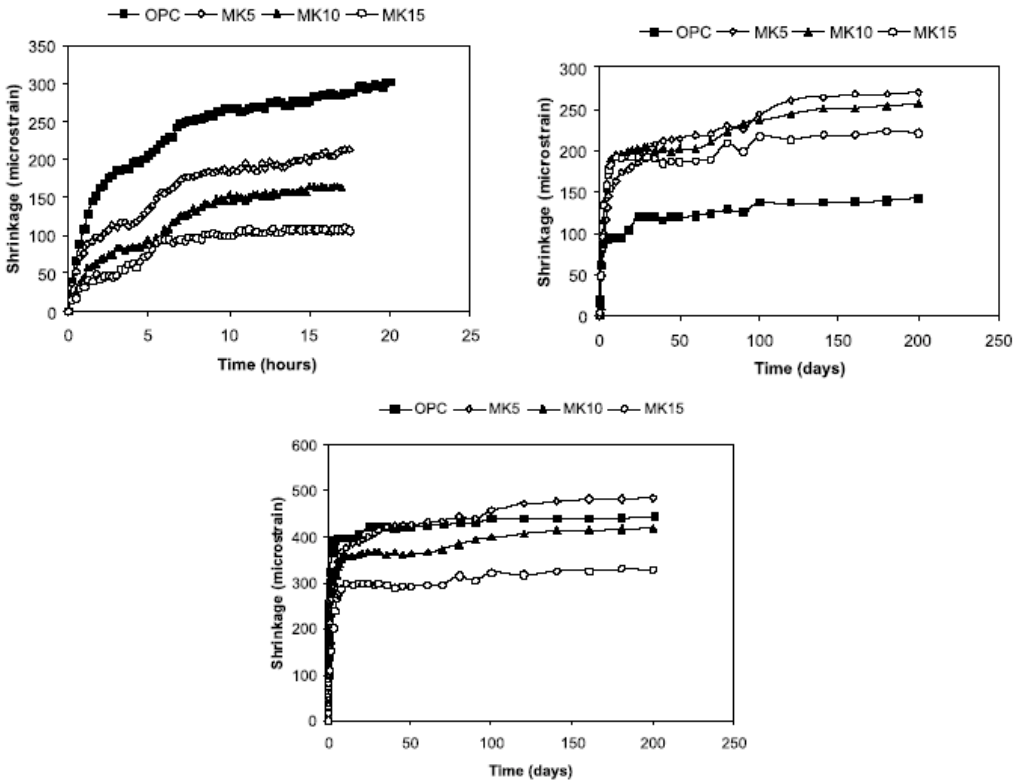

Figure 2.11. Effect of MK on the (a) early age, (b) long-term, and (c) total autogenous shrinkage of concrete [Brooks, 2001].

Wild *et al.* [Wild, 1998] studied autogenous and chemical shrinkage of MK-PC pastes for MK contents in the range 5-25%. Both autogenous and chemical shrinkage were found to increase over control pastes, reaching a maximum between 10% and 15% replacement, indicating an optimum in the combined effect of cement hydration and the removal of water from the system due to reaction of the MK at this composition. At

higher MK contents, both autogenous and chemical shrinkage were found to decrease sharply. Wild attributed this to the formation of increased amounts of lower density C_2ASH_8 and reduced amounts of higher density C_4AH_{13} compounds in the presence of greater MK contents, producing an overall volume increase and thus reducing autogenous shrinkage. Similar conclusions were made by Kinuthia *et al.* [Kinuthia, 2000], who found autogenous shrinkage to increase for 5 and 10% MK but decrease for 15 and 20% replacement, although this effect could also be related to a reduction in PC content.

In terms of free shrinkage alone, Caldarone *et al.* [Caldarone, 1994] found that replacement with 10% MK served to reduce shrinkage of concrete by nearly one third after 156 days of drying at 50% relative humidity. This phenomenon could be attributed, in part, to the fact that the reaction of MK consumed more free water in the system, leaving less evaporable water during shrinkage. This supports the conclusion that MK concretes have a lower porosity and finer pore structure, which encourages loss of water by self-desiccation rather than by diffusion to the surrounding environment.

Ding and Li [Ding, 2002] found free shrinkage of concretes containing MK or silica fume to decrease with increasing replacement percentage. Concrete mixtures containing 15% MK experienced 40% less free shrinkage than controls, while 15% silica fume mixtures shrank 33% less than controls. Ding and Li also calculated shrinkage rate, and found that compared with silica fume mixtures at the same replacement level, MK concretes showed a faster development of shrinkage during the first week of drying and a slower rate after that. Zhang and Malhotra [Zhang, 1995] reported similar findings -- although they initially shrank fastest, concrete with 10% MK had a lower drying shrinkage rate than control and silica fume concretes beyond one week of age.

2.4 Mechanical Properties

2.4.1 Strength

2.4.1a Compressive and Tensile Strength

Partial replacement with MK can improve concrete strength. However, it is not clear whether MK or silica fume produces greater increases in strength. If it is determined that MK increases strength as much or more than silica fume, MK might find greater application in HSC and HPC in the future.

The vast majority of papers about MK incorporation make some mention of strength. Caldarone *et al.* [Caldarone, 1994] produced concretes with 5% and 10% MK by weight of Type I cement, with w/cm of 0.40, which showed enhanced strengths at ages up to 365 days. These specimens showed strengths an average of 10% greater than concrete incorporated with the same amount of silica fume. At 365 days, the specimens prepared with 5% MK showed the highest strength of the group, 11.35 ksi, followed by 10% MK, 10% silica fume, and 5% silica fume (9.21 ksi). Control specimens had the lowest strengths at all ages.

Similar results were reported by Wild *et al.* [Wild, 1996], who tested concretes ranging from one to 90 days in age, produced at a w/cm of 0.45 with cement complying with BS12:1989. He found that 20% replacement with MK was optimal for achieving maximum long-term strength enhancement. A summary of Wild *et al.*'s results is shown in Table 2.3.

Table 2.3. Compressive strengths of metakaolin-concretes [Wild, 1996].

MK (%)	Density (kg/m^3)	Compressive strength (N/mm^2)				
		1 day	7 days	14 days	28 days	90 days
0	2490	19.07	50.23	57.10	62.60	72.43
5	2440	21.50	53.80	58.97	63.50	71.63
10	2460	22.43	62.30	69.23	71.00	80.07
15	2470	20.23	64.80	74.67	76.00	83.70
20	2480	19.33	66.47	75.73	82.47	85.13
25	2470	15.73	62.50	69.77	73.93	82.23
30	2480	14.53	60.53	72.33	76.73	81.80

These authors concluded that there are three elementary factors influencing the contribution that MK makes to strength when it partially replaces cement in concrete. These are the filler effect, the acceleration of PC hydration, and the pozzolanic reaction of MK with CH. According to Wild *et al.*, the filler effect is immediate, the acceleration of PC hydration has maximum impact within the first 24 hours, and the pozzolanic reaction makes the greatest contribution to strength somewhere between 7 and 14 days of age. Wild *et al.* also concluded that the positive contribution made by MK does not continue beyond 14 days, irrespective of the replacement level. This result was not confirmed by other researchers [Ding, 2002] and the table above indicates otherwise.

Wild *et al.* [Sabir, 2001] later showed that increasing the specific surface of MK from 12 to 15 m^2/g reduces the age at which maximum strength enhancement occurs in MK mortars, illustrating the effect of particle size on reaction rate. Because of the increased surface area, MK was able to react more rapidly, leading to a faster rate of strength evolution. This increase in fineness also resulted in an increase in the optimum level of replacement of cement by MK, meaning that more of the cement could be

replaced by this MK without the system suffering a lag due to dilution. Interestingly, this change in fineness did not influence the long-term (90 day) strength.

Ding and Li [Ding, 2002], who examined 5, 10, and 15% replacement with either MK or silica fume, found that both were effective in increasing strength beyond 14 days. At all ages, MK and silica fume performed similarly, increasing concrete strength to almost the same extent over controls. MK increased strength nearly linearly during the first 28 days of curing and then slowed down -- 65-day strength was only 6-8% greater than 28-day strength. Li and Ding [Li, 2003] further investigated 10% replacement with MK, combining it with PC alone or with both PC and ultra-fine slag. The compressive strength of the mortar mixture containing only MK was always greater than the control mixture, and was approximately 8 MPa greater by 28 days. Further, although initially lower, the MK-slag mixtures showed the highest 28-day strength.

Curcio *et al.* [Curcio, 1998] examined compressive strength development in mortars containing 15% MK. Specimens cast with three of the four MK materials tested showed higher rates of strength evolution than controls at ages up to 28 days. Samples cast with silica fume (S) and the fourth MK (M4), which was coarser but of approximately the same chemical composition, did not accelerate strength gain. Beyond 28 days, as shown in Figure 2.12, differences between controls and specimens containing admixtures were smaller.

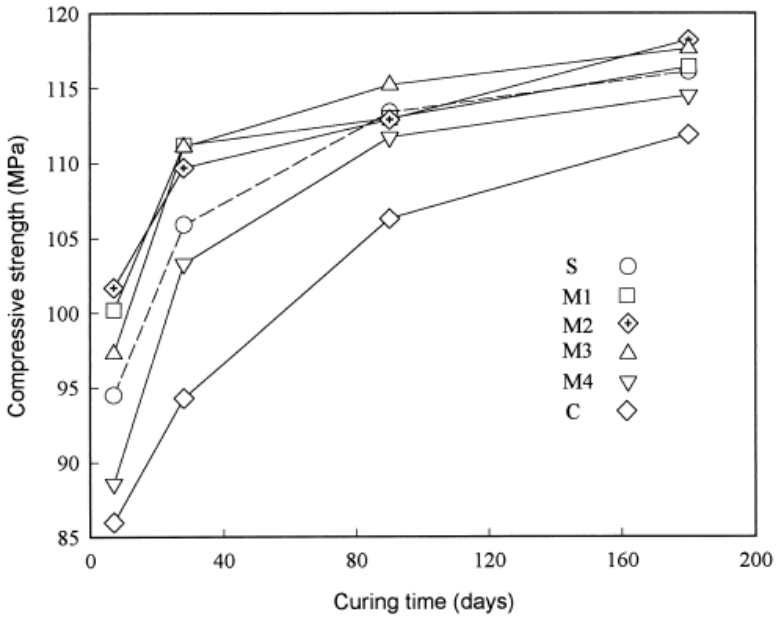

Figure 2.12. Compressive strength v. curing time for control mortars (C) and mortars containing 15% MK (M1-M4) or silica fume (S) [Curcio, 1998].

Vu *et al.* [Vu, 2001] studied a specific kaolin indigenous to northern Vietnam in order to determine the degree to which kaolin could replace PC in local mortar and concrete production. He found that the optimum PC replacement level increased with mortar maturity for all water-to-cement ratios. For early age mortars (up to seven days), 10% replacement with MK was optimal, while 15-20% was best in the 7-28 day range and 20-25% replacement resulted in the highest strength mortars 28 days and older. This implies that the pozzolanic reaction of MK may not make its peak contribution to strength until later in the hydration process. Vu also examined the effects of varying water content, and found that less MK was necessary to achieve maximum strength increases at lower w/cms. For mortars with a w/cm of 0.32, 10% replacement was optimum; for w/cm=0.44, 20% was optimum.

Qian *et al.* [Qian, 2001] measured both compressive and tensile strength of concretes incorporating MK. Compressive strength was found to increase substantially with increasing MK content. In samples with 15% replacement, compressive strength had increased 51% over controls by three days of age. In fact, the compressive strengths of samples containing 10% and 15% MK were higher at three days than the 28-day control strength, confirming that MK has a pronounced effect on early strength. Courard *et al.* [Courard, 2003] came to a similar conclusion, reporting that mortars had achieved 79% of their 28-day compressive strength by just three days of age. Qian [Qian, 2001] found that tensile strength also increased systematically with increasing MK content. The average tensile strength increases over controls were as follows: 7% (5% MK), 16% (10% MK), and 28% (15% MK). This was the only study reporting MK's effects on tensile strength.

2.4.1b Flexural Strength (Modulus of Rupture)

Very few studies have been published that have focused specifically on the influence of MK on modulus of rupture (MOR). Although there is little existing literature, there is good agreement that MK improves the flexural strength of concrete.

In a 1998 paper, Dubey and Banthia [Dubey, 1998] examined both MK and silica fume and their influence on flexural strength of high-performance steel fiber-reinforced concrete. As controls, specimens were cast with 10% SCMs but without fibers and vice versa. Both MK and silica fume increased MOR approximately 15% over the 100% PC sample in the prisms not containing fibers. The specimen containing 1% fibers and no SCMs had an MOR value similar to these, around 7.2 MPa. From the complete load-

displacement curves, Dubey and Banthia observed that the post-peak performance of fiber-reinforced concrete with MK was superior to other composites. That is, MK incorporation served to increase toughness. Silica fume concrete, on the other hand, exhibited a relatively brittle behavior and showed poor energy absorption performance, as evidenced by a steep drop in load after peak indicating a greater rate of softening and damage in these composites. Strength and toughness values are shown in Table 2.4.

Table 2.4. Modulus of rupture and toughness values for MK-concretes [Dubey, 1998].

Mix	Mix description	f_c', MPa	MOR, MPa	Absolute toughness T_{JCI}, N-m	Flexural toughness factor σ_b, MPa
CF	Control + 1.0 percent fibers	68.0	7.19	39.18	5.88
SF	Control + 10 percent silica fume + 1.0 percent fibers	70.1	8.37	32.01	4.80
MF	Control + 10 percent HRM + 1.0 percent fibers	72.2	8.39	41.45	6.40
SMF	Control + 5 percent silica fume + 5 percent HRM + 1.0 percent fibers	71.4	8.39	36.78	5.81

Qian *et al.* [Qian, 2001] measured the flexural strength of concrete beams in four-point bending for varying amounts of MK replacement at both 28 and 80 days of age. In either case, 5% replacement had little effect. For higher replacement levels, however, MOR increased significantly: by 28 days, it increased 32% and 38% for 10% and 15% replacement, respectively. These results are shown in Figure 2.13.

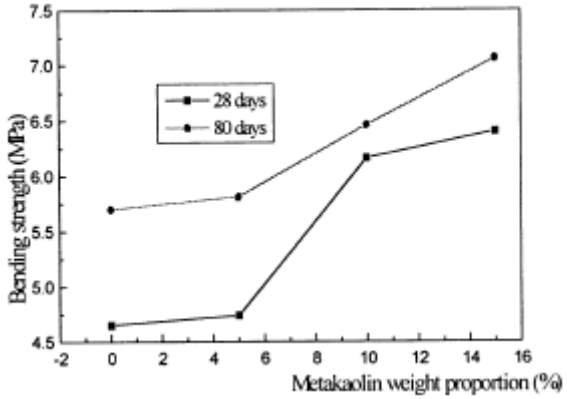

Figure 2.13. Flexural strength of concrete beams with various replacement levels [Qian, 2001].

Vu *et al.* [Vu, 2001] monitored flexural strength of MK-PC mortar prisms, although this study focused more on durability than strength evolution. These authors found that compressive and flexural strengths increased as a result of replacement with MK, even in concentrated sulfate environments. Compressive strength increased approximately 20% in 20% MK specimens. Flexural strength showed a less pronounced increase, as degradation due to sulfate attack first manifested itself at the specimens' surfaces, leading to spalling, mass loss, and thus lower MOR values.

Palomo *et al.* [Palomo, 1999] conducted a unique study that assessed MK without cement. He prepared a sodium hydroxide solution, added water glass (sodium silicate), and then mixed with MK in a planetary mixer while incrementally adding sand. Small prisms (1×1×6 cm) were cast from the paste, oven-cured for 2 h, and then immersed in jars containing various solutions. Rather than examining expansion, Palomo investigated the evolution of flexural strengths in these prisms. For the first three months, the strengths fluctuated, regardless of immersion medium. During this fluctuation stage, prisms submerged in sulfuric acid solution consistently had the lowest flexural strengths

of the group. After three months, however, when strength began to develop consistently, the prisms in seawater performed inferior to all other specimens (5 MPa). Those contained in sulfuric acid, sodium sulfate, and deionized water all reached approximately the same flexural strength (7 MPa). Through XRD, Palomo identified a primarily amorphous material containing small amounts of a crystalline zeolite belonging to the Faujisite family, which appears to act as reinforcement of the cement matrix. This indicates that MK may be alkaline-activated with concentrated NaOH to produce zeolitic precursors with excellent mechanical strength and good stability in aggressive environments (at least up to 270 days).

2.4.2 Modulus of Elasticity

There is little existing literature regarding the effect of metakaolin on the modulus of elasticity (MOE) of concrete. As it has been shown to increase compressive strength and to densify the microstucture, it follows that MK might also lead to increased elastic modulus, or stiffer concrete. From the literature, MOE generally seems to increase with increasing MK content, although the rate of increase is lower than that for compressive strength.

The study performed by Qian *et al.* [Qian, 2001] reported that at three days curing, concrete containing 15% MK had an elastic modulus of 26.2 GPa, as compared to 24.1 GPa for the control sample at this age. At 60 days of age, 15% MK and control concretes showed MOE values of 34.7 and 30.4 GPa, respectively.

Khatib and Hibbert [Khatib, 2004] evaluated dynamic modulus of elasticity for w/cm=0.50 concretes containing 0, 10, or 20% MK. They found that MK increased

MOE at all curing times, and that 10% and 20% replacement increased MOE to the same extent over controls. There was a sharp increase towards the end of the examination period: between 28 and 90 days, MOE increased from 38 kN/mm^2 to 50 kN/mm^2. Unfortunately these authors did not continue their study beyond 90 days to see if the effect persisted.

Caldarone *et al.* [Caldarone, 1994] reported increases in MOE associated with MK usage, as well. These authors performed ASTM C 469 to determine the static modulus of elasticity of concrete prepared with a w/cm=0.40 and 5% or 10% MK. MOE was measured at two ages, 28 and 90 days, and reported values were based on the average of two moist-cured 6 × 12" cylinders. At 28 days, concrete containing 5% MK had increased MOE 15% over controls, while concrete containing 5% SF increased MOE by 13%. Results from this study are shown in Table 2.5 below.

Table 2.5. Static modulus of elasticity for w/cm=0.40 concretes [Caldarone, 1994].

Testing Age	**Static Modulus of Elasticity (ksi)**				
	Control	**5% MK**	**10% MK**	**5% SF**	**10% SF**
28 Days	4805	5515	5640	5435	5590
91 Days	4980	5685	5880	5575	5855

2.5 Durability

In addition to strength, MK incorporation is widely regarded as an effective means to increase concrete durability. This is achieved primarily in the ITZ, which is characterized by a higher porosity, a higher local w/cm, and differing mineralogical and chemical composition than the bulk paste. It has been suggested that these properties of the ITZ can be detrimental to some composite properties, including resistance to chloride

and sulfate transport. MK, which has been shown to affect the chemistry and microstructure of the ITZ, may thus play a role in reducing ion transport and improving concrete durability. Three aspects of durability will be discussed herein: chloride permeability, sulfate attack, and alkali-silica reaction.

2.5.1 Chloride Permeability

The rapid chloride permeability test (RCPT), as described in ASTM C 1202, is a common test used to determine the resistance of concrete to chloride ion penetration. This test provides an indirect measure of chloride permeability by monitoring the charge passed (in Coulombs) through a concrete sample. One side of the concrete cylinder is exposed to a NaCl solution, and when a 60 V potential is applied, charge-carrying Cl^- ions will diffuse through to the other side of the cylinder, which is in contact with a NaOH solution. Unfortunately, these results cannot be used to directly predict the rate of chloride penetration under field conditions, since they do not incorporate the mass transport coefficients that true service life models require. Bulk diffusion, or ponding, tests are necessary to determine apparent chloride diffusion coefficients, but these tests are bulky and are lengthy in duration, and as a result are less commonly performed than RCPT or similar accelerated tests [Gruber, 2001].

Asbridge *et al.* [Asbridge, 2001] examined the influence of MK on chloride diffusion kinetics in mortars with varied volume fractions of aggregate, and hence varied volume and contribution of the material in the ITZ. The aggregate used to prepare the model mortars was a silicate glass bead supplied by British Optical. Chloride diffusion was measured both under steady-state and non-steady-state conditions. Steady-state

measurements were collected by mounting a 3-mm thick disc in a diffusion cell containing 1 M NaCl on one side and 0.035 M NaOH on the other. The increase in chloride concentration in the dilute NaOH compartment was monitored by periodically removing 100 μL aliquots for chloride determination. Non-steady-state measurements were made by removing the top surface (cast face) of a cylindrical specimen, sealing the remaining three sides, and submerging in a NaCl/NaOH solution for 168 days. After exposure and removal of the wax seal and the outermost 4 mm from the specimen diameter, profile grinding was performed in 3-mm increments from the top surface. These "grindings" were dried, treated with HNO_3, and filtered, and the filtrate was analyzed for chloride content.

In control samples, steady-state diffusion increased with aggregate content, but did not vary significantly in samples containing MK. The same phenomenon was observed in the non-steady-state analysis. Diffusivity and capillary porosity both increased markedly in control samples, indicating that the ITZ had a higher overall porosity than the bulk paste. Interestingly, the chloride diffusivity increased sharply at aggregate volume fractions above 35%, whereas capillary porosity increased linearly with aggregate content. This suggests some interconnection of higher porosity ITZ regions, which results in percolation and facilitates chloride transport. The use of 10% MK as a partial replacement of cement reduced non-steady diffusivity by an order of magnitude, and there was little variation regardless of aggregate content. Capillary porosity did increase in MK specimens with increasing amounts of aggregate, but the increase was not as great as in control samples. This supports the hypothesis that the use of MK increases permeation path tortuosity and thereby inhibits percolation.

Boddy *et al.* [Boddy, 2001] conducted a similar study, examining both steady- and non-steady-state bulk diffusion. Surface chloride concentration and bulk diffusion coefficients were measured in addition to RCPT. After three years of ponding, the diffusion coefficients were still decreasing, as expected, due to further hydration and infilling of porosity (Table 2.6). The best performance at all ages was exhibited by a concrete with 0.30 w/cm and 12% MK content. At just 28 days, this concrete exhibited a diffusion coefficient of 2.9×10^{-12} m^2/s and allowed 230 Coulombs to pass in the RCPT, as compared to measurements of 9.6×10^{-12} m^2/s and 2350 Coulombs for the 0.30-w/cm control. Also, at all ages, replacing 8% of the cement in a 0.40 w/cm concrete yielded approximately the same diffusivity as a 0.30 w/cm concrete containing no SCMs.

Table 2.6. Bulk diffusion coefficients, C_0 ($\times 10^{-12}$ m^2/s), and surface concentration, D_a (%), from chloride ponding tests [Boddy, 2001].

	28 days		90 days		140 days		365 days		1095 days	
Mix design	C_0	D_a	C_0	D_a	C_0	D_a	C_0	D_a	C_0	D_a
1 — 0.40 w/cm, 0% HRM	0.33	19.1	0.34	11.8	0.64	6.1	0.63	6.3	–	–
2 — 0.40 w/cm, 8% HRM	0.69	8.2	0.58	5.7	0.61	3.8	0.68	2.3	0.73	1.7
3 — 0.40 w/cm, 12% HRM	0.58	5.8	0.53	3.5	0.60	3.2	0.58	1.7	0.68	1.0
4 — 0.30 w/cm, 0% HRM	0.42	9.6	0.44	5.9	0.56	5.4	–	–	0.52	3.4
5 — 0.30 w/cm, 8% HRM	0.52	3.7	0.49	2.9	0.72	2.2	0.83	1.4	0.76	0.8
6 — 0.30 w/cm, 12% HRM	0.50	2.9	0.48	2.7	0.73	1.5	0.69	0.9	0.69	0.5

Batis *et al.* [Batis, 2004] selected a local Greek kaolin, calcined it, and tested it in mortars containing reinforcing steel. Batis used this MK to replace either sand or cement, and utilized several methods to evaluate corrosion resistance in the presence of a 3.5% NaCl solution. Based on half-cell potential development, mass loss, carbonation depth, and corrosion rate determination, Batis concluded that MK made a positive anti-corrosive impact. Replacement with either 20% MK for sand or 10% MK for cement improved

corrosion behavior most significantly, while higher replacement levels made no contribution.

Courard *et al.* [Courard, 2003] measured chloride diffusion via a diffusion cell containing saturated $Ca(OH)_2$ solution on one side and 1 M NaCl in saturated $Ca(OH)_2$ solution on the other. At periodic intervals, chloride concentration was determined by titration of a 20 cm^3 sample of the solution. PC mortars showed a breakthrough time of only 13 days (time necessary for initiation of Cl^- ion transfer through the sample), while 5% MK replacement resulted in a breakthrough time of 45 days and an apparent diffusion coefficient of 4.71×10^{-12} m^2/s. Specimens containing 20% MK still had not "broken through" at the end of one year, and exhibited coefficients lower than 1×10^{-12} m^2/s (Figure 2.14).

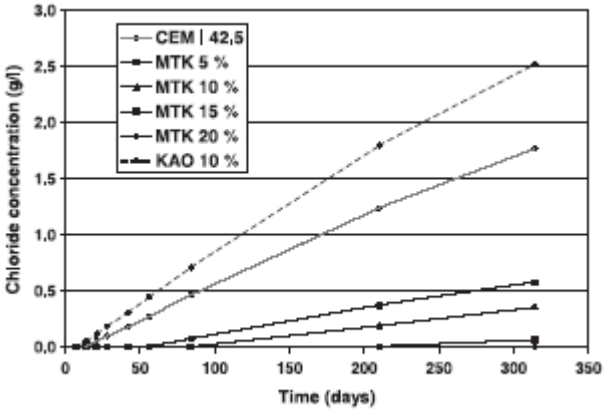

Figure 2.14. Chloride diffusion rates in mortars [Courard, 2003].

2.5.2 Sulfate Resistance

Another aspect of durability that MK replacement affects is resistance to sulfate attack. This is perhaps the most common and widespread form of chemical attack on concrete. Sulfates are often present in groundwater, particularly when high proportions

of clay are present in the soil, or in local concentrations in the vicinity of industrial wastes, such as mine tailings, slag heaps, and rubble fills. Sulfates are a major constituent of seawater and may be present in rainwater due to air pollution. Hazardous wastes, agricultural effluent, and sewage may also contain significant concentrations of sulfate. Sulfate attack is a complex process that may involve cracking and expansion of concrete as a whole, as well as softening and disintegration of the cement paste [Mindess, 2003].

Based on its ability to refine the pore structure and improve the strength of concrete, MK seems a likely candidate for promoting sulfate resistance. However, MK is chemically different from many other SCMs in that it has a very high alumina content. The reaction products that MK and CH form are not only C-S-H, but also include C_4AH_{13}, C_3AH_6, and C_2ASH_8. A clear correlation has been drawn between the tricalcium aluminate (C_3A) content of a portland cement and its susceptibility to sulfate attack [Kurtis, 2000]. If sulfate is present, ettringite is formed from reaction of ingressing sulfates, C_3A, and monosulfoaluminate. The formation of ettringite during sulfate attack can, but does not always, produce significant volume expansion and can be detrimental to concrete life [Mindess, 2003]. In addition, sulfate ions will react with CH to form gypsum, which then can lead to a decrease in pore solution pH, destabilization of hydration products, and decalcification of the C-S-H. The net effect of this form of chemical attack is loss of adhesion and strength.

In a 1997 study, Khatib and Wild [Khatib, 1998] examined a commercial MK and portland cements with either an intermediate or a high C_3A content. Expansion due to sulfate attack was found to decrease systematically with increasing MK content for both

cement types (Figure 2.15). Mortars containing high C_3A cement and 0-10% MK showed rapid expansion and deterioration between 40 and 70 days of exposure to a 5% sodium sulfate solution. Mortars containing high C_3A cement and 15 or 20% MK showed a small but sharp expansion during this window, but subsequently stabilized and contracted slightly. For the intermediate C_3A content mortars, the expansion process was delayed significantly. Those containing 10% or more MK exhibited essentially no expansion, while those containing 0% or 5% did not begin expanding until 150 days and did not grow rapidly until approximately 350 days.

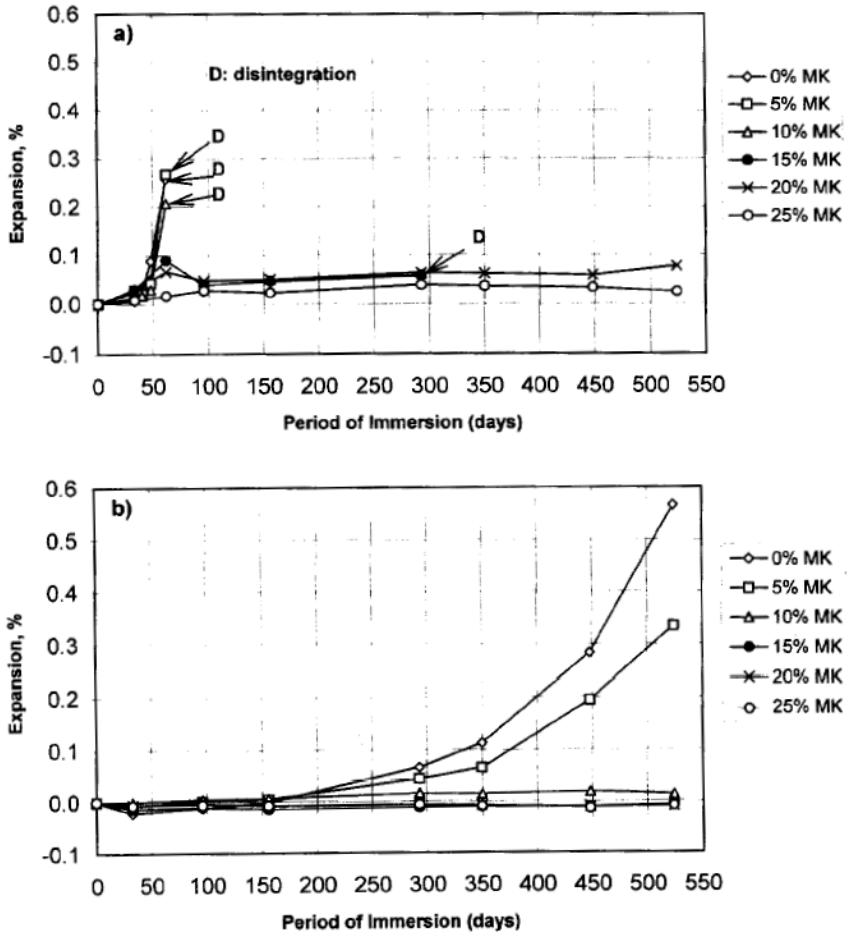

Figure 2.15. Expansion of MK mortar bars v. sodium sulfate exposure time for (a) high and (b) intermediate C_3A portland cements [Khatib, 1998].

Courard *et al.* [Courard, 2003] measured sulfate resistance in a procedure similar to the mortar bar method described in ASTM C 1012. PC mortar prisms experienced expansion after only a few days of exposure to sodium sulfate. After 84 days, variation in length was 3.7%. In contrast, prisms incorporated with 10% MK shrank initially and then did not change length significantly in either direction for the duration of the test (one year).

Roy *et al.* [Roy, 2001] conducted an extensive investigation consisting of 18 single blends and one control mixture in order to compare MK with FA and SF. Mortars were prepared with replacement levels ranging from 7.5% to 22.5% and at w/cms of 0.30, 0.36, or 0.40. Chemical resistance was determined in accordance with ASTM C 267. The aggressive chemical environments consisted of various acids (acetic, hydrochloric, nitric) and a mixture of magnesium sulfate and sodium sulfate. Results were quite inconsistent, but generally showed SF mixtures to possess the least chemical resistance and FA to have the greatest. MK mixtures fell in between. These results are somewhat questionable, however, as these authors also found chemical resistance to increase with decreasing SCM replacement percentage and increasing w/cm.

2.5.3 Alkali-Silica Reaction (ASR)

Alkali-silica reaction occurs between alkalis contained in cement paste and certain forms of reactive silica within the aggregate. Common forms of reactive silica include opal, chert, and natural volcanic glass. These materials have different alkali reactivity depending on their degree of crystallinity, crystal size and strain, and internal porosity.

The mechanism of ASR is relatively complex, beginning with depolymerization, dissolution, repolymerization of an alkali-silica gel product, and swelling of the gel in the presence of water. If a sufficient amount of water is present, the gel volume can increase, generating local tensile stresses in the concrete and eventually leading to cracking, which can increase the permeability (furthering the reaction) and decrease the strength and stiffness of the concrete. The best protection against ASR is achieved by:

1. avoiding susceptible aggregate,
2. reducing water content (to reduce concrete permeability),
3. specifying a low-alkali cement, and
4. reducing the overall alkali content of the concrete by limiting the cement content.

SCMs, including MK, have been shown to reduce the effects of ASR, as well. Secondary reactions involving SCMs promote refinement and densification of the concrete microstructure, reducing permeability and limiting the availability of water. In addition, when SCMs are used as partial replacement for cement, their effect is to dilute the cement, which reduces the alkali content of the concrete system and the pH of the pore solution, thereby increasing the solubility of calcium and promoting the formation of non-expanding gel in place of swelling N(K)-S-H. Adequate protection is typically attained by replacing cement with 15-20% Class F fly ash, 35-40% Class C fly ash[2], 10-15% silica fume, or ~50% slag. Recent studies involving MK have indicated that replacement levels of 10-15% should be effective in mitigating ASR [Aquino, 2001; Ramlochan, 2000].

[2] Class F fly ashes are produced from bituminous coals, while Class C fly ashes are produced from lignitic coals. Generally a greater amount of Class C fly ash is required to control expansion by ASR. It is believed that the higher CaO content in Class C fly ash results in a C-S-H with a greater C/S which is less capable of binding Na^+ and K^+. The greater availability of these alkali cations in the pore solution is believed to further the alkali-silica reaction.

Aquino *et al.* [Aquino, 2001] compared silica fume and MK in a 2001 study utilizing a high-alkali cement and dolomitic limestone aggregate substituted with 5% Beltane opal. Mortars were prepared at a w/cm of 0.56, sand-to-cement ratio of 2.25, and 10% replacement with SCMs. Results of ASTM C 1260, the accelerated mortar bar method, showed that although the MK specimens initally expanded at a faster rate, the silica fume specimens expanded more by the end of the testing period (approximately 0.25% at 21 days). The control specimen containing reactive aggregate (Control B) expanded the most -- over 0.50% -- while the control prepared with only inert aggregate (Control A) did not show significant expansion (0.03%). These results are shown in Figure 2.16.

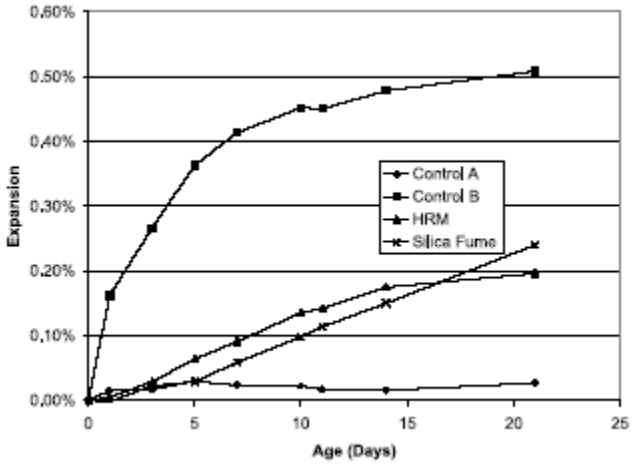

Figure 2.16. Results of ASTM C 1260 [Aquino, 2001].

Ramlochan *et al.* [Ramlochan, 2000] examined a MK from Georgia that was water-processed to remove impurities. Concrete prisms contained either of two reactive coarse aggregates, reactive sand, cement, and 0-20% SCM. Three Type I cements with varying alkali contents were used. Similar mortar bars were cast. These were tested

according to ASTM C 1260, while the concrete prisms underwent the two-year evaluation prescribed by the Canadian standard CAN/CSA A23.2-14A. For all combinations of aggregate and cement, 15% MK was sufficient to suppress ASR expansion to within the specified limit criteria (0.04% for concrete, 0.10% for mortar); for concrete prisms containing the Sudbury aggregate, a greywacke-argillite gravel, 10% replacement with MK was sufficient (Figure 2.17). Ramlochan suggested that the mechanism by which MK may suppress ASR expansion is entrapment of alkalis by the supplementary hydrates and a consequent decrease in the pH of the pore solution. This was supported by sampling pore solutions of paste samples over a two-year period and titrating to determine OH^- concentration.

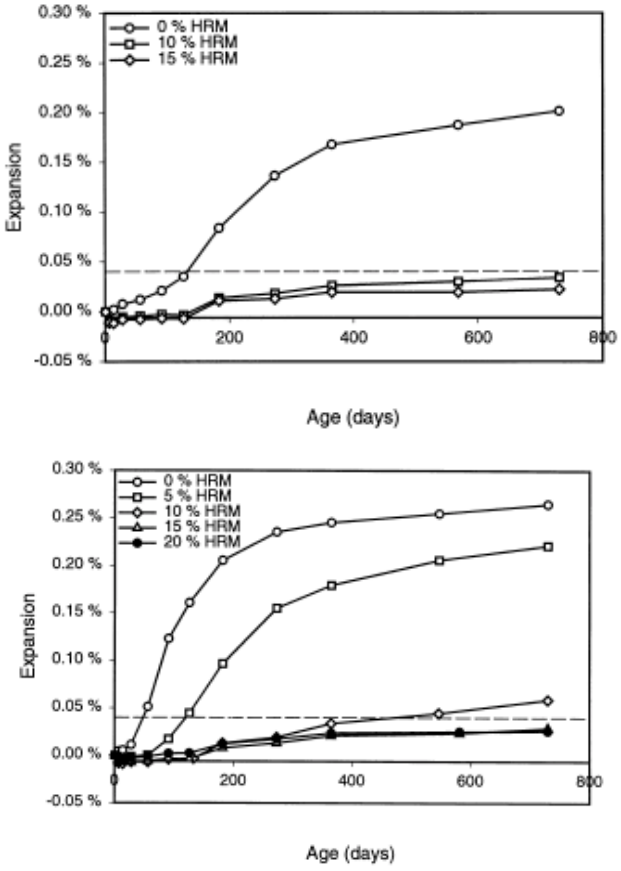

Figure 2.17. Expansion of concrete prisms containing metakaolin, cement A, and (a) Sudbury or (b) Spratt aggregate [Ramlochan, 2000].

2.6 Summary

There is good agreement in the existing literature that MK improves the properties of concrete. In general, MK has been shown to impart the following benefits:

- increased compressive strength,
- increased tensile strength,
- increased flexural strength, and
- decreased porosity and permeability (and thus increased resistance to chemical attack).

However, MK has also been shown to increase shrinkage and heat evolved during hydration, which can be detrimental. Since it is possible to tailor composition and particle size, each MK produced must be evaluated for efficacy in cementitious systems. Overall, MK has great promise as an SCM, and the utilization of MK will likely increase in the future.

Chapter III

Experimental Methods

3.1 Materials

The two metakaolins examined in this study, MK235 (*Kaorock*) and MK349 (*Kaorock F*), were provided by Thiele Kaolin Company in Sandersville, Georgia. These metakaolins differ primarily in their fineness, with MK349 having a smaller particle size and greater surface area (25.4 vs. 11.1 m^2/g). Both were produced using vertical hearth fluid bed calciners, into which the clay was fed at the top and the product collected from the bottom. MK235 was produced from coarse particle sized Cretaceous kaolin, while MK349 was produced from fine particle sized Tertiary kaolin. Photographs and SEM micrographs of these metakaolins are shown in Figures 3.1 and 3.2. Physical characteristics, as reported, are shown in Table 3.1. Particle size distributions, acquired at a Horiba Instruments/Retsch Incorporated Particle Technical Seminar, are reported in Figure 3.3. A DTA thermogram of the MKs and the other raw materials used in this study is shown in Figure 3.4. This plot shows a sharp crystallization peak just below 1000 °C, confirming that the MKs are reactive and were not over-calcined.

Figure 3.1. MK235 (left) and MK349 (right).

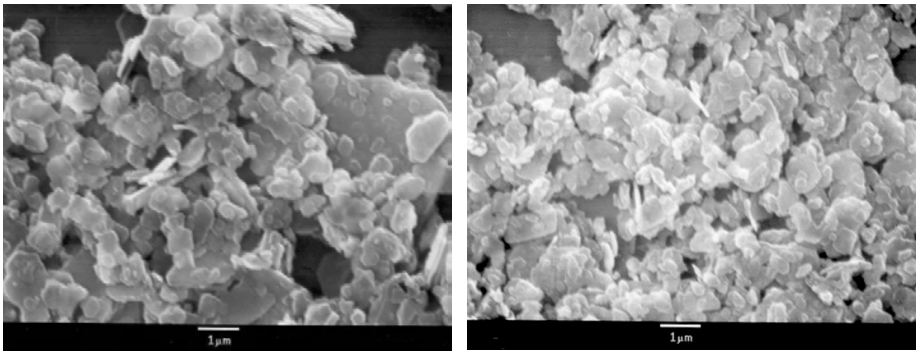

Figure 3.2. Scanning electron micrographs of MK235 (left) and MK349 (right).

Table 3.1. Physical characteristics of the two metakaolin samples examined.

Characteristics	MK235	MK349
Oxide Analysis (%)		
SiO_2	51.5	52.5
Al_2O_3	44.7	44.5
TiO_2	2.1	1.7
Fe_2O_3	0.4	0.9
Sedigraph PSD (%)		
< 2.0 µm	67	90
< 1.0 µm	41	83
< 0.5 µm	9	53
< 0.2 µm	4	4
Surface Area (m^2/g)	11.1	25.4
Bulk Density (lb/ft^3)	18	9
(kg/m^3)	288	139

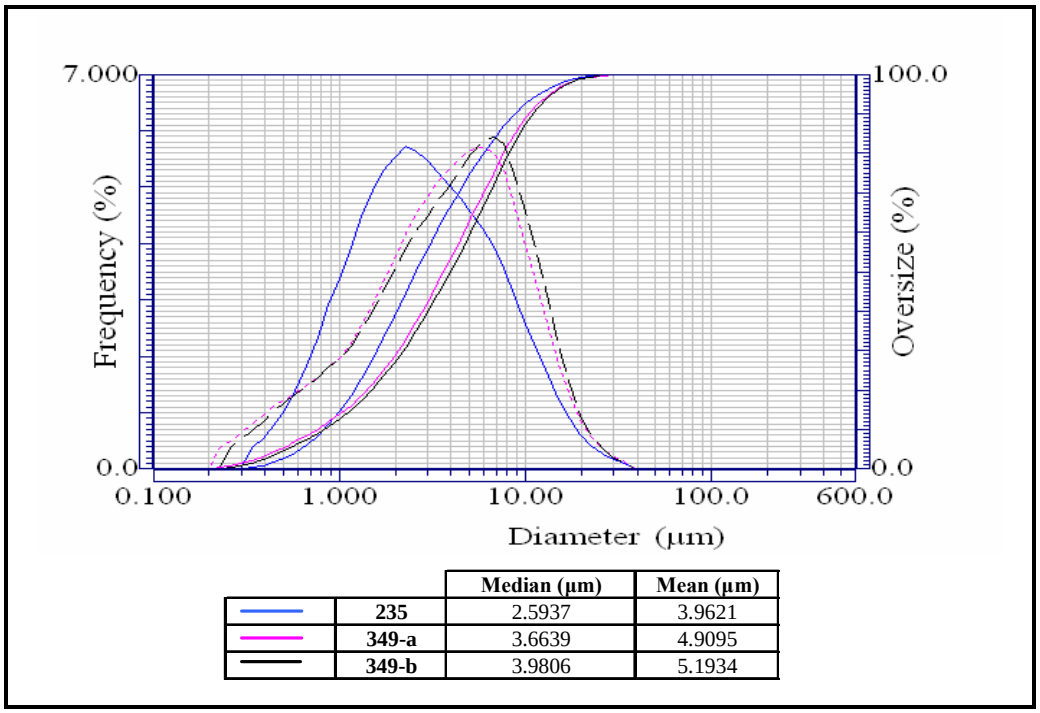

		Median (µm)	Mean (µm)
	235	2.5937	3.9621
	349-a	3.6639	4.9095
	349-b	3.9806	5.1934

Figure 3.3. Particle size data acquired by laser analysis.

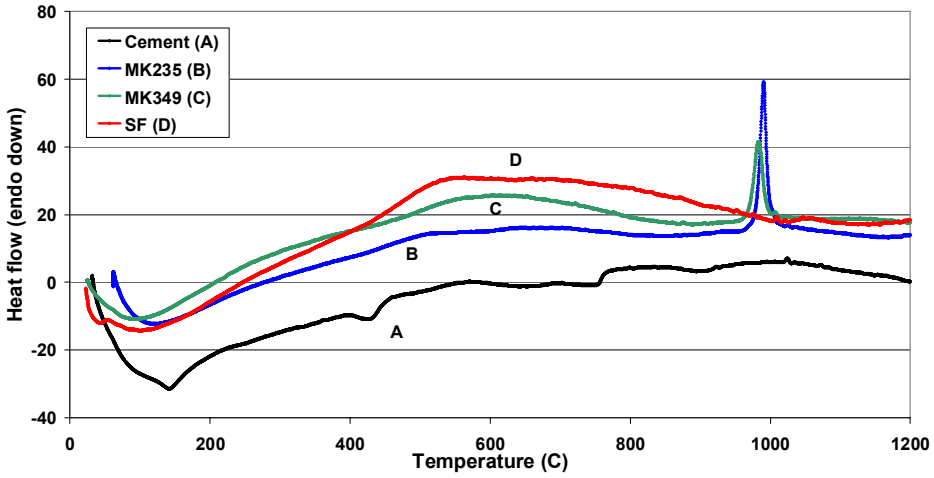

Figure 3.4. DTA thermogram of raw materials.

Commercially available Type I cement, obtained from Lafarge, was used for all paste and concrete mixtures. Results from a chemical oxide analysis of the cement, along with the Bogue potential composition, are given in Table 3.2. For comparative purposes,

companion mixtures were also prepared using Grace Force 10,000 D silica fume, a dry densified microsilica powder. An oxide analysis is given in Table 3.2. Aggregates were #67 3/4"- (19 mm) MSA crushed granitic gneiss stone and 2.38 fineness modulus natural sand, as well as mixed quartz/chert/feldspar alkali-reactive sand from El Paso, Texas for the ASR testing (Figure 3.5). Commercially available superplasticizer, which conforms to the ASTM C 494 Type F designation, was also used. Tap water was used for mixing concretes; de-ionized water was used for mortars, pastes, and all chemical solutions.

Table 3.2. Chemical oxide analysis, weight %, for Type I cement and silica fume and Bogue potential composition for the cement.

Component	Cement	Silica Fume
SiO_2	21.26	97.12
Al_2O_3	4.79	0.01
Fe_2O_3	3.14	0.05
CaO	64.10	0.37
MgO	2.35	0.28
Na_2O	0.02	0.04
K_2O	0.36	0.58
TiO_2	0.19	0.02
MnO_2	0.04	0.04
P_2O_5	0.03	0.08
SrO	0.03	0.01
BaO	0.04	0.00
SO_3	2.63	0.04
Loss on Ignition	1.04	1.36
Insoluble Residue	0.11	N/A
Moisture	N/A	0.43
C_3S	55.24	N/A
C_2S	19.28	N/A
C_3A	7.38	N/A
C_4AF	9.54	N/A

Figure 3.5. Alkali-reactive sand used in ASR test, ASTM C 1260.

3.2 Mixture Proportions

In this study, the early age properties of fresh concrete and mechanical performance and durability of hardened concrete were examined. All tests were conducted using the following four sample groups:

1. an ordinary cement paste or concrete,
2. pastes or concrete substituted with 8% MK235 by mass replacement for cement,
3. pastes or concrete substituted with 8% MK349 by mass replacement for cement, and
4. pastes or concrete substituted with 8% silica fume by mass replacement for cement.

Pastes, mortars, or concretes were prepared at three water-to-cementitious materials ratios (w/cm) -- 0.40, 0.50, and 0.60 -- for each of the above sample groups, unless ASTM tests made specific requirement for w/cm. Concrete raw materials were batched and mixed for approximately 15 minutes in accordance with ASTM C 192 using a 2.5 ft^3-capacity (71 L) Lancaster Counter Current Batch mixer, according to the mixture designs given in Table 3.3. The following mixing procedure was used:

1. Add coarse aggregate to mixer.
2. Start mixer.
3. As mixer is spinning, add fine aggregate.
4. As mixer is spinning, add cement.
5. As mixer is spinning, add metakaolin or silica fume, if using.
6. Allow dry materials to mix for 5 minutes.
7. Add water.

8. Add superplasticizer, if using (use small dosages and wait at least 1 minute before adding more).
9. Mix for 3 minutes.
10. Rest for 3 minutes.
11. Mix again for 2 minutes.
12. Perform slump.
13. Return concrete to mixing bowl and continue mixing for 10 minutes.

Mortars and pastes were mixed with a Hobart mixer per ASTM C 305 for at least five minutes after the addition of water. SCMs were incorporated into mortar mixtures concurrently with or immediately following cement -- after aggregates, but prior to water.

Table 3.3. Concrete mixture designs for control mixtures and mixtures with SCMs at 8% by weight replacement for cement.

		1 yd^3 or 1 m^3										Nominal Density	
w/cm		Water		Coarse (SSD)		Fine (SSD)		Cement		SCM			
		lb	kg	lb	kg	lb	kg	lb	kg	lb	kg	lb/yd^3	kg/m^3
0.4	Control	340	201	1709	1014	1127	668	850	505	--	--	4026	2388
	w/ SCM	340	201	1709	1014	1127	668	782	464	68	41	4026	2388
0.5	Control	340	201	1709	1014	1279	759	680	403	--	--	4008	2377
	w/ SCM	340	201	1709	1014	1279	759	626	372	54	31	4008	2377
0.6	Control	340	201	1709	1014	1374	815	567	336	--	--	3990	2366
	w/ SCM	340	201	1709	1014	1374	815	522	310	45	26	3990	2366

Concrete samples were removed from plastic-covered molds 24 hours after casting and placed in a 23 °C fog room for the remainder of the active testing period. Mortar and cement paste samples, with the exception of the Vicat samples, were demolded at 24 hours and placed in a 23 °C limewater curing tank. A summary of the tests conducted on fresh and hardened samples, their corresponding ASTM standards, and the dimensions of samples used for each is shown in Table 3.4.

Table 3.4. Tests conducted and cast specimen dimensions.

Description	Designation	Dimensions	
		in	mm
Slump	C 143	N/A	N/A
Setting time	C 191	N/A	N/A
Chemical shrinkage	N/A	N/A	N/A
Autogeneous shrinkage	N/A	N/A	N/A
Free shrinkage	C 157	1×1×11.25, 3×3×11.25	25×25×286, 76×76×286
Compressive strength	C 39	3×6	76×152
Splitting tensile strength	C 496	3×6	76×152
Modulus of rupture	C 78	3.5×4.5×16	89×114×406
Modulus of elasticity	C 469	6×12	152×305
Chloride permeability	C 1202	4×8	102×203
Sulfate resistance	C 1012	1×1×11.25	25×25×286
Alkali-silica reaction	C 1260	1×1×11.25	25×25×286

3.3 Methods

3.3.1 Early Age Properties

Early age properties of pastes and concrete, including slump, unit weight, setting time, and heat evolution were measured. Slump was measured according to ASTM C 143. Superplasticizer was used as necessary in order to achieve a target slump of 3-4" (76-102 mm) for all mixtures. Unit weight was calculated based on an average of five 3×6" (76×152 mm) concrete cylinders.

Time to initial and final set was measured using a Vicat apparatus, as shown in Figure 3.6, according to ASTM C 191. Three samples were used for each measurement. Because pastes made with metakaolin required a higher water content to become workable, setting time tests were conducted both at a normal consistency (varying w/cm) as determined by ASTM C 187, as prescribed by the standard, and at a constant w/cm of 0.34. This was the w/cm necessary for MK349 to reach normal consistency -- the highest value determined by ASTM C 187. In order for the other three experimental groups to

approach normal consistency (approximately 15 mm penetration with the Vicat needle), these pastes were allowed to remain in the mixing bowl as necessary before placing in the ring molds and moist cabinet.

Figure 3.6. Vicat needle apparatus
[Humboldt Manufacturing - Vicat Consistency Testers].

Heat of hydration was evaluated via isothermal calorimetry using a Thermometric TAM Air eight-channel heat conduction calorimeter maintained at 25 °C. This type of instrument measures heat evolved by comparing the temperatures of a sample and an inert reference that are held under isothermal conditions. Heat flow data is collected as a function of time. Pastes contained 200 g total cementitious material and a w/cm of 0.50 and were mixed for five minutes using a Sunbeam hand mixer on low speed. In addition to 8%, 15% replacement with SCMs was examined. Polyethylene ampules (Figure 3.7) were filled with approximately 20 g of paste, with empty ampules serving as references. All experiments were conducted in replicates of three and data was collected for at least 48 h. When running multiple mixtures concurrently, the calorimeter and data collection

process were started upon addition of water to the first mixture. As subsequent mixtures were produced, the time that water was added was recorded so that these curves could be offset when analyzing the data.

Figure 3.7 Polyethylene ampules used for isothermal calorimetry.

Differential thermal analysis may be formally defined as a technique for recording the difference in temperature between a substance and a reference material as the two specimens are subjected to identical heating or cooling regimes. Phase changes that occur in the sample which lead to the absorption or evolution of heat can be detected relative to the inert reference. The resulting curve, plotted as heat flow versus time or temperature, will show peaks representing these phase changes, with the area contained in a peak representing enthalpy [Bhadeshia, 2002].

Differential thermal analysis was conducted using a Perkin Elmer DTA 7. Samples of approximately 54 mg were heated at 10 °C/min, in argon atmosphere, to 1200 °C. Pastes contained 8% SCM and a w/cm of 0.40. Samples were mixed by hand, for at least five minutes, using a spatula and a glass plate, and were cast in 1 cm cube molds.

The ages examined were 4 h, 8 h, and 24 h. These were chosen based on the heat of hydration curve and corresponded to ages before, at, and after the primary heat peak. Samples were also run at seven and 28 days of age. Samples examined during the first 24 h of curing were tested as mixed; seven and 28 day samples were demolded after 24 h and stored in limewater until ready to test.

DTA was used to show the temperature ranges over which phase transitions occurred and to reveal whether different compounds were present at different ages. Perkin Elmer analysis software was used to compare DTA relative peak amplitudes (mW), areas (mJ), and enthalpies (J/g). These were then compared to the corresponding values obtained for the decomposition of 54 mg of pure, laboratory grade CH to yield an approximate CH content [Sha, 2001]. The interior of the DTA is pictured in Figure 3.8.

Figure 3.8. DTA samples, in alumina sample cups, inside the instrument.

Thermogravimetric analysis was used to measure the CH content of pastes containing 8% SCMs and w/cm of 0.40. This technique measures mass change as a function of temperature. In the particular TGA utilized in this study, the sample was

suspended, in a titanium foil boat, from a platinum wire hanging in the center of a vertical tube furnace. As it was heated, the mass change was measured from the displacement of a counterbalance on the opposite end of the platinum wire, which was thermally isolated from the furnace. Pastes were prepared in the same manner as the DTA pastes and were examined at the same ages. Samples of approximately 450 mg were heated to 900 °C at a rate of 10 °C/min in dry air atmosphere. CH content was determined based on the weight loss over the temperature range where CH decomposition was shown, through DTA, to occur (400-530 °C) [Poon, 2001; Wild, 1997]. The thermogravimetric analyzer and sample boat utilized are shown in Figure 3.9.

Figure 3.9. TGA specimen in titanium boat.

3.3.2 Shrinkage

Three types of shrinkage were monitored: chemical, autogenous, and free shrinkage. Briefly, chemical shrinkage is a result of the volume difference between reactants and products in a hydrating cement system. Autogenous shrinkage occurs due to the lowering of the cement paste internal relative humidity. Free, or drying, shrinkage

is the contraction that results as a paste, mortar, or concrete loses water to the environment. All shrinkage examinations were conducted at a w/cm of 0.40, and SCMs were used at 8% replacement.

Chemical shrinkage was evaluated on four replicate samples by a method modified from Geiker and Knudsen [Geiker, 1982; Knudsen, 1985]. This method involves introducing a known volume of cement paste (approximately 10 g, sample thickness < 10 mm) into a small glass vial fitted with a graduated pipette, thereby allowing volume change to be measured over time (Figure 3.10). These pastes were mixed concurrently with autogenous shrinkage pastes using a Hobart mixer. Vials were capped with rubber stoppers. Pipettes were inserted through holes in the stoppers, sealed with Parafilm, and topped off with hydraulic pump oil to prevent evaporation of water.

Figure 3.10. Chemical shrinkage setup.

Autogenous shrinkage was measured on four replicate samples using rigid corrugated polyethylene tubes capped on both ends to prevent loss of moisture to the environment. This well-accepted technique is described by Jensen and Hansen [Jensen,

1995]. Linear deformation of these tubes was monitored using a comparator, as shown in Figure 3.11. Both chemical and autogenous shrinkage samples were kept in an environmental chamber at 20 °C and 50% relative humidity. Data was recorded daily.

Figure 3.11. Autogenous shrinkage specimen in dilatometer.

Free, or bulk, shrinkage was measured according to ASTM C 157 on three or four replicate samples, for concrete and mortar prisms, respectively. A sand-to-cement ratio of 2.25 was used to cast mortar prisms of 1×1×11.25" (25×25×286 mm), and the mixture design shown in Table 3.3 was scaled down to make 3×3×11.25" (76×76×286 mm) concrete prisms. All contained a w/cm of 0.40. These were removed from molds 24 hours after casting and allowed to cure in limewater for the remainder of one week. At that point, samples were moved to an environmental chamber at 23 °C and 50% relative humidity to evaluate drying shrinkage. Measurements were recorded on days 1, 3, 5, 7, 10, and 14, and then every seven days for the following six weeks.

To further quantify the underlying causes of shrinkage, surface area and porosity were measured in controls and samples containing 8% SCMs (w/cm=0.40) at one, seven, and 28 days of age. To stop hydration and prevent carbonation, samples were crushed in an ethanol slurry and solvent-exchanged in ethanol for one week. Samples were then dried in an 80 °C oven until constant mass was achieved and stored in a desiccator until tested.

Nitrogen adsorption was performed on a Coulter SA 3100 using Rapitube flasks and approximately 0.3 g of powdered starting material (Figure 3.12). This technique involves dosing the sample with a known amount of nitrogen and measuring the volume of adsorbate gas retained by the sample. This volume is determined based on the residual pressure in the sample chamber formed by the molecules that do not adsorb. The process is repeated at the same temperature and at incremental pressures to form an isotherm data set.

Surface area was measured on the adsorption isotherm according to the BET (Brunauer, Emmett, Teller) method, while pore size distribution was measured on the desorption isotherm according to the BJH (Barrett, Joyner, Halenda) method. The BET surface area is calculated from a multilayer adsorption theory that assumes the first layer of molecules adsorbed involves adsorbate-adsorbent energies and subsequent layers are governed by the energy of vaporization of this adsorbate-adsorbent interaction. BET specific surface area is measured on the adsorption isotherm in the relative pressure range of 0.050 to 0.200. BJH, measured along the desorption isotherm, accounts for the area of pore walls and relates the nitrogen equilibrium relative pressure to the size of the pores where capillary condensation takes place [Gregg, 1982].

Figure 3.12. Sample flask used for BET and BJH testing.

3.3.3 Mechanical Properties

Compressive strength was measured on three replicate samples according to ASTM C 39. Cylinders of 3×6" (76×152 mm) were compressed at a rate of 20,000 lb/min (1480 N/s). Splitting tensile strength was also measured on three replicate 3×6" (76×152 mm) cylinders loaded at a rate of 5,000 lb/min (370 N/s), as outlined in procedure ASTM C 496. Compression and tension tests were conducted on 1, 3, 7, 28, and 90 days of age using an 800,000 lb-capacity (3600 kN) compression machine with a digital indicator. Photographs of these tests are shown in Figure 3.13.

Figure 3.13. Compressive (left) and splitting tensile (right) strength testing configurations.

Modulus of rupture was evaluated at ages of 1, 3, 28, and 90 days using a 400,000 lb-capacity (1800 kN) universal testing machine. This machine has several loading ranges and was set at its lowest capacity to give the best accuracy in these measurements. Prisms were cast at 3.5×4.5×16" (89×114×406 mm), and ASTM C 78 (third-point loading) was followed, using steel supporting rods and rubber pads, as shown in Figure 3.14. Three samples were tested in flexure for each condition.

Figure 3.14. Third-point loading experimental configuration.

Modulus of elasticity was determined per ASTM C 469, using 6×12" (152×304 mm) cylinders and a compressometer. This test was conducted on three replicate samples per mixture at day 28 of age on the 400,000 lb-capacity (1800 kN) universal load frame. Figure 3.15 is an image of the elastic modulus testing setup.

Figure 3.15. Method for determining modulus of elasticity in compression.

3.3.4 Durability

The rapid chloride permeability test (RCPT), as described in ASTM C 1202, was performed on three replicate specimens. This test provides an indirect measure of chloride permeability by monitoring the charge passed (in Coulombs) through a concrete sample. Samples 4" (102 mm) in diameter and 2" (51 mm) thick were cut from 4×8" (102×203 mm) concrete cylinders at 28 days of moist (fog room) curing. Samples were prepared according to the conditioning procedure outlined in ASTM C 1202. The rounded faces were sealed with epoxy and the specimens were placed in a vacuum desiccator. After three hours, the specimens were submerged in de-aerated water and the

pump allowed to run for one additional hour. Finally, air was allowed to re-enter the desiccator and the specimens were left to soak for 18 h before being loaded into applied voltage cells. A potential difference of 60 V DC was maintained across the ends of the specimens, one of which was immersed in a 3.0% by mass sodium chloride solution, the other in a 0.3 N sodium hydroxide solution (both prepared using de-ionized water). The total charge passed, in Coulombs, has been found to be related to the resistance of the specimen to chloride ion penetration. The equipment used, produced by Germann Instruments, is shown in Figure 3.16.

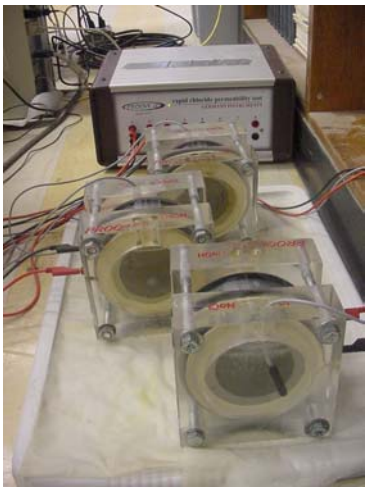

Figure 3.16. RCPT apparatus and diffusion cells.

To assess sulfate resistance, six replicate 1×1×11.25" (25×25×286 mm) mortar bars were prepared and measured for expansion according to ASTM C 1012. In addition to controls, two sets of samples were cast for each of the three SCMs, one at 8% and one at 15% replacement. ASTM C 1012 was modified slightly by preparing all mortar bars using a single w/cm of 0.485 and adding superplasticizer to those mixes with metakaolin and silica fume replacements to achieve suitable workability. Cast samples were placed

in metal roasting pans atop plastic sheeting and water heated to 35 °C, covered loosely with towels, and stored in a 35 °C oven for 24 h. Prisms were then demolded and stored in limewater for two additional days before initial length measurements were taken and exposure initiated. Samples were exposed to a 33,800 ppm sulfate solution (50 grams of Na_2SO_4 per liter of de-ionized water) at room temperature, as prescribed by the standard, and length change was recorded weekly. Solutions were changed on every measuring day. Mortar prisms and electronic comparator used for length measurements are shown in Figure 3.17.

Figure 3.17. Mortar prisms (left) and electronic comparator (right).

Additionally, as sulfate attack is more commonly associated with magnesium sulfate in the field, ASTM C 1012 was repeated using $MgSO_4$ and the sample matrix described above (four replicate samples). The amount of magnesium sulfate was adjusted to maintain an equivalent amount of sulfate (SO_4) as in the sodium study.

$MgSO_4$ = 120.4 g/mol
Na_2SO_4 = 142.1 g/mol
SO_4 = 96.1 g/mol

$SO_4/Na_2SO_4 = 96.1/142.1 = 0.676$

$33.8\%/0.676 =$ **49.98 g/L Na_2SO_4**

$(120.4/142.1) \times 49.98 =$ **42.35 g/L $MgSO_4$**

Potential for alkali reactivity was measured according to the accelerated mortar bar method (ASTM C 1260). This method has been shown reliable for evaluating the effectiveness of SCMs in suppressing ASR [Bérubé, 1995]. As with sulfate testing, a single water-to-cementitious materials ratio (0.47) was used and both 8% and 15% replacement levels were examined for samples (six replicates) containing SCMs. Gradation information for the alkali-reactive sand, which is slightly modified from the standard, and mortar mixture designs are shown in Tables 3.5 and 3.6, respectively. Mortar bars (1×1×11.25" or 25×25×286 mm) were cast and cured for 24 h in a moist cabinet at room temperature, demolded, and then cured for an additional 24 h in de-ionized water at 80 °C. Subsequently, they were stored in a 1 N sodium hydroxide solution, prepared with de-ionized water, at 80 °C, and length change data was collected for 28 days.

Table 3.5. ASR testing, aggregate gradation.

Sieve	Mass retained, g	Mass retained, %
#8	132	10
#16	330	25
#30	396	30
#50	396	30
#100	66	5
Total	1320	100

Table 3.6. Mortar mixture designs for ASTM C 1260 (ASR test).

Mixture	Water (g)	Aggregate (g)	Cement (g)	SCM (g)
Control	276	1320	587	N/A
8%	276	1320	540	47
15%	276	1320	499	88

Chapter IV

Results and Discussion

4.1 General

Metakaolin addition yielded concrete with considerably higher strengths and improved durability over concretes without SCMs. Metakaolin incorporation increased chemical and autogenous shrinkage of pastes, but decreased free shrinkage of mortars and concretes relative to controls. In general, the finer MK349 appeared to be more effective in increasing strength and elastic modulus, while the coarser MK235 was more effective in increasing durability, although both were more effective than silica fume. Key results regarding early age properties, shrinkage, mechanical properties, and durability are presented herein.

4.2 Early Age Properties

4.2.1 Slump, Superplasticizer Dosage, Unit Weight

To achieve a target slump of 3-4" (76-102 mm), superplasticizer was required for all concrete mixtures, with the exception of the control mixtures at w/cms of 0.50 and 0.60. When using SCMs, the necessary superplasticizer dosage increased with decreasing w/cm. Mixtures containing either of the metakaolins required more superplasticizer than those containing silica fume. MK235 typically required 15% more

than the amount used with silica fume, and MK349 required 150% more than that value. Superplasticizer dosages, in mL, are given in Table 4.1. Both metakaolins produced concrete with unit weights similar to control samples, while silica fume yielded concrete of 1.13% lower unit weight than controls on average over the three w/cm.

Table 4.1. Superplasticizer dosage requirements (mL) for 1.5 ft^3 concrete.

	0.40	**0.50**	**0.60**
Control	15	0	0
MK235	24	13	11
MK349	48	34	20
SF	22	12	9

4.2.2 Setting Time

The water-to-cementitious materials ratios (w/cm) used to produce pastes of normal consistency determined by ASTM C 187 are shown in Table 4.2, and the measured initial and final setting times for these pastes are shown in Figure 4.1. In general, final set occurred approximately 30 minutes after initial set, which was sooner than expected, as others have reported one hour or longer between initial and final set [Brooks, 2000; Vu, 2001]. For the normal consistency pastes, the MK235-containing samples had longer times to initial and final set than the control sample (initial set at 155 minutes), while the paste containing the finer MK349 had shorter setting times. The paste containing silica fume had the fastest setting times -- approximately 135 minutes for initial set. These results agree with what has been reported in the literature [Brooks, 2000; Vu, 2001; Batis, 2004], and are likely related to the higher water contents required to achieve normal consistency in MK pastes.

The initial and final setting times determined for pastes at a constant w/cm of 0.34 are shown in Figure 4.2. This was the w/cm necessary for MK349 to reach normal consistency and was the highest value determine by ASTM C 187. In this series, all pastes containing SCMs had shorter times to initial and final set than the control sample (initial set at 305 minutes). Both metakaolin pastes exhibited faster setting times than the silica fume pastes, with the paste containing MK349 showing the fastest setting times of all four paste types at 145 minutes. This is likely due to the finer particle size of the MK349, which results in a much larger surface area available for reaction and thus a faster rate of hydration and setting. A similar result was found by Moulin [Moulin, 2001], who found MK pastes to have much shorter setting times than controls when the Vicat needle test was conducted at a constant w/cm of 0.40.

Table 4.2. Normal consistency of pastes, as determined by ASTM C 187.

	w/c or w/cm
Control	0.27
MK235	0.31
MK349	0.34
SF	0.28

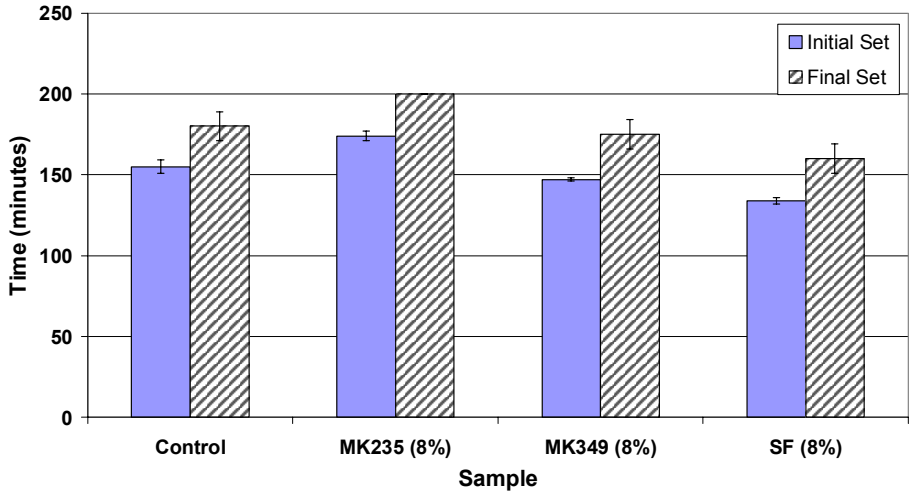

Figure 4.1. Vicat initial and final setting times at normal consistency (varying w/cm).

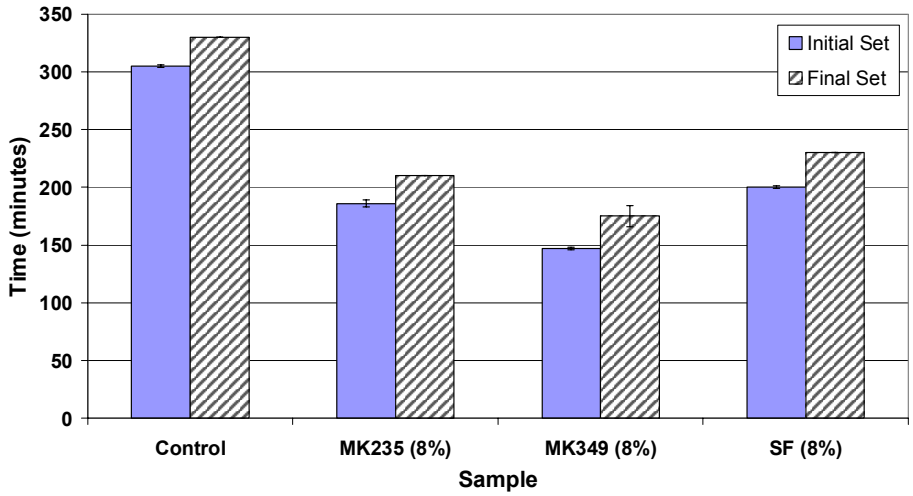

Figure 4.2. Vicat initial and final setting times at constant w/cm (0.34).

4.2.3 Heat of Hydration

Pastes containing metakaolin showed higher cumulative heat of hydration and faster rates of reaction than controls or silica fume pastes. Similar results were reported in the literature [Zhang, 1995; Frías, 2000; Bai, 2002]. Figure 4.3a shows the rate of heat

evolution and Figures 4.3b and 4.3c show the cumulative heat evolved -- all are normalized per gram of cementitious material. Silica fume incorporation reduced both the rate of heat evolution and the total heat evolved, relative to controls, likely due to the removal of cement from the system. This is supported by the fact that the 15% silica fume curve is lower than the 8% curve in both plots. Further, both silica fume rate curves follow the same general profile as the control, with the first peak, corresponding to C_3S hydration, reaching higher than the second peak (C_3A). This reflects dilution of the cement hydration and indicates that there is no secondary reaction occurring due to the presence of silica fume at these early ages.

Interestingly, all four metakaolin curves show the opposite trend: the second peak is higher than the first, indicating that some additional exothermic reaction(s) is (are) occurring in the MK pastes. These could be latent hyraulic or pozzolanic reactions, or possibly even a delayed dissolution of cement or MK phases. MK349, the finer material, showed the highest rate of heat evolution when used at a replacement level of 15%. This specimen produced approximately 0.68 J/g at its peak, which occurred at just over seven hours of age. This specimen also showed a significantly faster rate of reaction than other samples, with a greater slope on both the ascent to and descent from the peak. This resulted in a shift of this curve to the left of the other curves and a full-width half-max (FWHM) peak width of only 6.7 h.

The lowest rate of heat evolution was observed in the 15% silica fume sample, which only produced 0.42 J/g. This sample had a much broader hydration peak, with a FWHM of approximately 13.1 h. These results show that both metakaolins are highly

reactive at very early ages, and illustrate the influence of fineness on reaction rate. These results also indicate that the reactions MK is participating in are highly exothermic.

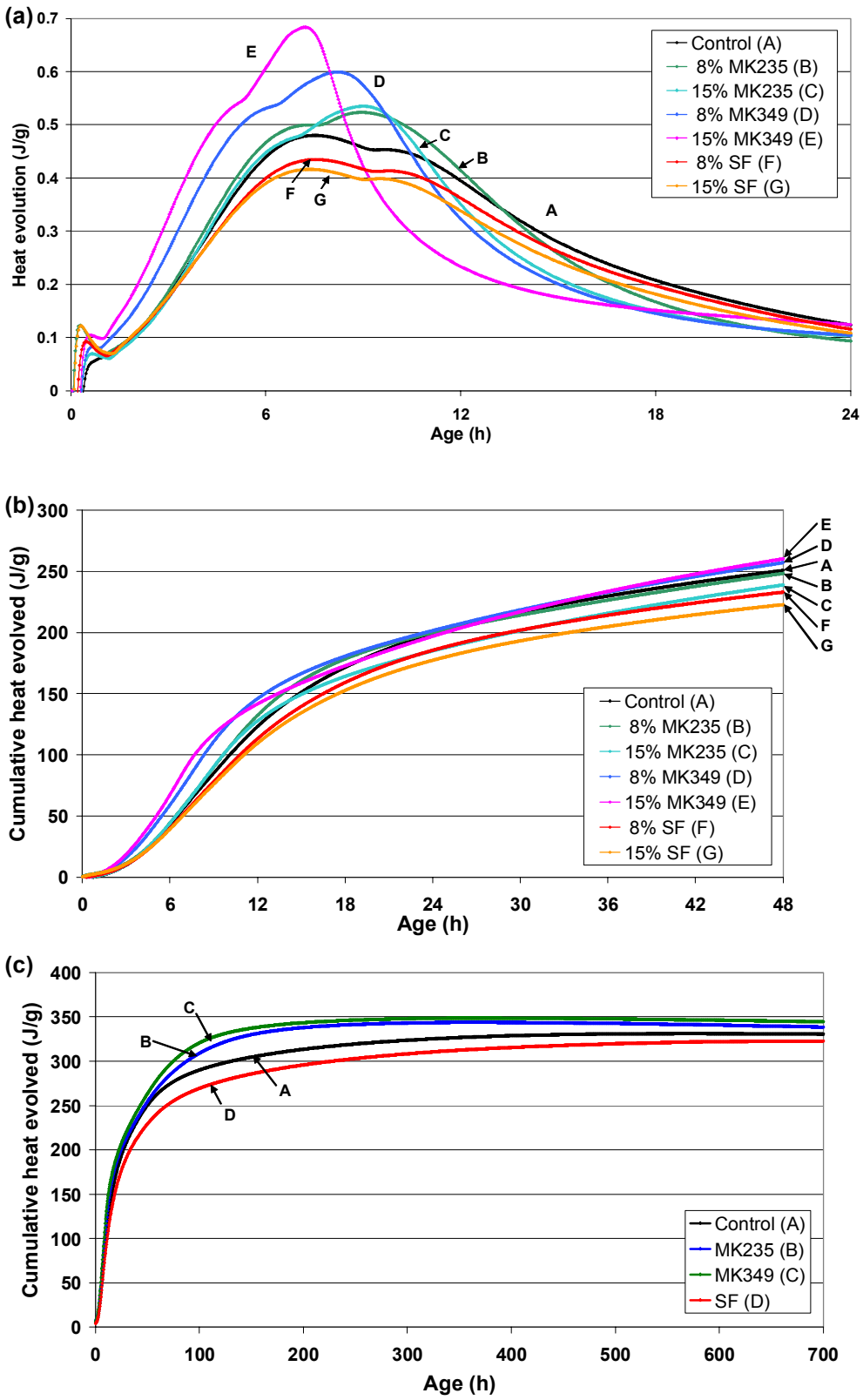

Figure 4.3. Isothermal calorimetry results showing (a) rate of heat evolution, (b) short-term, and (c) 28-day cumulative heat evolved per gram of cementitious material.

4.2.4 Calcium Hydroxide Content

Calcium hydroxide (CH) is a reaction product of C_2S and C_3S hydration. Unlike C-S-H, CH does not make a significant contribution to strength and can be detrimental to concrete durability. Further, CH occupies a large volume in the cement paste and tends to grow in any free space until impeded [Mindess, 2003]. When SCMs containing amorphous silica, like metakaolin or silica fume, are introduced, they react rapidly with newly forming CH compounds to produce supplementary C-S-H. In the case of metakaolin, as described in Chapter 2, various calcium aluminate compounds are also formed. Reduction of CH content is beneficial because more strength-giving material (C-S-H) may be produced and less CH can be leached out or reacted with during chemical attack [Sha, 2001]. Therefore, quantifying the CH content of a sample gives an indication of the progress of the pozzolanic reaction of MK and an approximate prediction of concrete durability. In addition, the relative reactivity of the different MK samples may be compared to one another and to silica fume.

Differential thermal analysis, performed on pastes at varying ages, showed CH decomposition to begin between 390 °C and 450 °C for all mixtures (Figures 4.4 and 4.5). Figure 4.4 is a thermogram of pure, laboratory grade CH, and is provided to illustrate the key parameters examined in DTA analysis. In general, the younger the paste, the earlier this transition began. The decomposition of CH was complete by 460 °C to 550 °C, with younger pastes finishing this transition at lower temperatures (Figures 4.6-4.9). Pastes made with MK349 as partial replacement for cement showed higher onset and ending temperatures than other mixtures, however only slightly.

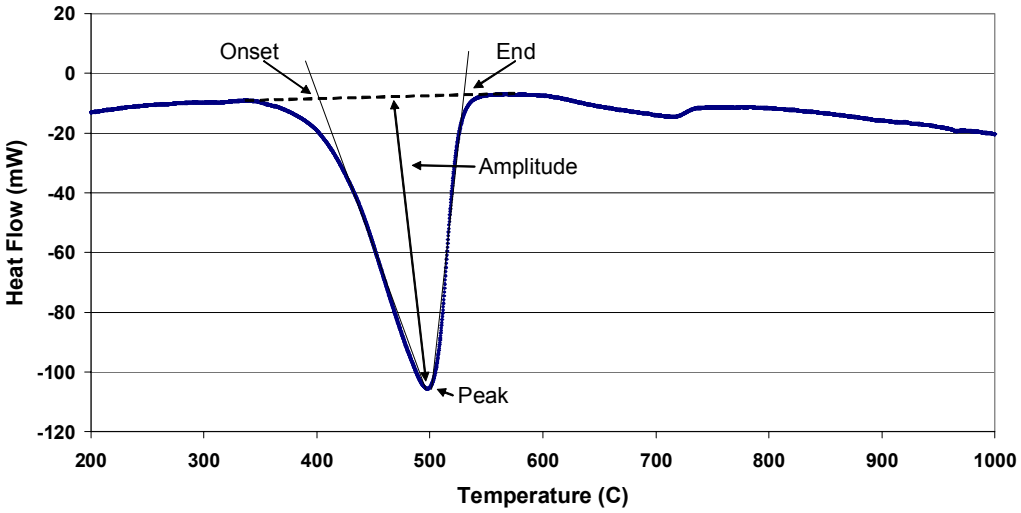

Figure 4.4. DTA thermogram of pure CH.

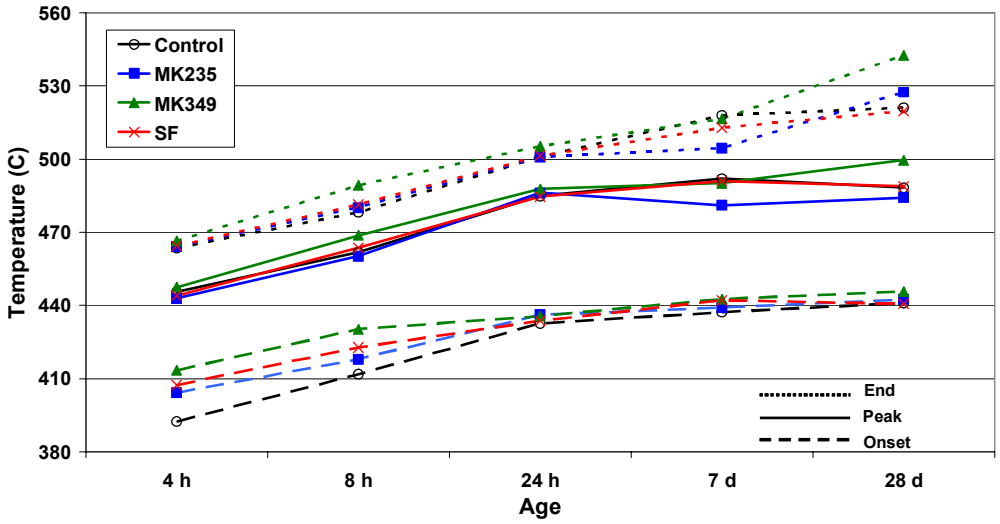

Figure 4.5. DTA onset, peak, and ending temperatures for CH decomposition in pastes at varying ages.

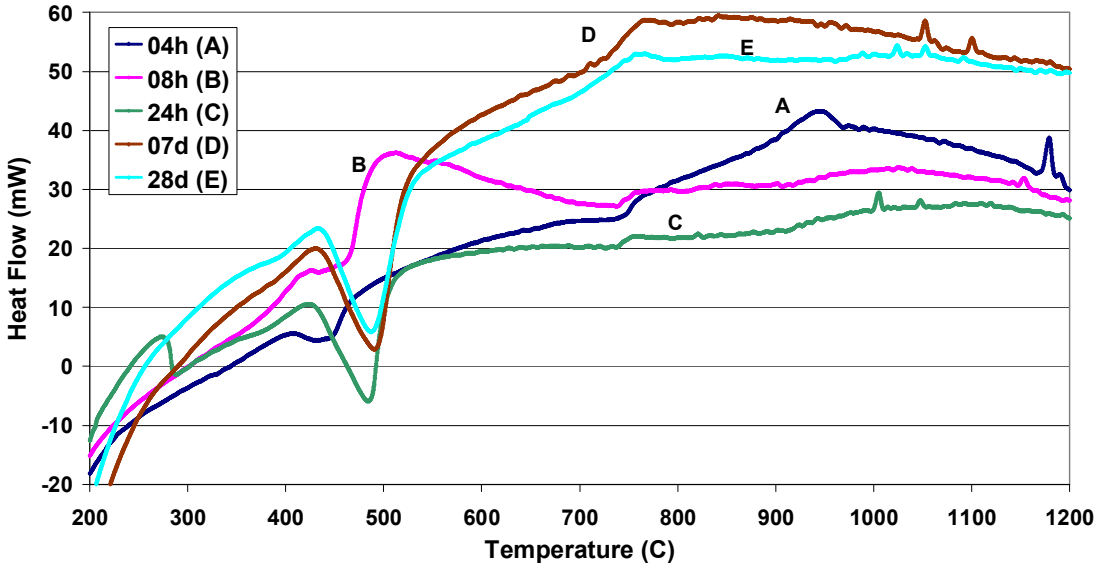

Figure 4.6. DTA thermogram showing heat flow (endotherms down) versus temperature for control specimens at varying ages.

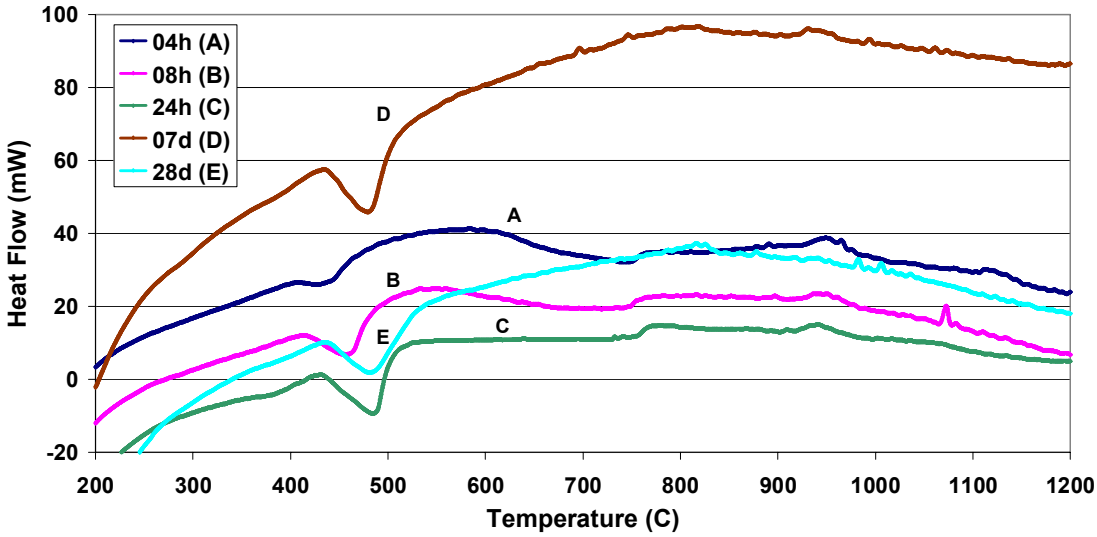

Figure 4.6. DTA thermogram showing heat flow (endotherms down) versus temperature for MK235 specimens at varying ages.

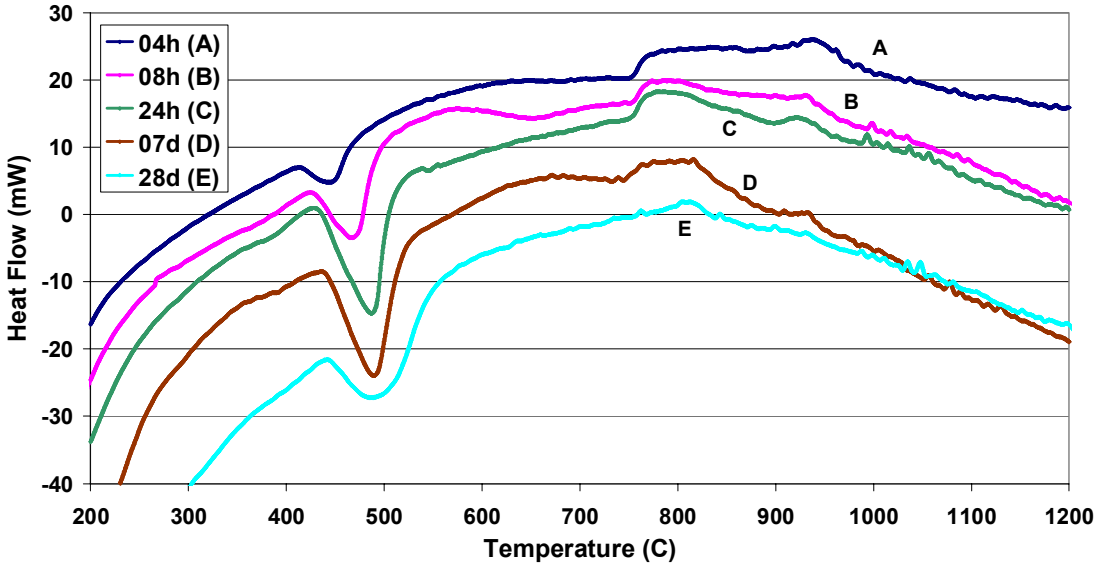

Figure 4.8. DTA thermogram showing heat flow (endotherms down) versus temperature for MK349 specimens at varying ages.

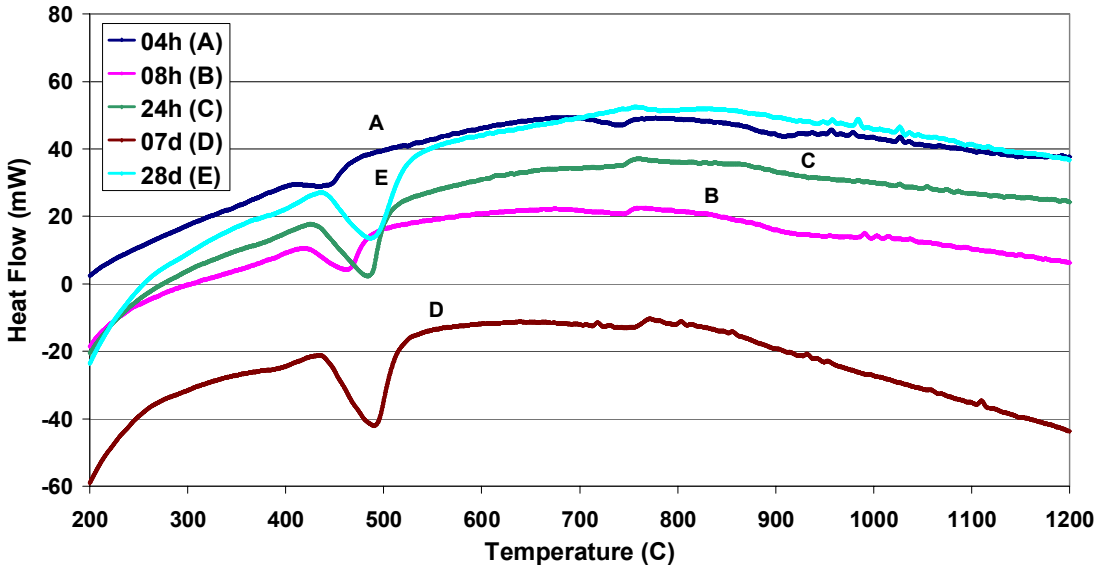

Figure 4.9. DTA thermogram showing heat flow (endotherms down) versus temperature for silica fume specimens at varying ages.

Relative amounts of CH may be determined by comparing DTA peak parameters such as amplitude and area. From Figures 4.10-4.12, it appears that CH content increased

up to 7 d in all samples, but remained fairly constant from 7 d to 28 d in the control and SF samples. In both MK samples, CH content decreased significantly, showing a much less pronounced peak at 28 d than at 7 d. Table 4.3 presents a comparison of peak amplitudes, areas, and enthalpies, determined using Perkin Elmer's Pyris Series software, for the various mixtures at 24 h, 7 d, and 28 d.

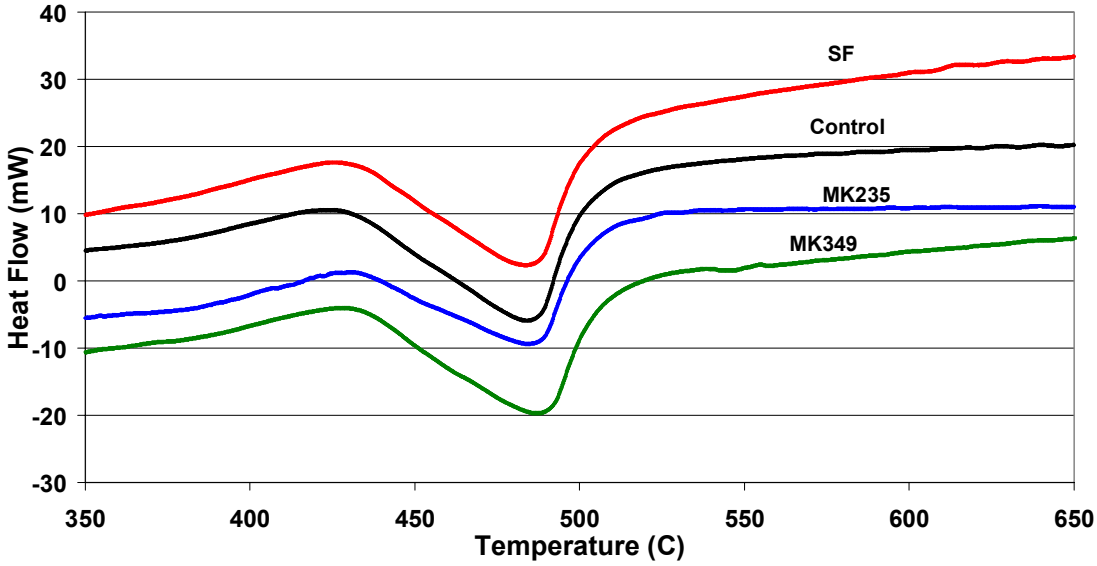

Figure 4.10. DTA thermogram showing CH decompostion peak at 24 h of age.

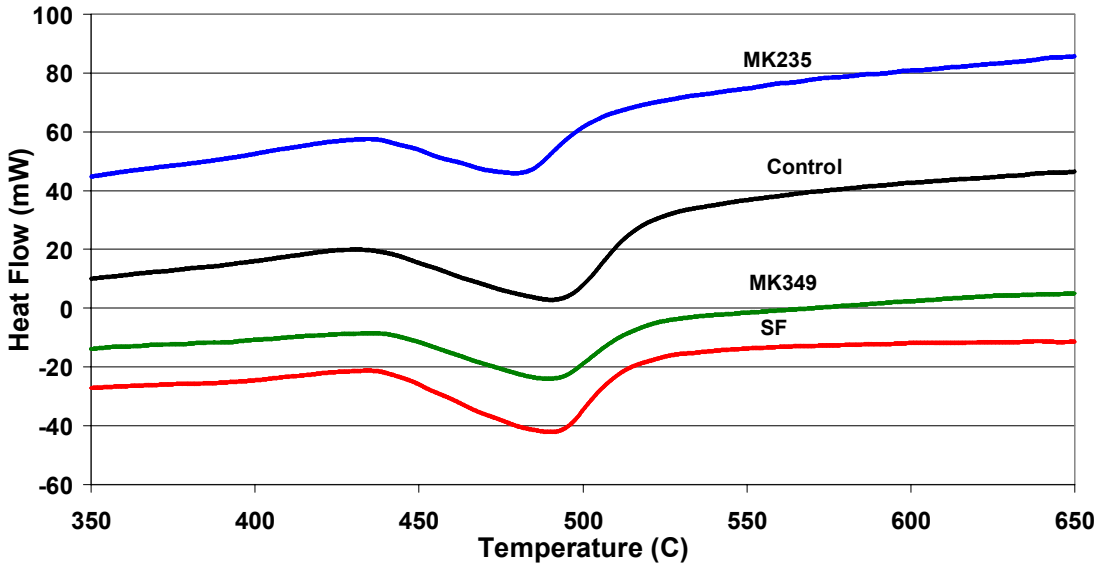

Figure 4.11. DTA thermogram showing CH decomposition peak at 7 d of age.

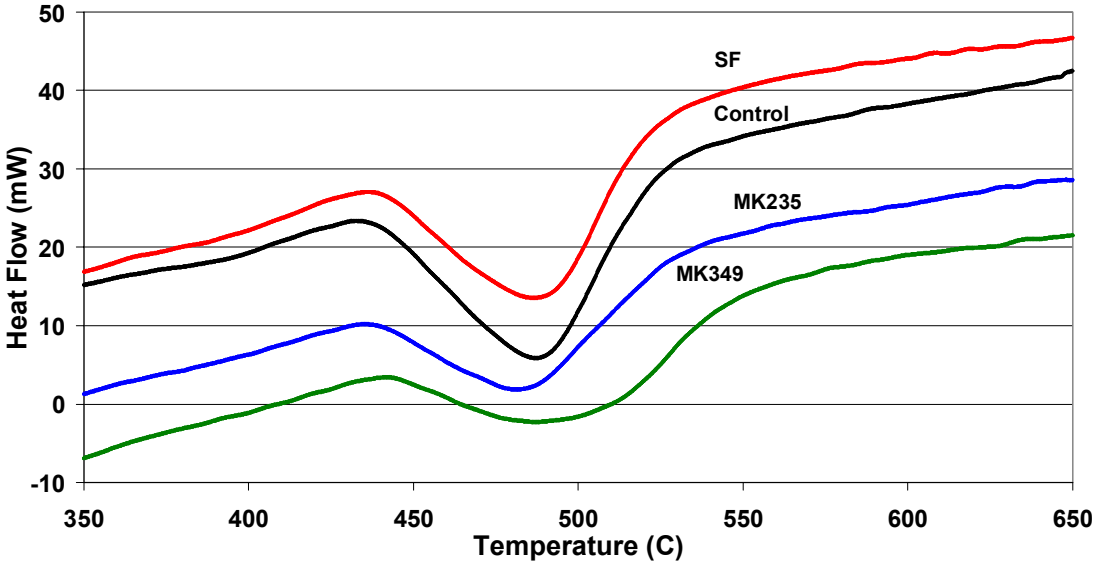

Figure 4.12. DTA thermogram showing CH decomposition peak at 28 d of age.

Table 4.3. DTA peak amplitudes, areas, and enthalpies.

	Age	Onset	Peak	End	Height	Area	Enthalpy
		°C	°C	°C	mW	mJ	J/g
Control	**4 h**	392.38	445.63	463.56	4.89	1101.85	20.79
	8 h	411.81	461.73	478.16	9.03	1901.27	35.47
	24 h	432.61	484.82	500.97	20.06	4920.88	92.85
	7 d	437.23	491.97	517.94	26.26	7452.14	135.49
	28 d	441.05	488.29	521.12	22.59	6526.72	122.22
MK235	**4 h**	404.16	442.83	464.10	4.08	858.70	15.87
	8 h	417.94	460.17	480.21	10.63	2517.56	46.54
	24 h	436.15	486.17	500.89	15.58	3594.30	67.69
	7 d	439.14	481.04	504.51	18.85	4497.80	83.91
	28 d	442.46	484.23	527.44	13.34	4033.48	75.53
MK349	**4 h**	413.36	447.44	466.45	5.09	1037.70	19.43
	8 h	430.28	468.71	489.29	11.50	2576.47	48.07
	24 h	435.67	487.79	505.25	18.82	4790.45	88.55
	7 d	442.64	490.14	516.59	18.78	4912.45	91.48
	28 d	445.79	499.52	542.56	11.33	4345.01	79.87
SF	**4 h**	407.30	444.06	464.37	3.99	831.26	15.39
	8 h	422.72	463.63	481.40	9.60	2059.56	38.00
	24 h	433.70	484.66	501.38	19.70	4864.90	89.59
	7 d	442.09	491.04	512.87	24.38	6217.37	116.00
	28 d	440.69	488.78	519.69	19.93	5695.61	106.06

Although DTA testing was performed primarily to determine the ranges where CH decomposition occurred (to be used with TGA) and for relative visual comparison of peak geometries, it is possible to quantify this data since the same amount of starting material (± 1 mg) was used for all tests. The area of a DTA peak, divided by the sample starting mass, is equivalent to the enthalpy associated with the phase transition. Thus, by comparing calculated enthalpies with the enthalpy of the same mass of pure CH, the CH content of these samples may be determined. This technique is used primarily with DSC, which gives a more accurate measure of enthalpy, but may be applied to DTA data to determine relative amounts of compounds present [Sha, 2001].

The enthalpy of decomposition for 54 mg of CH was found to be approximately 1520 J/g by DTA. It has been reported as 103 kJ/mol, or 1390 J/g [Taylor, 1997]. Masses of approximately 27 mg and 13.5 mg of pure CH were also run (Table 4.4). There was good agreement between the measured enthalpy values, and peak amplitude and area scaled fairly linearly with CH mass, indicating that this is a reasonable, though perhaps not exceptionally accurate, means of comparison. The CH contents of the pastes examined in this study are shown in Figures 4.13 and 4.14. Figure 4.13, calculated based on enthalpy, gives the most accurate measure of CH content. Figure 4.14, calculated based on peak amplitude, is provided for comparative purposes.

From this, it is clear that incorporation with MK reduces CH content of cement pastes, as expected. CH is produced by hydration of calcium silicate compounds, which forms the first node in the peak of the heat of hydration curve (Figure 4.3a) between six and ten hours. The majority of the CH in an HCP system is produced during this

acceleration period. Hydration continues indefinitely, at a much slower, diffusion-controlled rate, but is generally over 90% complete by 28 days of age.

In the case of the control and SF specimens, the C_2S and C_3S hydration reactions continued to produce a significant amount of CH between 1 and 28 days of age. In the MK specimens, however, there was only a slight increase in CH content between 1 and 7 days age, followed by a decrease between 7 and 28 days. By the end of the testing period, both MK pastes had CH contents of around 5%, versus 7% for SF and 8% for the control. This is a good indication that the pozzolanic reaction of MK continues beyond 14 days, unlike what has been reported in the literature [Wild, 1996], and that this reaction is consuming CH at a rate equal to or faster than the rate of CH production by calcium silicate hydration. Interestingly, CH content of both MK samples was higher than that of control and SF samples at 8 h of age. Beyond 8 h, CH content of MK pastes was always lower than in control or SF pastes. This indicates that the large peak observed in isothermal calorimtery curves around 8 h hydration (Figure 4.3a) does not correspond to the consumption of CH by MK, but is likely related to acceleration of C_3A hydration in the presence of MK.

Table 4.4. DTA key parameters for decomposition of pure CH.

Mass	**Onset**	**Peak**	**End**	**Height**	**Area**	**Enthalpy**
mg	**°C**	**°C**	**°C**	**mW**	**mJ**	**J/g**
54.2	438.76	522.15	551.04	198.22	82145.06	**1515.59**
27.6	412.65	497.65	523.35	97.86	40768.43	**1477.12**
12.8	400.14	474.74	495.53	54.46	20037.33	**1565.42**
					μ =	**1519.38**
					σ =	**44.27**

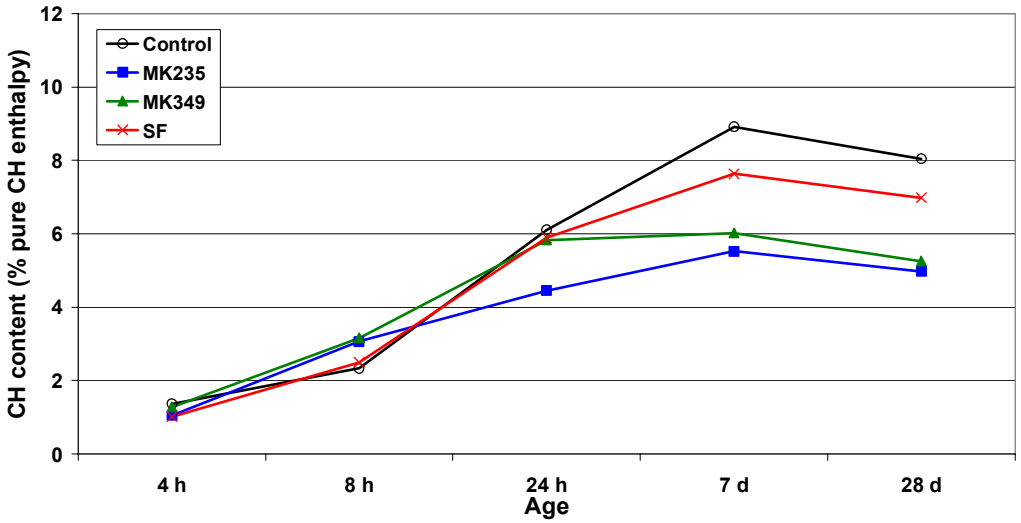

Figure 4.13. CH content of pastes, calculated from enthalpy, as measured by DTA.

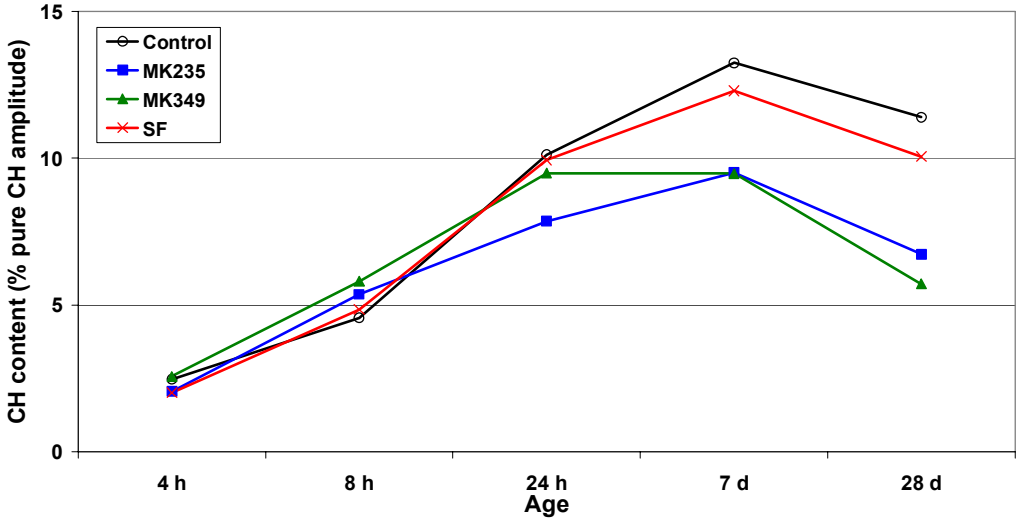

Figure 4.14. CH content of pastes, calculated from peak amplitude, as measured by DTA.

Results from thermogravimetric analyses are presented in Figure 4.15 and 4.16. CH contents are shown as percentages and were calculated as the mass loss due to CH decomposition relative to the ignited cement weight (4.15) and relative to the total mass

loss between 25 °C and 900 °C (4.16). Each figure contains three determinations of mass loss due to CH decomposition. These were calculated as follows:

(a) calculated based on the temperatures found through DTA: for 4 h and 8 h samples, a range of 400-480 °C was used; for 1-28 d samples, a range of 430-530 °C was used;

(b) calculated to include full DTA temperature range (400-530 °C) for samples of all ages;

(c) calculated, for all ages, as the mass loss in the temperature range 400-750 °C, which includes $CaCO_3$ decomposition (CH becomes $CaCO_3$ in the presence of carbon in the atmosphere).

These analyses yielded CH contents similar to the DTA calculations, and show the same general trend: blending with MK decreases CH content of pastes relative to controls, but not until at least 24 h of age. CH content decreased more rapidly in MK349 pastes than in MK235 pastes, though MK235 specimens generally showed the least CH by 28 days age. This indicates that the finer nature of MK349 allows it to initially react faster with CH, but that MK235 is equally or more effective at consuming CH overall. As with DTA testing, pastes made with silica fume as partial replacement for cement typically showed less CH than controls, but more than MK pastes. This confirms that SF has pozzolanic reactivity, but a slower reaction rate than either of the MKs.

The CH contents found through DTA and TGA analysis were slightly lower than what has been reported in the literature [Poon, 2001; Wild, 1997], but show the same trend, with both MK and SF serving to decrease CH content relative to controls. This discrepancy in values is likely due to the different nature of sample preparation necessary

for such young pastes. Most TGA studies examined pastes ranging from three to 90 days that were dried prior to testing. Because complete drying of a paste sample, whether by solvent exchange, vacuum, oven, or a combination of these, takes 7-14 days for completion [Juenger, 2001], this was not possible in the current study. As such, pastes contained varying amounts of free and bound water depending on their age, which resulted in varying amounts of cementitious material comprising their starting masses. TGA results were normalized based on ignited cement weight, yielding lower values than were expected.

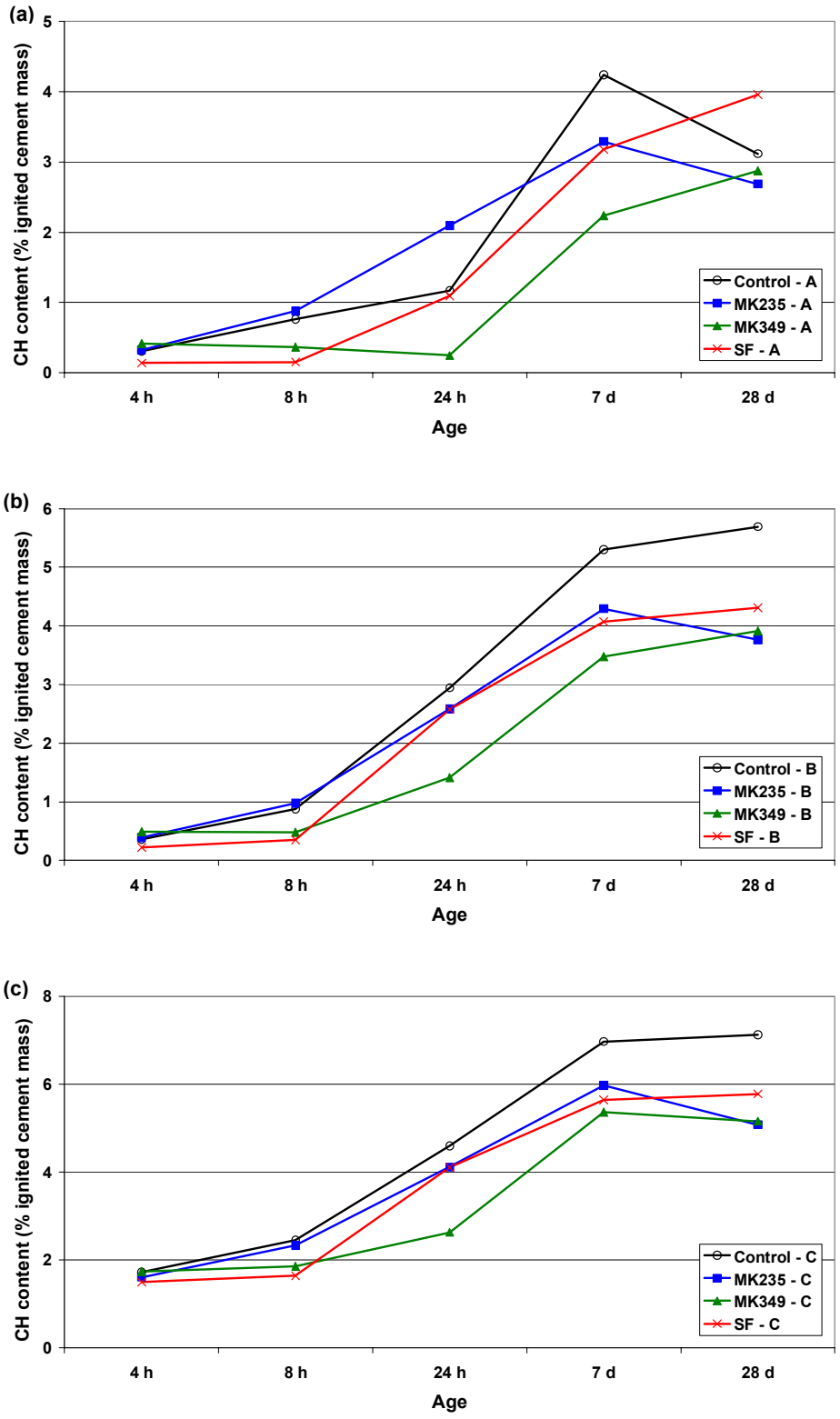

Figure 4.15. CH content calculated relative to ignited cement mass for (a) specific decomposition temperature range, (b) full range (400 °C - 530 °C), and (c) CH and $CaCO_3$ decomposition (400 °C - 750 °C).

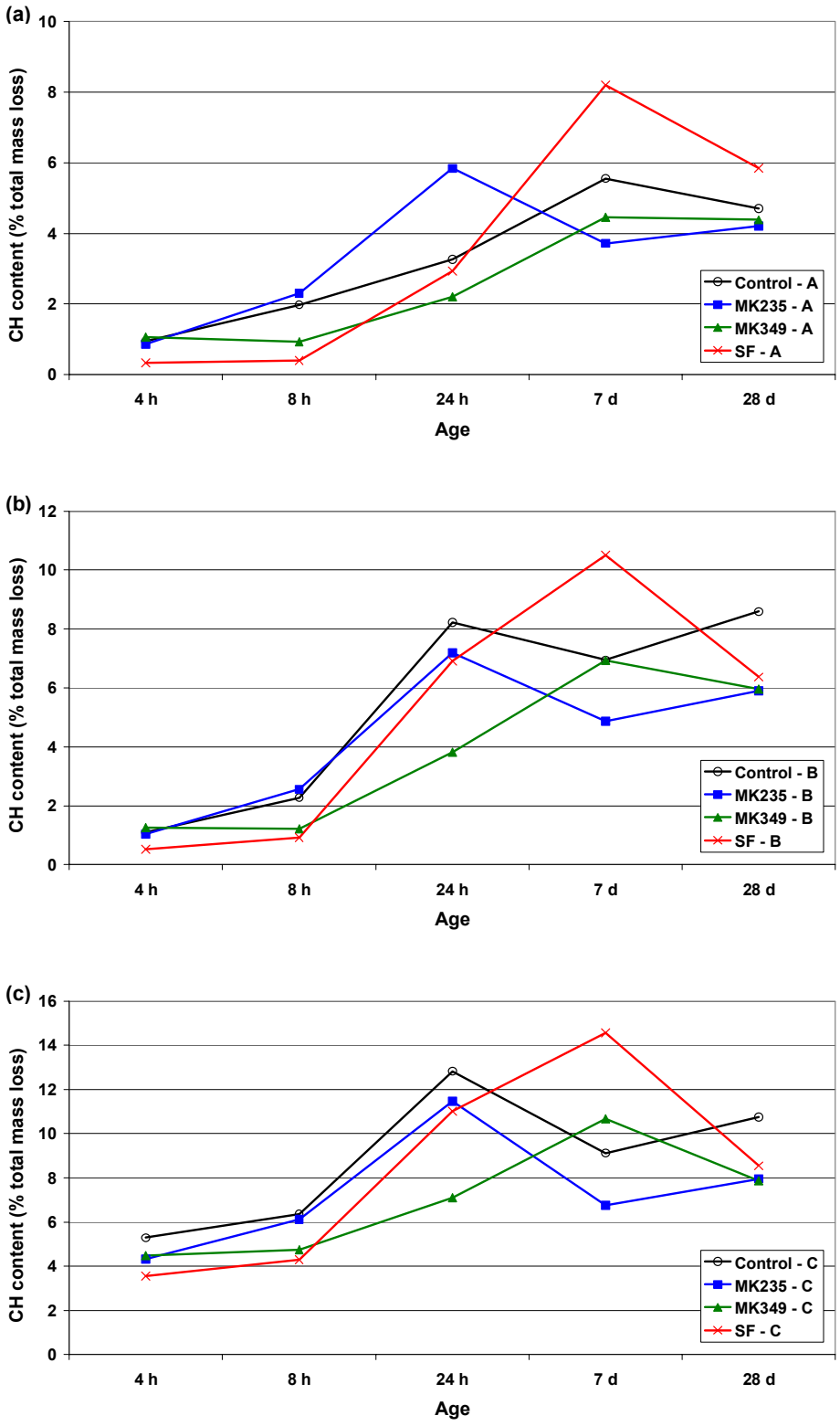

Figure 4.16. CH content calculated relative to total mass loss for (a) specific decomposition temperature range, (b) full range (400 °C - 530 °C), and (c) CH and $CaCO_3$ decomposition (400 °C - 750 °C).

4.3 Shrinkage

4.3.1 Chemical Shrinkage

Chemical shrinkage is a result of the volume difference between reactants and products in a hydrating cement system. As hydration proceeds, the volume occupied by the products is smaller than that of the reactants. Thus, unless additional water is supplied from an external source, this chemical shrinkage will result in the formation of empty pores within the cement paste microstructure of hardened systems [Bentz, 1999].

Pastes containing metakaolin showed greater chemical shrinkage than controls or silica fume pastes, with the MK235 paste showing the most chemical shrinkage -- approximately 8.5 mL/100 g at 28 days of curing (Figure 4.17). The MK349 paste was expected to show the greatest chemical shrinkage because of its high surface area and faster hydration reaction rate observed in isothermal calorimetry; the lower chemical shrinkage as compared to the coarser MK235 paste could be related to morphology and stacking behavior, but further investigation is necessary to isolate the potential causes for these observations. Wild *et al.* [Wild, 1998] also found chemical shrinkage to increase due to MK replacement, reaching a maximum between 10 and 15% replacement.

At 28 days, control samples had experienced the least chemical shrinkage: approximately 4 mL/100 g at 28 days. However, around seven weeks, silica fume samples actually started to expand, and continued to do so for the duration of the four-month testing period, such that they showed the least overall chemical shrinkage. This expansion is likely due to ASR involving silica fume agglomerations.

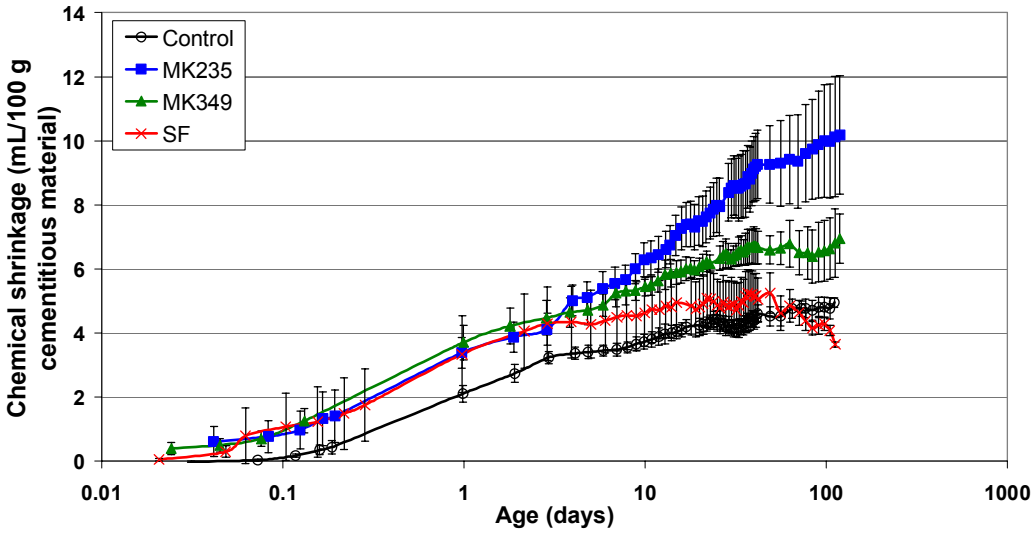

Figure 4.17. Chemical shrinkage of cement paste at w/cm=0.40, 8% replacement.

4.3.2 Autogenous Shrinkage

Autogenous shrinkage, which occurs due to the lowering of cement paste internal relative humidity and is related to capillary porosity, increased with the addition of metakaolin. Both metakaolin samples experienced greater autogenous shrinkage than controls, with MK349 pastes showing the most shrinkage (-2100×10^{-6} strain at 28 days). This was as expected. The acceleration of the hydration reaction and the pozzolanic reaction of MK will escalate self-desiccation, and due to the finer pore structure of the MK pastes, this self-desiccation should induce greater autogenous shrinkage [Brooks, 2001].

Because MK349 has a very fine particle size and the most pronounced accelerating effect on paste hydration, this result makes sense. However, since autogenous shrinkage has been shown to be related to chemical shrinkage (the empty porosity created after final set leads to a reduction in internal relative humidity and a measurable autogenous shrinkage of the material [Bentz, 1999]), the autogenous

shrinkage would have been expected to be greater in the MK235 sample, which showed the greatest chemcial shrinkage. In fact, the measured autogenous shrinkage value for MK235 was significantly lower than for MK349: -750 v. -2100 × 10^{-6} strain (mm/mm × 10^{-6}). Values were -200 and +200 × 10^{-6} strain for the silica fume and control pastes, respectively, as shown in Figure 4.18.

These results disagree with Brooks *et al.*'s [Brooks, 2001] finding that MK replacement decreased autogenous shrinkage within the first 24 h of curing, although Brooks did find MK to increase long-term autogenous shrinkage. Wild *et al.* and Kinuthia *et al.* [Wild, 1998; Kinuthia, 2000] both also found autogenous shrinkage to increase, reaching a maximum at approximately 10% replacement with MK. This indicates that the values obtained here, at 8% replacement, can be taken as an approximate worst case scenario (i.e. this replacement level yields the highest autogenous shrinkage that would be observed due to incorporation with these MKs). Additionally, our results correspond to setting times found at a constant w/cm. That is, pastes experiencing greater autogenous shrinkage have shorter times to initial and final set.

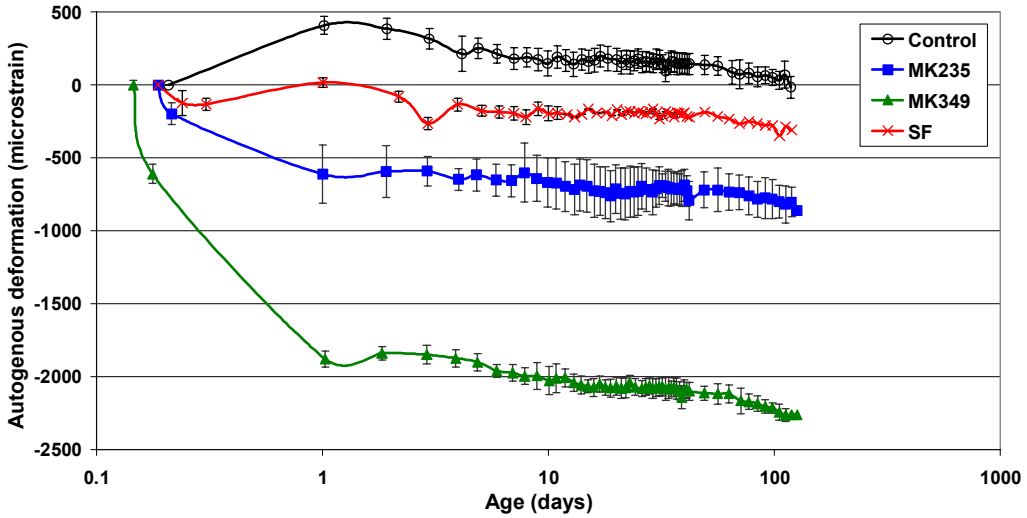

Figure 4.18. Autogenous deformation of cement paste at w/cm=0.40, 8% replacement.

4.3.3 Free Shrinkage

Metakaolin incorporation had varying effects on free shrinkage (Figures 4.19 and 4.20). Mortar bars made with MK235 shrank approximately 0.053% during the first two weeks of controlled drying. Overall, these samples showed the least bulk shrinkage over the duration of the six-week testing period. Mortars made with silica fume experienced the most shrinkage. Change in mass was also measured on the same mortar samples, and mass loss (Figure 4.19b) followed the same trend as shrinkage. That is, samples that shrank the most also generally lost the most mass during the testing period.

Concrete prisms made with MK235 also showed the least bulk shrinkage and the least mass loss during the first six weeks of drying, while prisms incorporating silica fume experienced the most shrinkage and mass loss (Figure 4.20). The reduction in free shrinkage can be attributed to a lower amount of evaporable water, as hydration and pozzolanic reaction in MK mortars and concretes consumed a significant amount of the free water. This is supported by the lower mass loss observed in MK specimens relative to other mixtures. Both Caldarone *et al.* [Caldarone, 1994] and Ding and Li [Ding, 2002] also found replacement with MK to decrease free shrinkage relative to controls.

In summary, metakaolin replacement resulted in increased chemical and autogenous shrinkage, but reduced free shrinkage. Brooks *et al.* [Brooks, 2001] reported the same finding. This suggests that MK mortars and concretes have a lower porosity and finer pore structure, which encourages loss of water by self-dessication rather than by diffusion to the outside environment. These results show that even significant increases in chemical and autogenous shrinkage may not be detrimental, as they do not lead to increases in free shrinkage beyond 24 h as measured by standard tests.

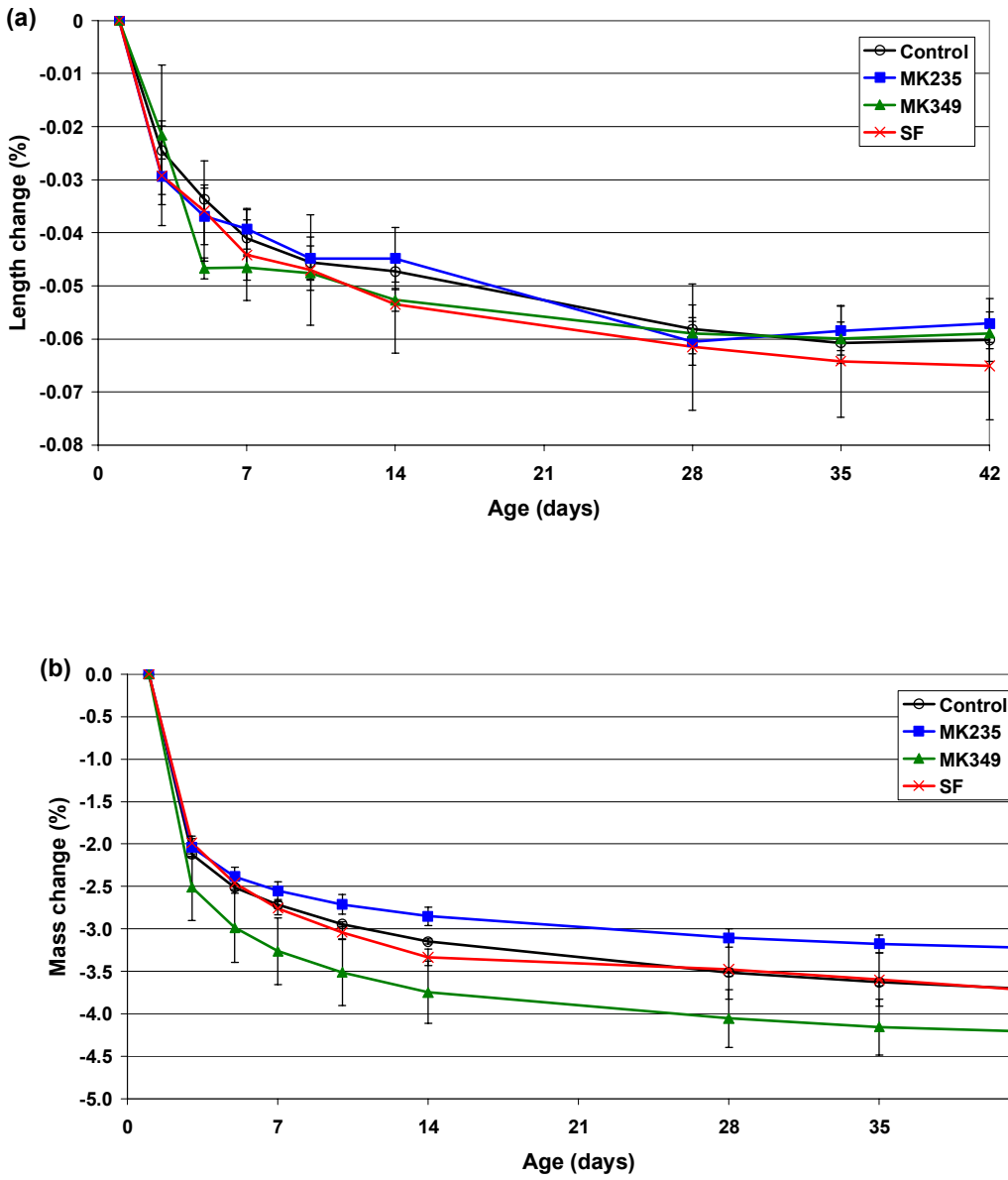

Figure 4.19. Free shrinkage of mortar prisms at w/cm=0.40, 8% replacement: (a) length change and (b) mass change.

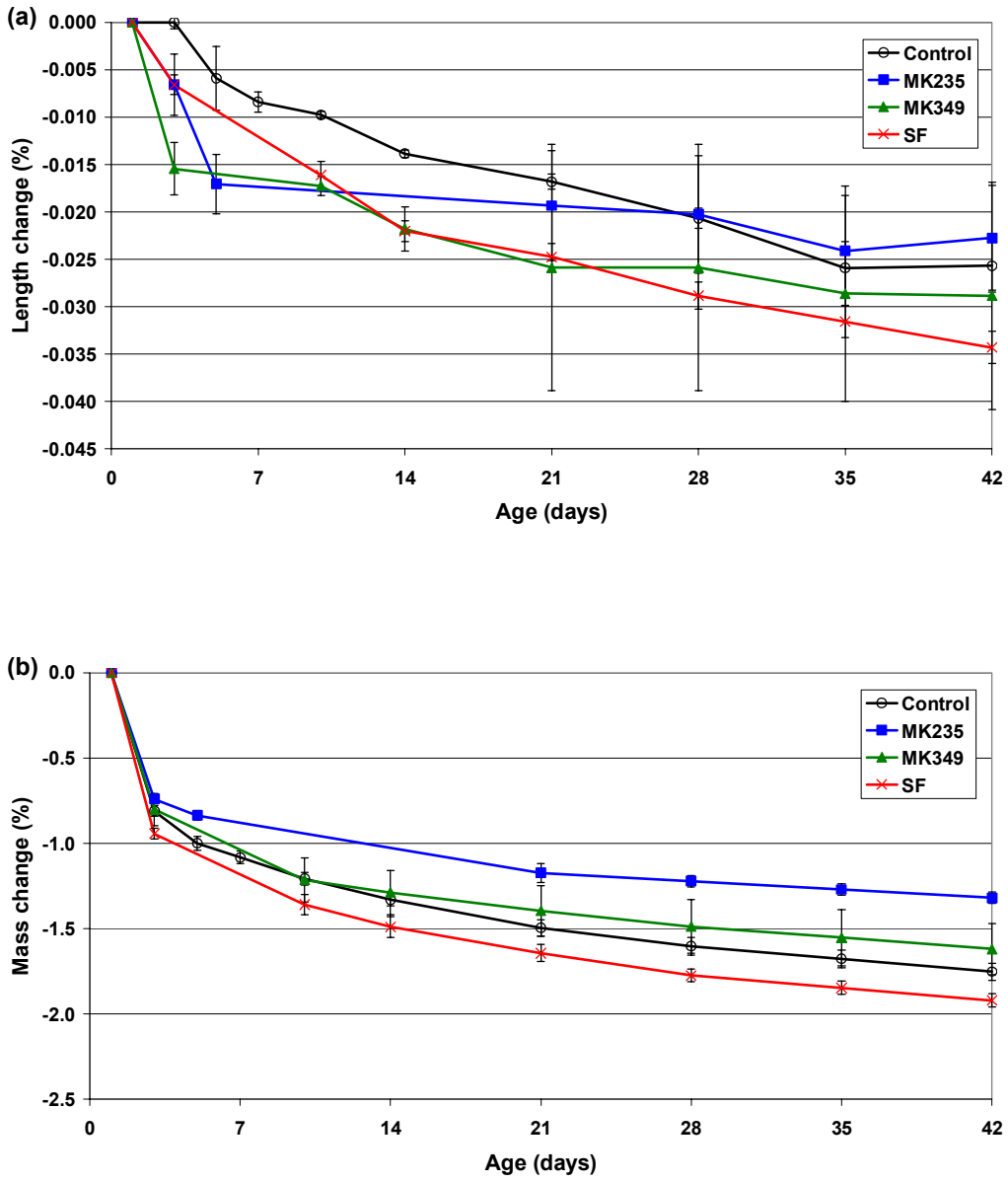

Figure 4.20. Free shrinkage of concrete prisms at w/cm=0.40, 8% replacement: (a) length change and (b) mass change.

4.3.4 Porosity

Nitrogen adsorption was used to measure BET specific surface area, total porosity, and pore size distribution. Samples tested at one day of age did not show significant differences in these quantities, though both pastes containing metakaolin showed slightly higher surface areas and total porosities than control and silica fume pastes (Figures 4.21 and 4.22). At 28 days, all samples examined showed increases in total porosity. The control and MK349 pastes also showed an increase in surface area, while the MK235 paste showed a decrease. Tests on silica fume pastes at 28 days age could not be performed due to problems with the instrument.

In terms of pore size distribution, samples containing MK actually showed a relatively greater amount of large pores and smaller amount of fine pores than other samples at one day of age (Figure 4.23a). By 28 days, however (Figure 4.23b), MK pastes showed a much greater proportion of pores smaller than 10 nm in diameter. MK349 pastes had 63% of their porosity in these very fine pores, as compared to 57% and 43% for the MK235 and control pastes, respectively. This is likely due to an infilling of porosity and a greater amount of C-S-H being produced by the pozzolanic reaction of MK, leading to a greater number of very small pores. Based on setting time (Figure 4.2) and shrinkage data (Figures 4.17 and 4.18), the silica fume pastes would have been expected to fall in between, showing more fine porosity than controls but less than MK pastes. Similar findings were reported in the literature [Khatib, 1996].

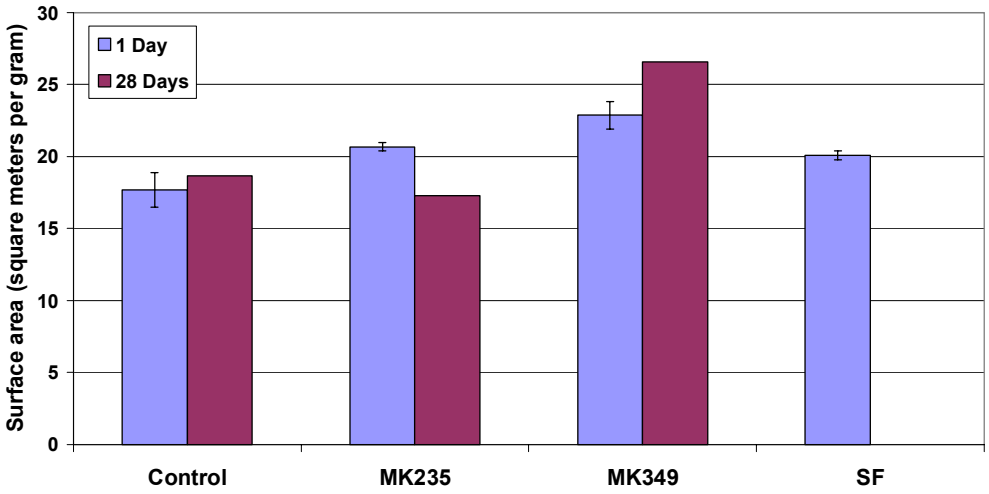

Figure 4.21. BET specific surface area of cement pastes containing 8% SCMs.

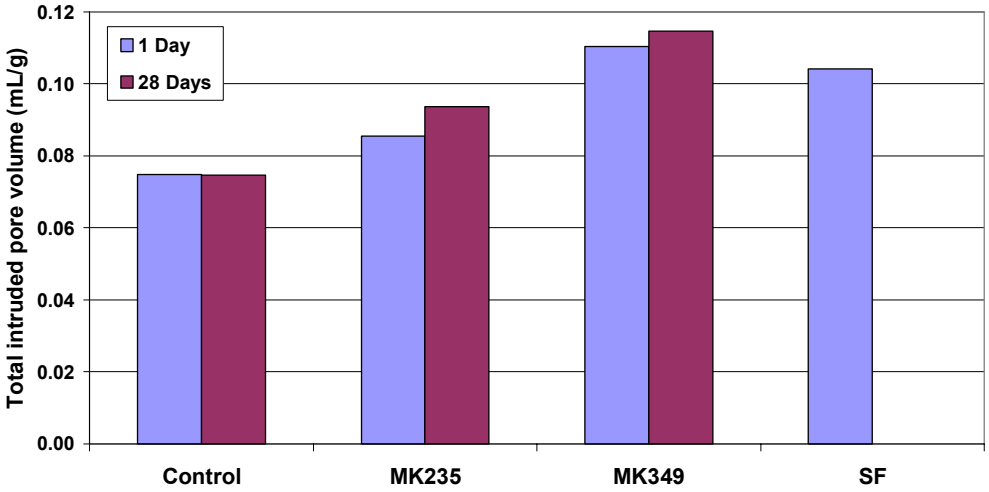

Figure 4.22. Total porosity of cement pastes containing 8% SCMs.

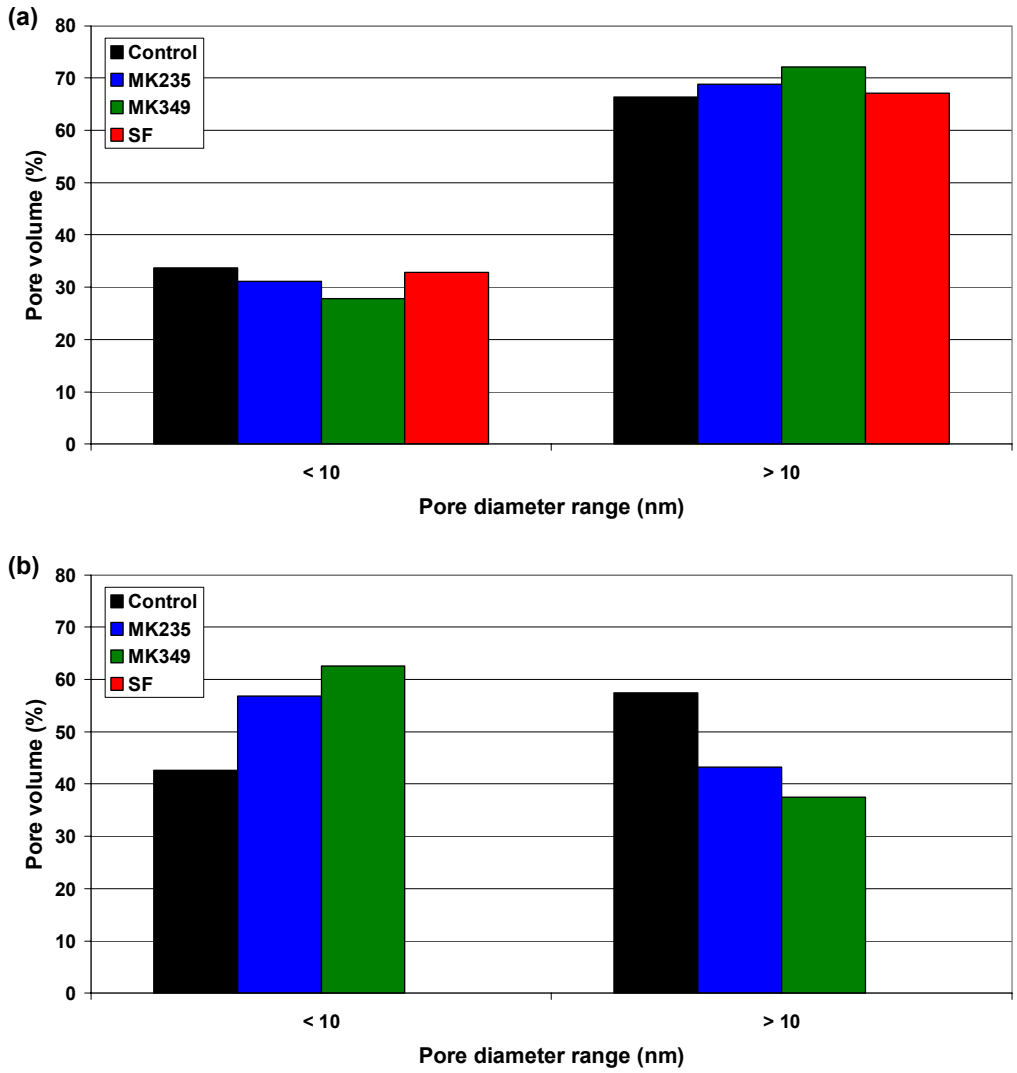

Figure 4.23. Pore size distribution of cement pastes containing 8% SCMs at (a) one day and (b) 28 days age.

4.4 Mechanical Properties

4.4.1 Compressive Strength

A significant increase in compressive strength as compared to the ordinary concrete controls was observed for both metakaolin samples at 8% replacement for cement, with the finer MK349 having a more pronounced effect, particularly at the lower w/cm and generally at later ages (i.e., seven days or more). For all mixtures, the

compressive strength increased with decreasing w/cm, as expected. The maximum compressive strength observed was nearly 11,000 psi (75 MPa), which occurred in the MK349 concrete with w/cm=0.40 at 28 days. Strength increases due to MK349 fineness were less apparent at higher w/cm likely because ample water was available for hydration and particle surface area became less critical. These results are shown in Figure 4.24. An increase in the rate of strength gain for the MK349 was apparent after three days at a w/cm of 0.40 and after seven days at 0.50 (Figure 4.25).

For the w/cm=0.40 concretes, MK349 produced strength increases of 30-50% over controls at the same ages (Table 4.5). MK235 concretes exhibited compressive strengths that were 15-30% greater than controls at this water content across all ages. These represent increases of approximately 280% and 220%, respectively, over the one-day control strength, as compared to an increase of only 150% in the control specimens by 90 days age. These results confirm what has been reported in the literature: MK produces significant (e.g. 15-50% as compared to controls in this study) compressive strength increases in concrete (Table 4.6).

Wild *et al.* suggested that there are three elementary factors influencing the contribution that MK makes to strength when it partially replaces cement in concrete [Wild, 1996]. These are the filler effect, the acceleration of PC hydration, and the pozzolanic reaction of MK with CH. According to Wild *et al.*, the filler effect, which results in more efficient paste packing, is immediate, the acceleration of PC hydration has maximum impact within the first 24 hours, and the pozzolanic reaction makes the greatest contribution to strength somewhere between 7 and 14 days of age. Based on this, it follows that the finer MK349 should have a greater strength-enhancing effect than the

coarser MK235. Its finer particle size would lead to a better packing and filling capacity at the aggregate/paste interface, and the increased surface area of the finer material should cause a greater acceleration of PC hydration and a faster pozzolanic reaction rate.

This is supported by the correlation between our measured heat of hydration and compressive strength data. The increased cumulative heat and rate of heat evolution observed corresponds to increased strength and an enhanced rate of strength gain in the MK349 specimens. This acceleration effect is illustrated by the rate of compressive strength gain plots in Figure 4.25. Here, particularly at a w/cm of 0.40, MK349 concretes gain strength most rapidly, exhibiting approximately 150% of the one-day control strength by just three days age. By contrast, the control specimens did not show a 150% increase in strength until 28-90 days age. This confirms that the increased heat evolved during hydration of the MK349 mixtures corresponds to increased compressive strength, and suggests an enhanced rate of production of strength-giving aluminate compounds at very early ages.

Silica fume addition resulted in concrete of strength comparable to the control mixtures, which was unexpected. As a result, all of the mixtures containing silica fume were recast using a new supply of the material; however, results from this second round of testing were similar, although higher early strength was apparent at lower w/cm. As shown in Figure 4.24, results were inconsistent across the three w/cm, but generally strength did not develop until later ages. The cause(s) for these lower-than-anticipated strengths with silica fume concrete are not clear, but similar results have recently been reported in the metro-Atlanta region [Wolfe, 2004] and in the literature [Curcio, 1998; Poon, 2001]. Agglomerations were not readily apparent when examining these samples

by optical microscopy, thus it is assumed that adequate silica fume dispersion was achieved in these mixtures.

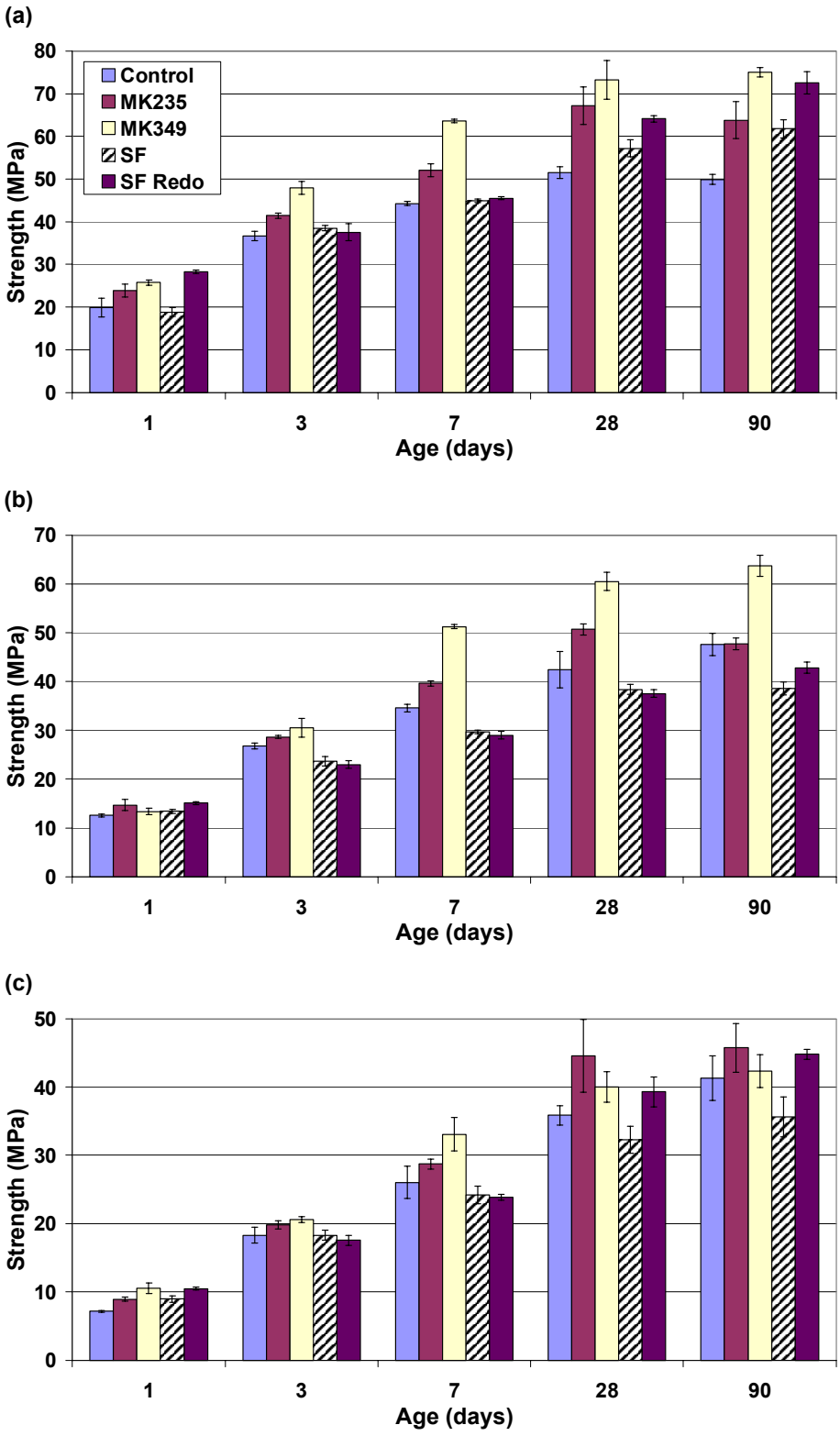

Figure 4.24. Average peak compressive strength versus concrete age for (a) w/cm=0.40, (b) w/cm=0.50, and (c) w/cm=0.60.

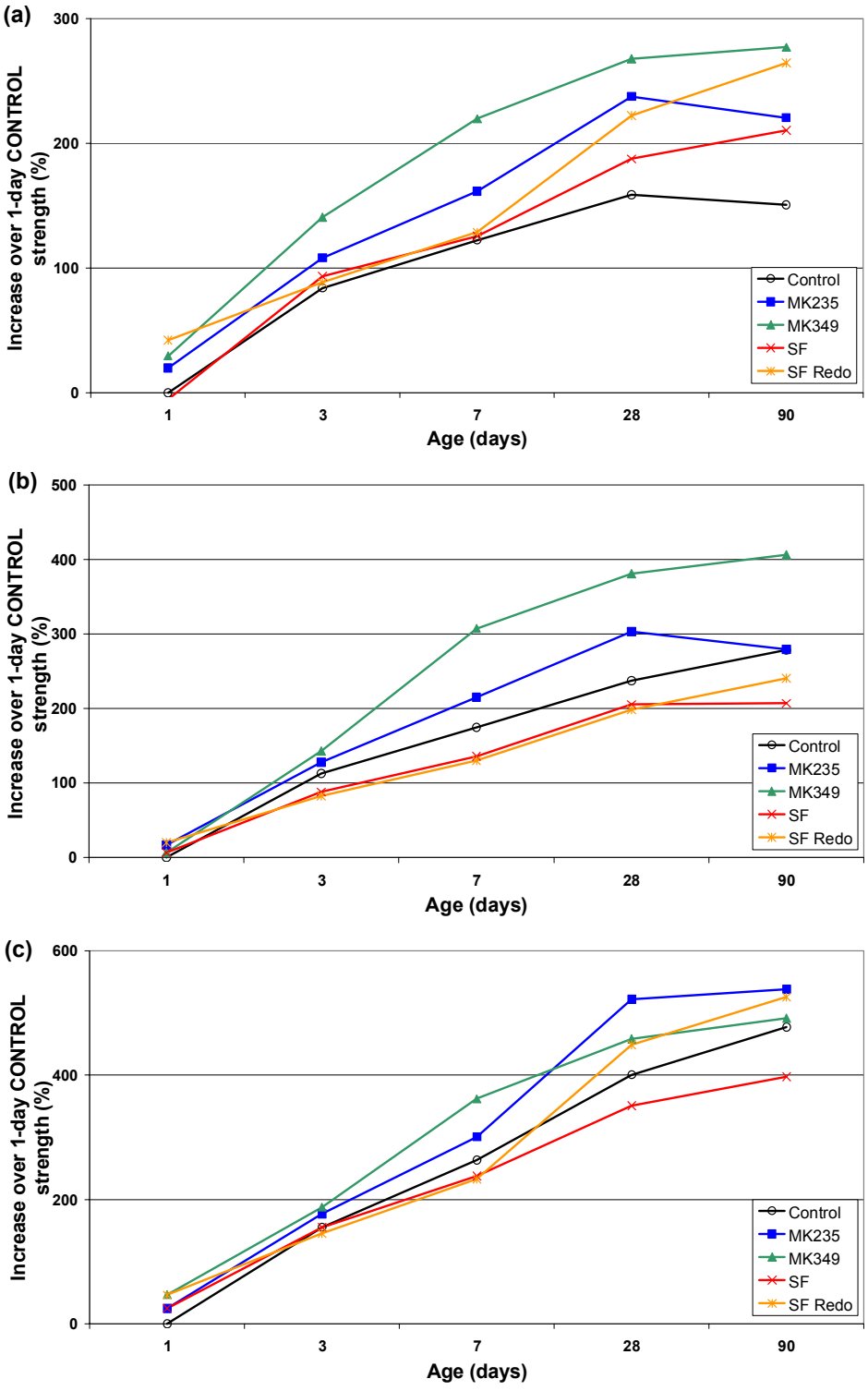

Figure 4.25. Rate of compressive strength development, shown as a percent increase over 1-day control strengths for (a) w/cm=0.40, (b) w/cm=0.50, and (c) w/cm=0.60.

Table 4.5. Compressive strength gain for w/cm=0.40 MK-concretes.

Age (Days)	Increase over MK235 1-day strength (%)	Increase over Control 1-day strength (%)	Increase over Control strength, same age (%)
1	0.0	19.9	19.9
3	73.7	108.2	13.2
7	118.1	161.5	17.6
28	181.5	237.5	30.5
90	167.3	220.5	27.9
Age (Days)	**Increase over MK349 1-day strength (%)**	**Increase over Control 1-day strength (%)**	**Increase over Control strength, same age (%)**
1	0.0	29.6	29.6
3	85.7	140.6	30.8
7	146.6	219.6	43.7
28	183.8	267.8	42.2
90	190.9	277.0	50.4

Table 4.6. Increases in compressive strength (f'c) over controls due to partial replacement with metakolin, as reported/measured at 28 days age.

Author/Material	w/cm	% Replacement	% f'c Increase over Control
Caldarone et al. (1994)	0.40	10	54
Curcio et al. (1998)	0.33	10	17
Ding & Li (2002)	0.35	10	28
Qian et al. (2001)	0.38	10	69
Vu et al. (2001)	0.36	10	6
Vu et al. (2001)	0.44	10	23
Wild et al. (1996)	0.45	10	13
MK235*	0.40	8	30
MK235*	0.50	8	19
MK349*	0.40	8	42
MK349*	0.50	8	43

* present study

4.4.2 Splitting Tensile Strength

Splitting tensile strength results also generally showed increases with metakaolin use as compared to ordinary concrete controls. Splitting tensile strengths for the metakaolin mixtures generally ranged between 3 and 4 MPa across the three w/cm at 28 days (Figure 4.26), which was about 15% greater than the tensile strengths of controls at this age. This is similar to what was reported by Qian *et al.* [Qian, 2001]: average tensile

strength increases over controls were 7% and 16% for MK replacement levels of 5% and 10%, respectively. Both MK235 and MK349 improved concrete performance in this test, but neither was dominant, and standard deviations for all test results were relatively large. The silica fume used did not greatly affect splitting tensile strength, as compared to controls. This type of test is not routinely performed (hence the lack of existing literature), both because concrete is relatively weak in tension and because there is not a reliable correlation between values of tensile strength measured by splitting tension and by direct tension [Mindess, 2003].

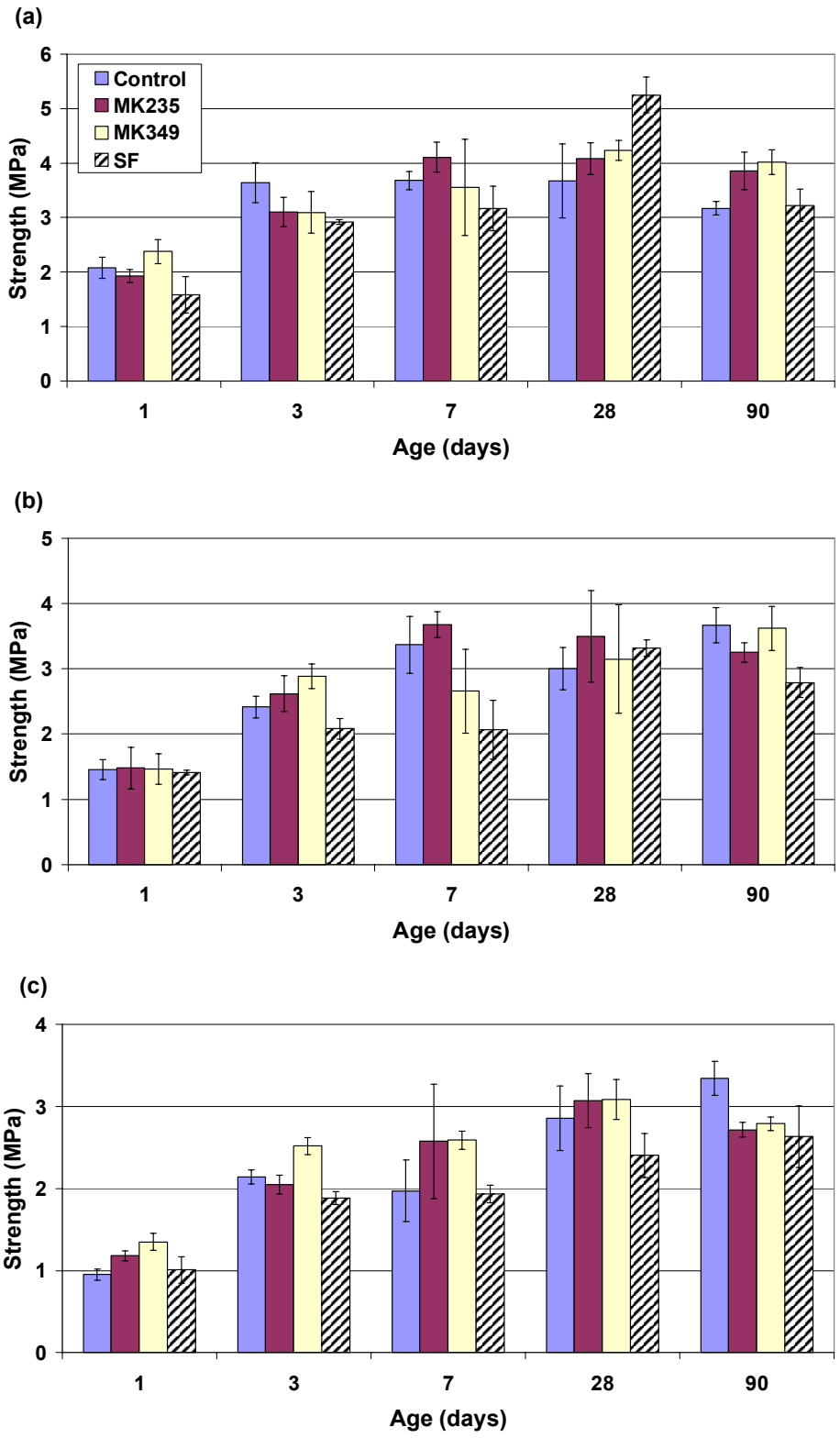

Figure 4.26. Average peak splitting tensile strength versus concrete age for (a) w/cm=0.40, (b) w/cm=0.50, and (c) w/cm=0.60.

4.4.3 Modulus of Rupture

Metakaolin incorporation generally increased flexural strength by 20-40% when 0.40-w/cm concrete prisms were subjected to four-point bending (Figures 4.27 and 4.28, Table 4.7). There was an increase of 1-2 MPa associated with the use of both metakaolins, although there was not a clear trend indicating that one was superior. Prisms cast with silica fume as a partial replacement for cement showed a higher (approximately 20%) modulus of rupture than the control at w/cm=0.40, though mixtures at higher w/cms did not differ from controls. At w/cm=0.40, MK349 and silica fume prisms reached 600 psi (4.1 MPa) at one day of age, control and MK235 prisms at three days. At higher w/cms, MK349 samples reached 600 psi by day three, while other mixtures did not reach this value until 28 days of age. These results bear particular relevance to pavement construction and suggest that metakaolin concrete could be used to shorten the time needed before pavements may be opened to traffic.

These results agree with what those of Dubey and Banthia [Dubey, 1998] and Qian *et al.* [Qian, 2001], who both found modulus of rupture to increase when MK was used as partial replacement for cement. Table 4.8 compares these authors' results to those found in our evaluation. Increases in flexural strength in MK-concretes are likely related to refinements in pore structure and denser, thinner interfacial transition zones, meaning proportionally less of this weaker phase.

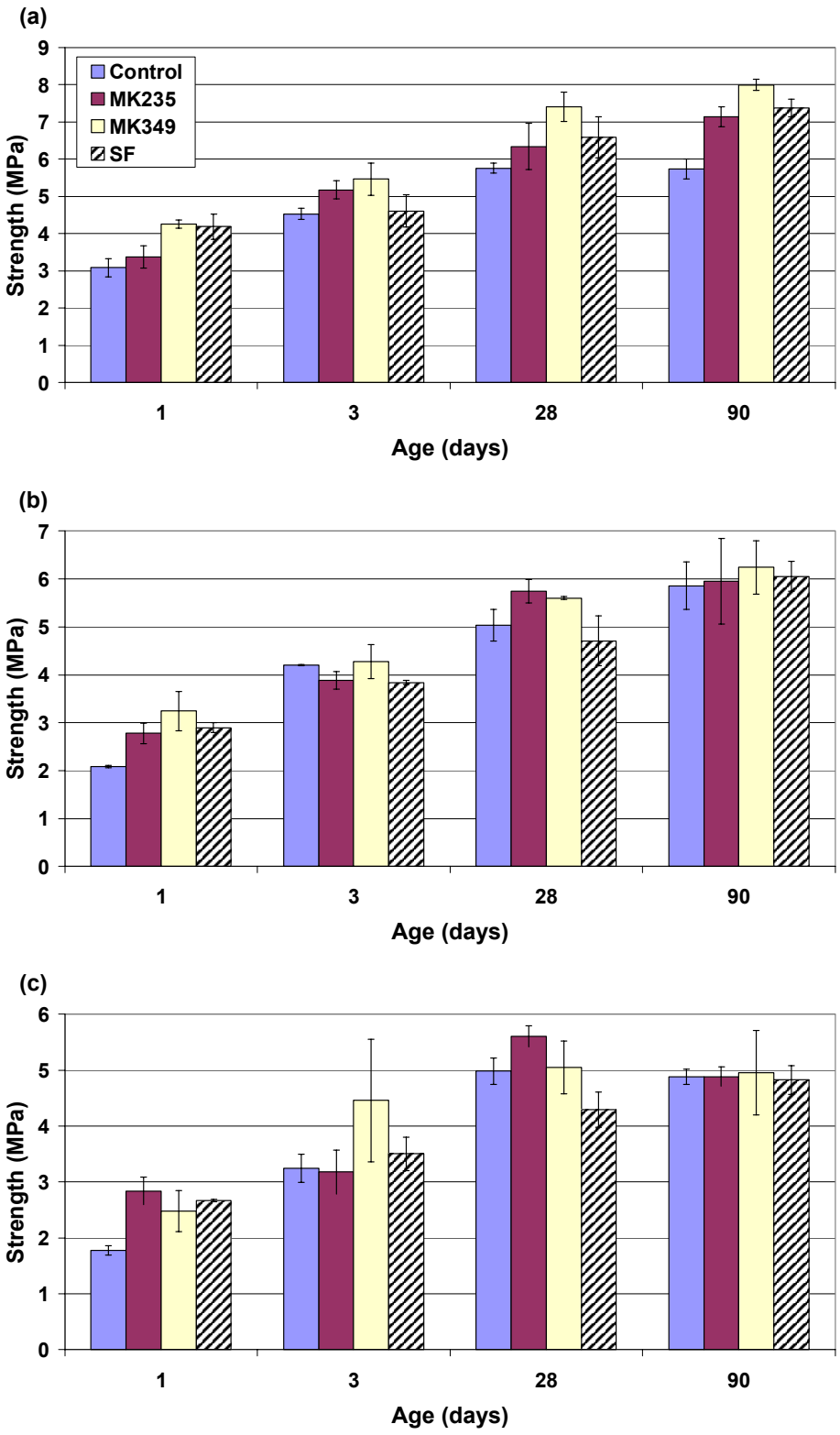

Figure 4.27. Average peak flexural strength (modulus of rupture) versus concrete age for (a) w/cm=0.40, (b) w/cm=0.50, and (c) w/cm=0.60.

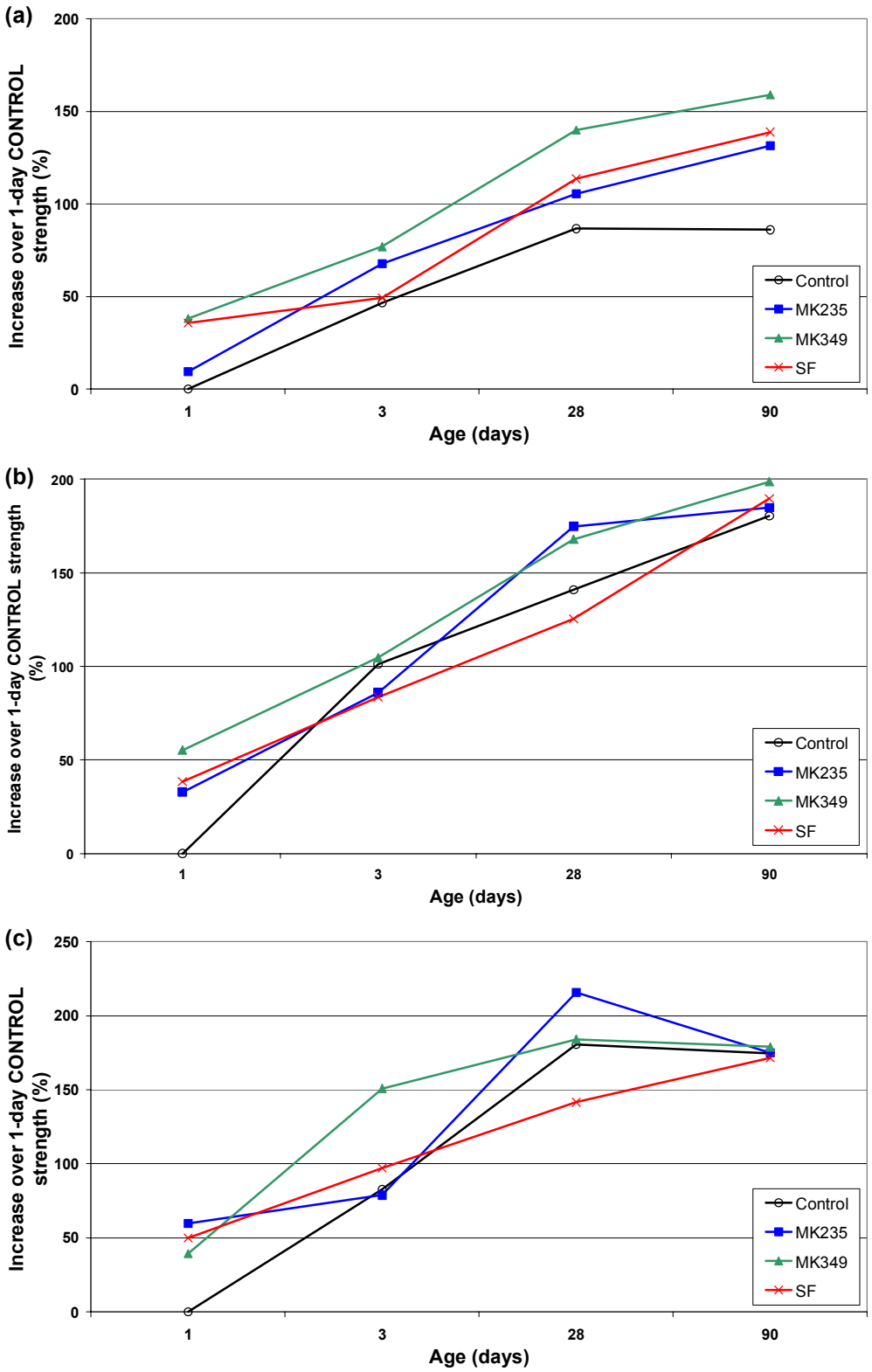

Figure 4.28. Rate of flexural strength development, shown as a percent increase over 1-day control strengths for (a) w/cm=0.40, (b) w/cm=0.50, and (c) w/cm=0.60.

Table 4.7. Flexural strength gain for w/cm=0.40 MK-concretes.

Age (Days)	Increase over MK235 1-day strength (%)	Increase over Control 1-day strength (%)	Increase over Control strength, same age (%)
1	0.0	9.4	9.4
3	53.4	67.7	14.4
28	87.8	105.4	10.1
90	111.6	131.4	24.4
Age (Days)	**Increase over MK349 1-day strength (%)**	**Increase over Control 1-day strength (%)**	**Increase over Control strength, same age (%)**
1	0.0	38.1	38.1
3	28.2	77.0	20.7
28	73.7	139.9	28.6
90	87.5	159.0	39.2

Table 4.8. Increases in modulus of rupture (MOR) over controls due to partial replacement with metakolin, as reported/measured at 28 days age.

Author/Material	w/cm	% Replacement	% MOR Increase over Control
Dubey & Banthia (1998)	0.35	10	15
Qian et al. (2001)	0.38	10	32
MK235*	0.40	8	10
MK349*	0.40	8	29

* present study

4.4.4 Modulus of Elasticity

Both metakaolins increased concrete's modulus of elasticity over controls, most significantly at lower water contents (Figure 4.29). MK235 and MK349 performed approximately the same, resulting in increases of 2-5 GPa (or 11-19%) across the three w/cm. As with compression testing, silica fume addition yielded unexpectedly low elastic modulus values. However, when recast and cured, new silica fume samples showed a modulus of elasticity 18-26% higher than controls, which was higher than both metakaolin samples, as depicted in Figure 4.16. The effect was most pronounced at w/cm=0.40, with silica fume yielding an elastic modulus of 37 GPa, versus 34 GPa for the metakaolins and 29 GPa for controls.

Our results are in accord with what has been reported in the literature [Qian, 2001; Khatib, 2004; Caldarone, 1994]. All of these authors have reported increases in elastic modulus associated with MK usage, ranging from 3 to 19%. Since metakaolin has been shown to increase compressive strength and to densify the microstructure, it follows that MK should also lead to increased elastic modulus, which is very sensitive to defects such as microcracks and voids. A summary of the above authors' results, along with our measurements, is given in Table 4.9. From this, the effect of w/cm is quite apparent. At a w/cm=0.50, increases of only 3-6% over controls were observed, while at a w/cm=0.40, modulus of elasticity increased approximately 18% over controls. As with the compressive strength data, this shows that the metakaolin has a greater effect at lower w/cm. However, unlike the compressive strength data where the finer material produced greater strengths, no apparent effect of metakaolin fineness was observed in the elastic modulus data.

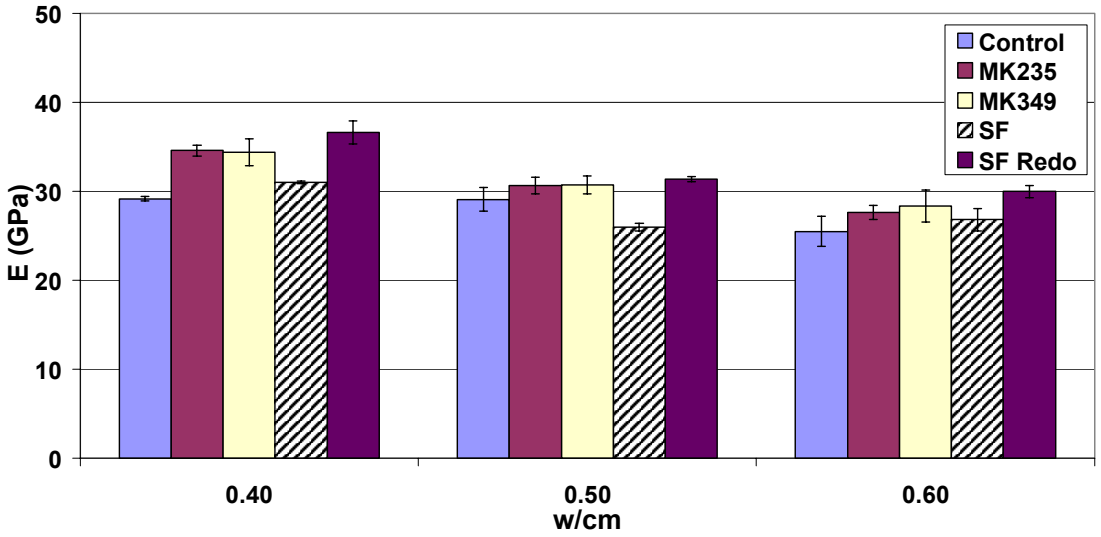

Figure 4.29. Modulus of elasticity, E, at 28 days of age.

Table 4.9. Increases in modulus of elasticity (MOE) due to partial replacement with metakolin, as reported/measured at 28 days age.

Author/Material	w/cm	% Replacement	MOE (GPa)	% MOE Increase over Control
Calderone et al. (1994)	0.40	10	38.9	18
Khatib & Hibbert (2004)	0.50	10	38.0	3
Qian et al. (2001)	0.38	10	33.2	11
MK235*	0.40	8	34.6	19
MK235*	0.50	8	30.7	5
MK349*	0.40	8	34.4	18
MK349*	0.50	8	30.8	6

* present study

4.5 Durability

4.5.1 Chloride Permeability

The metakaolin mixtures showed markedly lower permeability than controls, as measured by RCPT (Figure 4.30). For all w/cm, the control samples were considered to have a high permeability (above 4000 Coulombs). MK235 proved to be the most effective in reducing charge passed, with values in the low or very low range (below 2000 Coulombs) for all w/cms. Concrete cast with MK349 produced RCPT results which were only slightly higher than the MK235 samples at 0.40 (14%) and considerably higher at 0.60 (47%). These values ranged from very low at w/cm=0.40 to moderate for 0.60. Silica fume addition also reduced permeability as compared to controls, with values in the low to moderate range, though the silica fume did not produce reductions in permeability as great as either of the metakaolins. However, there is some uncertainty as to whether the RCPT is appropriate for SF-concrete, as the silica fume itself may be conductive [Wee, 2000].

Asbridge *et al.* [Asbridge, 2001] and Boddy *et al.* [Boddy, 2001] also found MK to significantly decrease resistance to chloride ion penetration. In Boddy *et al.*'s study, a w/cm=0.30 concrete with 12% MK exhibited an RCPT value of 230 Coulombs at 28 days

age, as compared to 2350 Coulombs in the 0.30-w/cm control. This decrease of approximately one order of magnitude was also observed in our evaluation for the w/cm=0.40 concrete specimens with 8% MK (590 v. 5020 Coulombs). These RCPT results suggest that blending with MK greatly densifies the matrix, which reduces permeability in addition to increasing strength, as observed in MK-concretes. Improvements due to MK incorporation are likely achieved primarily in the transition zone, which is known to be the most porous and permeable region in a standard concrete system.

The finer material, MK349, was expected to show greater reductions in permeability than the coarser MK235 due to its larger surface area, faster reaction rate (Figure 4.3a), and more pronounced strength-enhancing effect (Figures 4.24 and 4.25). MK235 also produced the greatest amount of chemical shrinkage, which was unexpected. These results suggest that MK235's action is somehow different than MK349's, in terms of either the type or the rate of reactions in which it is participating. From Figure 4.17, it appears that the three pastes containing SCMs were showing approximately the same degree of chemical shrinkage until seven days, when the MK235 began shrinking more rapidly. This implies initiation or acceleration of a reaction in the MK235 system that is producing denser reaction compounds which occupy a smaller volume and therefore lead to the greater chemical shrinkage from 7 days forward. From the RCPT data, collected at 28 days, it seems likely that these denser compounds are better able to inhibit penetration and percolation of chloride ions.

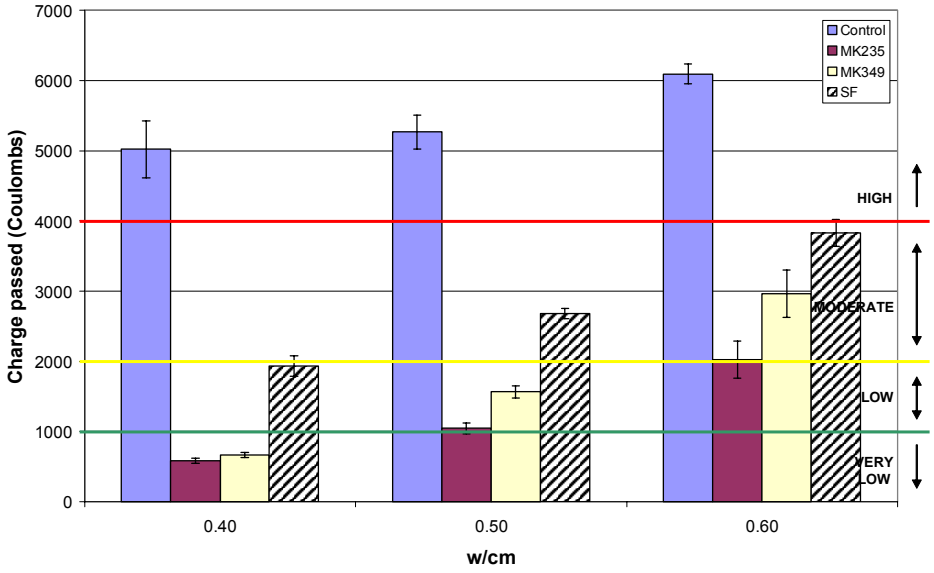

Figure 4.30. Rapid chloride permeability results at 28 days of age.

4.5.2 Sulfate Resistance

Sulfate resistance was measured by ASTM C 1012, which monitors expansion of mortar prisms that are submerged in a 33,800 ppm sulfate solution at room temperature. Several months of measurements are reported in Figure 4.31; standard deviations are reported in Table A.1 to prevent overcrowding. Unexpectedly, the 8% MK349 prisms began showing expansion first, whereas the control sample would have been expected to expand earliest and the most overall. Images of these prisms at 260 days of age are shown in Figure 4.32. The 8% MK235 prisms have not shown significant expansion yet, but are beginning to show signs of deterioration, including cracking near their gage studs, due to the sulfate exposure (Figure 4.33). Due to these unexpected results, the full matrix of mortar prisms was recast and a second round of tests started in January, 2005.

Preliminary results from these new samples are shown in Figure 4.34, with standard deviations in Table A.2.

Mortar prisms were also subjected to $MgSO_4$ exposure, as magnesium sulfate is more typically encountered in the field than is sodium sulfate. Initial results from this analysis are shown in Figure 4.35. Standard deviations are tabulated in A.3. Although ASTM C 1012 provides no strict limit on expansion, it has been suggested that expansion of 0.05% to 0.10% at 180 days would indicate moderate sulfate resistance and expansion of less than 0.05% at 180 days would indicate high sulfate resistance during ASTM C 1012 exposure. Data collection is ongoing, but the results are expected to indicate that mixtures resistant to sulfate attack can be produced using either of the metakaolins examined or silica fume at either 8% or 15% weight replacement.

Based on its ability to improve the strength (Figures 4.24 and 4.25) and refine the pore structure of concrete (Figures 4.23 and 4.30), MK seems a likely candidate for promoting sulfate resistance. It is suspected that much of MK's action occurs within the interfacial transition zone. This region, located around aggregates, typically has a higher porosity, a higher local w/cm, and differing chemical and mineralogical composition than the bulk paste. The ITZ is more permeable and is mechanically weaker than the other two phases, and cracks often initiate here, allowing uninhibited penetration of chemical solutions and eventually leading to component failure. Previous results of Khatib and Wild [Khatib, 1998] and Roy *et al.* [Roy, 2001], in addition to our strength and RCPT results, suggest the MK should increase resistance to sulfate attack. Additionally, as CH is one of the reactants in sulfate attack and MK has been shown to reduce CH content (Figures 4.13-4.16), sulfate resistance should be improved.

However, it is possible that the high alumina content of MK could be detrimental. If low-sulfate calcium aluminate phases are formed by MK reaction in the cement paste, these could react with ingressing sulfates to promote formation of additional ettringite or gypsum, leading to volume expansion, cracking, and accelerated penetration of sulfates. This being said, it should be noted that the expanding 8% MK349 specimens still showed less than 0.10% expansion at 180 days, indicating moderate sulfate resistance. Further, were the alumina compounds in MK349 contributing to the sulfate-induced expansion, the 15% MK349 samples would have been expected to show greater expansion than the 8% samples due to their higher alumina content.

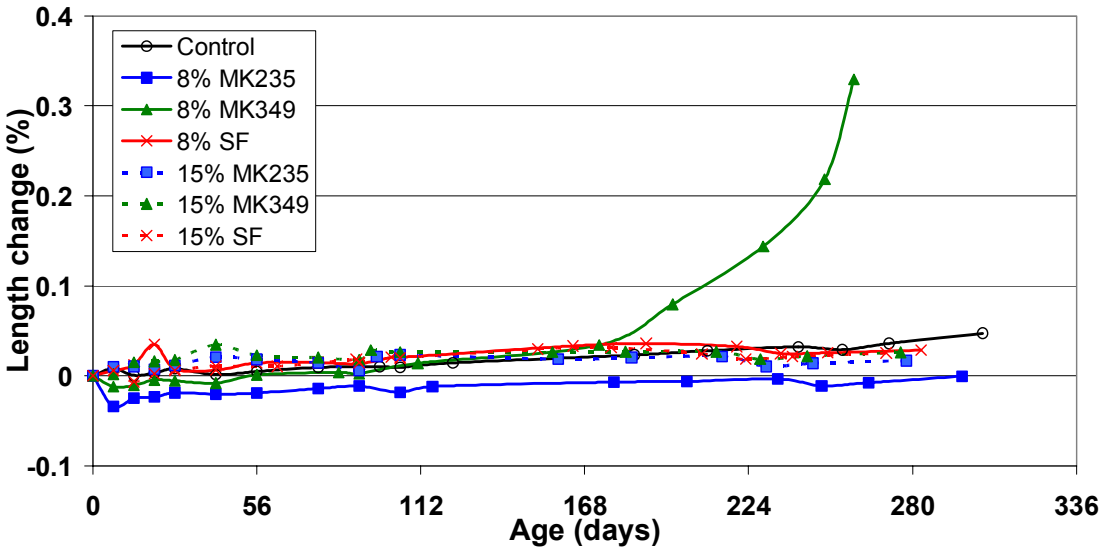

Figure 4.31. Mortar bar expansion due to sodium sulfate exposure, w/cm=0.485.

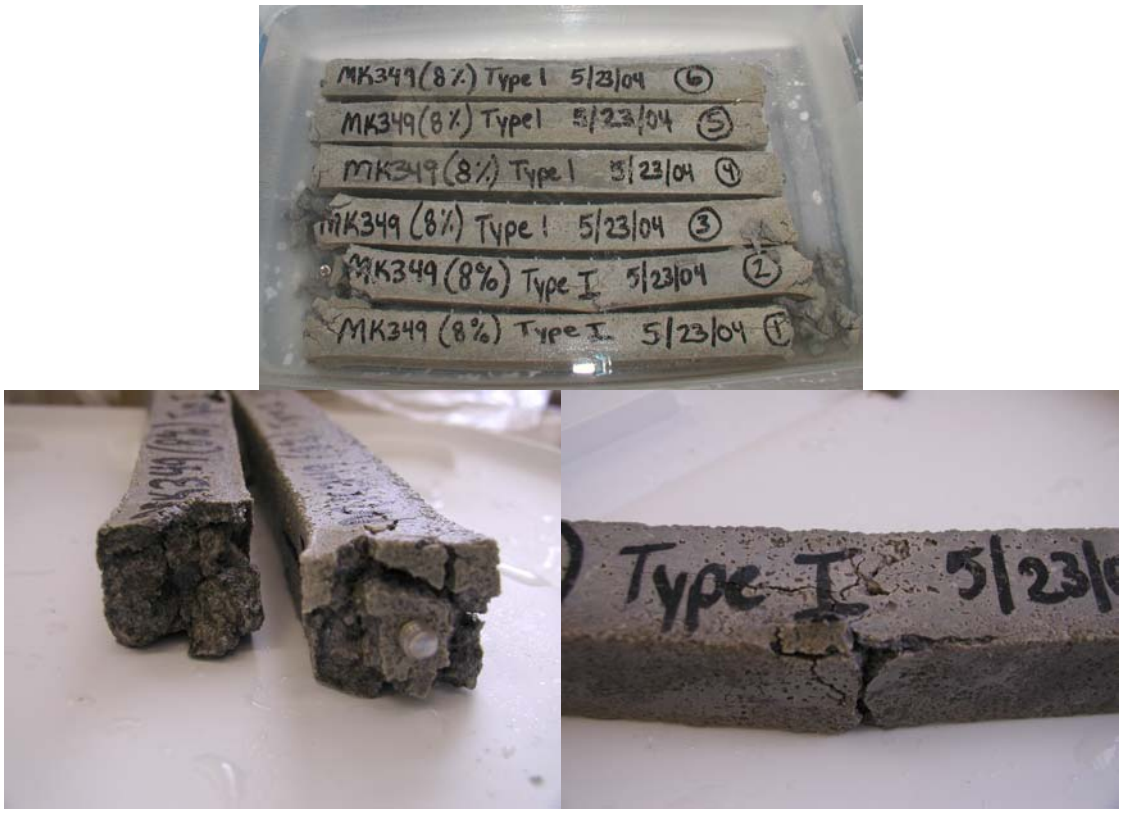

Figure 4.32. Images of 8% MK349 mortar prisms after 260 days of sodium sulfate exposure.

Figure 4.33. Image of 8% MK235 mortar prisms after 300 days of sodium sulfate exposure.

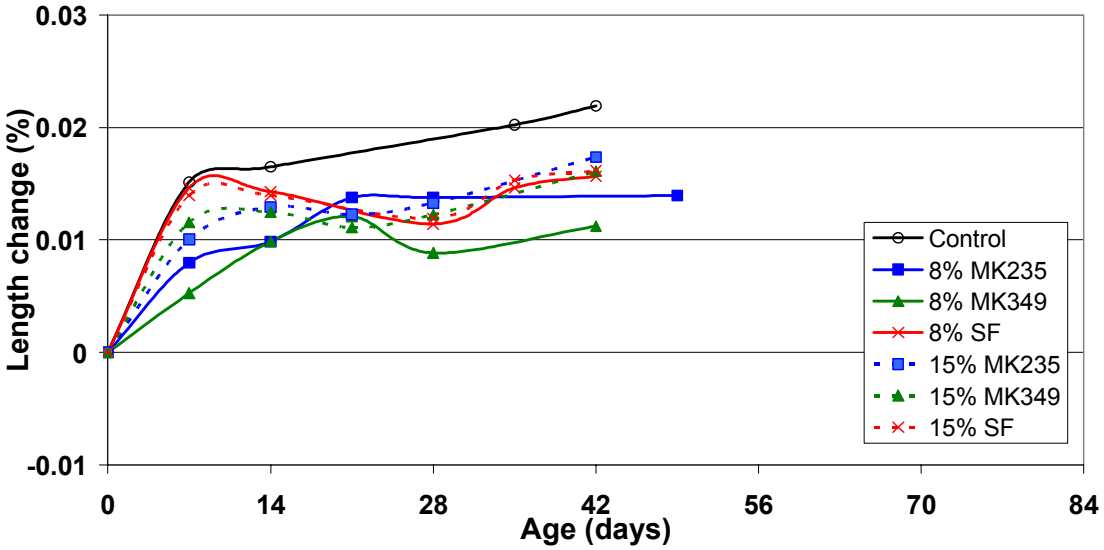

Figure 4.34. Mortar bar expansion due to sodium sulfate exposure, w/cm=0.485, trial two.

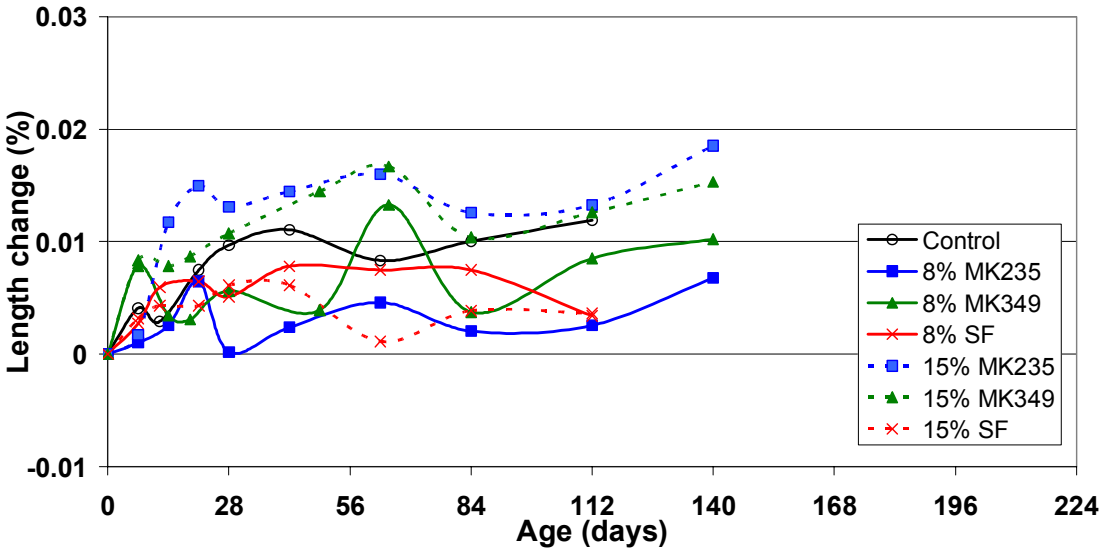

Figure 4.35. Mortar bar expansion due to magnesium sulfate exposure, w/cm=0.485.

4.5.3 Alkali-Silica Reaction

ASR test results are shown in Figure 4.36. These tests were performed using a highly reactive aggregate to determine the effect of varying matrix composition on expansion by ASR. According to ASTM C 1260, expansion of less than 0.10% at 14 days of age indicates acceptable performance, and expansion of greater than 0.20% indicates unacceptable performance. Based upon these criteria, the 15% MK235 mixture passed, the 8% MK235 and 15% MK349 specimens fell into the intermediate range (showing between 0.10% and 0.20% expansion at 14 days), and all other mixtures failed. These results show that both metakaolins reduce expansion due to ASR and to a greater extent than silica fume at the same rate of addition. Additionally, 15% replacement with either metakaolin sample produced greater reductions in expansion than 8% replacement, and MK235 was more effective than MK349 in mitigating expansion due to ASR.

These results confirm what has been reported in the literature [Ramlochan, 2000; Aquino, 2001]. Although the alkali-reactivity of an aggregate can vary widely, our evaluation and both of these studies found 15% replacement with MK sufficient to suppress ASR expansion of a highly reactive system to within the specified limit criterion (0.10% for mortars). The mixed quartz/chert/feldspar sand used in our evaluation was extremely reactive, which suggests that most alkali-reactive aggregates should require less metakaolin to achieve acceptable protection from ASR. As with other forms of chemical attack, this increased resistance to ASR is likely due, for the most part, to refinements in the ITZ. Densification and minimization of this region by secondary reaction with MK reduces permeability and limits the availability of water, thereby resulting in concrete with enhanced durability.

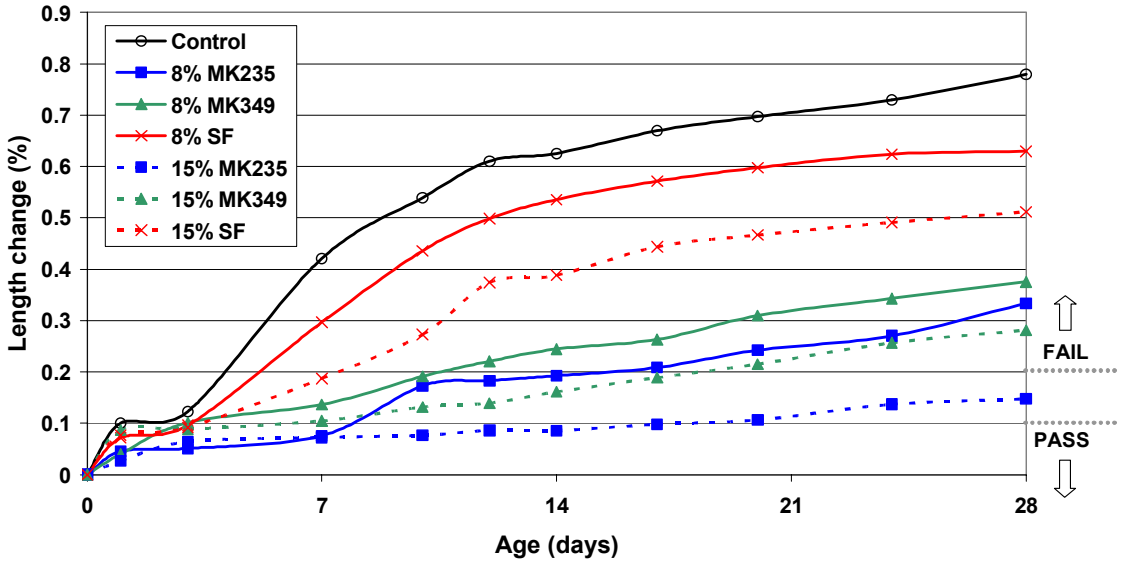

Figure 4.36. Expansion due to alkali-silica reaction, w/cm=0.47.

Chapter V

Conclusions

5.1 Summary of Research Methods and Results

The performance of two metakaolins, which varied primarily in their surface area and particle size distribution, was examined and compared to the performance of ordinary (control) and silica fume pastes, mortars, and concretes. The following conclusions may be drawn:

1. With regard to workability and setting time, both metakaolins examined generally required more superplasticizer to achieve adequate concrete workability. The finer MK349 caused the greatest reductions in workability, likely due to its larger surface area. Both metakaolins also shortened setting time of pastes by 35-50% as compared to controls and 10-30% as compared to companion silica fume mixtures at the same w/cm. Both of these observations indicate that the metakaolins are consuming water by absorption, adsorption, or reaction.

2. Isothermal calorimetry illustrated the acceleration effect that metakaolin has on cement hydration. Both MK materials resulted in an increase in the rate of heat evolution, and both showed enhanced aluminate peaks, with the finer MK349

exhibiting the most pronounced accelerating effect. Additionally, both metakolins were shown, through DTA and TGA, to reduce the CH content of pastes, suggesting that concretes admixed with these materials should exhibit durability superior to controls.

3. Greater shrinkage, both chemical and autogenous, was observed in mixtures containing SCMs as compared to ordinary cement and concrete control mixtures. MK235 mixtures showed the greatest chemical shrinkage, while MK349 mixtures showed the greatest autogenous shrinkage. However, free shrinkage decreased with the use of both metakolins, with the coarser MK235 resulting in the least drying shrinkage.

4. Increased concrete strength, as compared to control and silica fume mixtures, was measured for concretes produced with both metakaolins. The finer metakaolin, MK349, yielded the highest compressive, splitting tensile, and flexural strengths. Both metakolins also yielded increased elastic moduli relative to controls, although the silica fume specimens showed the greatest moduli of the group. The positive influence of the metakaolin fineness was more apparent at lower w/cm: at three days, the MK349 specimens exhibited increases in strength of 31%, 14%, and 13% over controls for w/cms of 0.40, 0.50, and 0.60, respectively.

5. With regard to the durability tests reported here, concretes produced with metakaolin at 8% by mass cement exhibited reduced permeability, as measured by

RCPT. The coarser metakaolin produced greater reductions in permeability, yielding Coulomb values in the very low or low range for all w/cms. In accelerated alkali-silica tests (ASTM C 1260), the best performance was achieved in mortars with 15% by weight replacement of cement with MK235. Tests to determine resistance to sulfate-induced expansion are incomplete and are presently inconclusive.

Both metakaolins examined led to increases in strength, elastic modulus, and resistance to chemical attack, as compared to controls. In general, the finer MK349 seemed more effective in enhancing concrete mechanical performance, while the coarser MK235 seemed more effective in improving concrete durability.

5.2 Recommendations for Use of Thiele Metkaolins

Based on this research, both metakaolins have great potential to improve the mechanical and durability properties of concrete. In general, replacement of 8% of the cement in a system should produce significant strength increases and provide adequate protection against corrosion, alkali-silica reaction, and sulfate attack. Replacement with 15% MK results in even greater decreases in permeability and superior resistance to chemical penetration.

5.3 Future Testing

Although characterization of these metakaolins was quite comprehensive, future testing might be desirable to pin down the underlying mechanisms of metakaolin's action.

In terms of early age properties, results were clear and consistent, with the finer metakaolin showing higher reactivity. This is supported by MK349's higher heat of hydration, shorter setting time, larger reduction in workability, and greater rate of strength gain. However, as both metakaolins required a higher dosage of superplasticizer than silica fume mixtures, ternary blends containing metakaolin and other SCMs (including fly ash, which is known to improve workability) should be investigated to develop mixture designs with improved strength and durability, which can be made workable at lower cost (i.e., lower superplasticizer dosage). Blending with fly ash should also help reduce the heat evolved during early hydration.

Because shrinkage results were inconsistent and somewhat confusing, further evaluation is necessary to better understand the shrinkage behavior of metakaolin concretes. ASTM C 157, the only of the evaluations performed on concrete specimens, does not capture shrinkage within the first 24 h of curing. To assess this very early shrinkage, concrete prisms should be cast with embedded waterproof, low-modulus strain gauges. This will allow shrinkage in concrete samples to be measured from the time of setting. Shrinkage-reducing chemical admixtures might also be examined.

Strength increases were observed in metakaolin mixtures across all ages and w/cm, as compared to control and silica fume mixtures. An increase in the rate of compressive strength gain for the MK349 was evident after three days at a w/cm of 0.40 and after seven days at 0.50 (Figure 4.25), but the underlying mechanism is not readily apparent. Calorimetry experiments performed for longer periods, perhaps up to 28 days, may provide additional understanding. Flexural testing results bear particular relevance

to pavement construction and suggest that metakaolin concrete could be used to shorten the time needed before pavements may be opened to traffic.

In terms of durability, more long-term data is necessary to predict how metakaolin-concretes will perform under field conditions. Resistance to damage from freeze-thaw cycling should be investigated. Although metakolins greatly reduced the charge passed in rapid chloride permeability testing, long-term ponding tests may be desirable to fully understand the extent of corrosion resistance that metakaolin can offer. Sulfate testing should continue until mortar bars have expanded beyond the length of the comparator. ASR should be further evaluated via the long-term concrete prism test outlined in ASTM C 1293. This should paint a more accurate picture of the reaction, as it will include effects of the interfacial transition zone. Additionally, ternary blending with fly ash or slag might be explored as a means for mitigating ASR, as 15% replacement with metakaolin is expensive and gives poor workability.

Appendix

Table A.1. Mortar bar expansion due to sodium sulfate exposure (ASTM C 1012), averages and standard deviations.

Control			8% MK235			8% MK349			8% SF		
Age (Days)	Mean	Standard Deviation	Age (Days)	Mean	Standard Deviation	Age (Days)	Mean	Standard Deviation	Age (Days)	Mean	Standard Deviation
7	0.008	0.020	7	-0.034	0.019	7	-0.012	0.028	7	0.006	0.002
14	0.000	0.018	14	-0.025	0.017	14	-0.011	0.027	14	0.012	0.005
21	0.003	0.019	21	-0.024	0.017	21	-0.005	0.028	21	0.035	0.028
28	0.008	0.017	28	-0.019	0.016	28	-0.006	0.027	28	0.008	0.002
42	0.001	0.018	42	-0.021	0.018	42	-0.008	0.027	42	0.006	0.004
56	0.005	0.018	56	-0.019	0.018	56	0.001	0.029	56	0.014	0.003
77	0.009	0.018	77	-0.014	0.019	84	0.004	0.029	77	0.015	0.005
98	0.010	0.018	91	-0.012	0.017	91	0.002	0.032	91	0.013	0.005
105	0.009	0.021	105	-0.019	0.033	111	0.014	0.029	102	0.021	0.004
123	0.014	0.018	116	-0.012	0.017	173	0.034	0.039	105	0.021	0.009
185	0.023	0.017	178	-0.007	0.015	198	0.079	0.097	164	0.033	0.006
210	0.028	0.015	203	-0.006	0.016	229	0.144	0.157	189	0.036	0.008
241	0.032	0.017	234	-0.004	0.016	237	0.130	0.107	220	0.032	0.007
256	0.029	0.017	249	-0.011	0.014	244	0.103	0.071	235	0.025	0.007
272	0.036	0.018	265	-0.008	0.014	250	0.218	0.201	251	0.025	0.008
304	0.047	0.035	297	-0.001	0.014	260	0.329	0.345	283	0.028	0.008

15% MK235			15% MK349			15% SF		
Age (Days)	Mean	Standard Deviation	Age (Days)	Mean	Standard Deviation	Age (Days)	Mean	Standard Deviation
7	0.010	0.004	7	0.002	0.008	7	0.006	0.002
14	0.010	0.003	14	0.015	0.005	14	-0.007	0.001
21	0.007	0.004	21	0.016	0.002	21	0.002	0.002
28	0.011	0.007	28	0.017	0.004	28	0.006	0.002
42	0.021	0.018	42	0.035	0.007	42	0.011	0.010
56	0.018	0.005	56	0.023	0.004	63	0.011	0.002
77	0.014	0.006	77	0.020	0.007	77	--	--
91	0.006	0.012	91	0.018	0.010	90	0.018	0.003
97	0.021	0.006	95	0.028	0.002	91	0.015	0.008
105	0.023	0.007	105	0.026	0.007	105	0.020	0.003
159	0.018	0.007	157	0.026	0.004	152	0.030	0.003
184	0.020	0.006	182	0.027	0.004	177	0.031	0.004
215	0.021	0.006	213	0.027	0.004	208	0.024	0.004
230	0.010	0.006	228	0.018	0.004	223	0.018	0.003
246	0.014	0.005	244	0.022	0.004	239	0.021	0.003
278	0.017	0.006	276	0.026	0.004	271	0.025	0.004

Table A.2. Mortar bar expansion due to sodium sulfate exposure (ASTM C 1012), averages and standard deviations, trial two.

Age (Days)	8% MK235		8% MK349		8% SF		Control	
	Mean	Standard Deviation	Mean	Standard Deviation	Mean	Standard Deviation	Mean	Standard Deviation
7	0.008	0.001	0.005	0.001	0.015	0.001	0.015	0.001
14	0.010	0.001	0.010	0.002	0.014	0.001	0.016	0.001
21	0.014	0.001	0.012	0.001	--	--	--	--
28	0.014	0.001	0.009	0.002	0.011	0.001	--	--
35	--	--	--	--	0.015	0.001	0.020	0.001
42	--	--	0.011	0.002	0.016	0.001	0.022	0.001
49	0.014	0.001	--	--	--	--	--	--
Age (Days)	**15% MK235**		**15% MK349**		**15% SF**			
	Mean	Standard Deviation	Mean	Standard Deviation	Mean	Standard Deviation		
7	0.010	0.001	0.012	0.001	0.014	0.001		
14	0.013	0.001	0.012	0.000	0.014	0.001		
21	0.012	0.001	0.011	0.001	--	--		
28	0.013	0.001	0.012	0.001	0.012	0.001		
35	--	--	--	--	0.015	0.001		
42	0.017	0.001	0.016	0.001	0.016	0.001		
49	--	--	--	--	--	--		

Table A.3. Mortar bar expansion due to magnesium sulfate exposure (ASTM C 1012), averages and standard deviations.

Control			8% MK235			8% MK349			8% SF		
Age (Days)	Mean	Standard Deviation	Age (Days)	Mean	Standard Deviation	Age (Days)	Mean	Standard Deviation	Age (Days)	Mean	Standard Deviation
7	0.004	0.001	7	0.001	0.003	7	0.008	0.002	7	0.003	0.001
12	0.003	0.001	14	0.003	0.003	14	0.003	0.002	12	0.006	0.001
21	0.007	0.001	21	0.006	0.002	19	0.003	0.002	21	0.006	0.002
28	0.010	0.001	28	0.000	0.002	28	0.006	0.002	28	0.005	0.001
42	0.011	0.002	42	0.002	0.002	49	0.004	0.001	42	0.008	0.000
63	0.008	0.002	63	0.005	0.003	65	0.013	0.001	63	0.007	0.001
84	0.010	0.002	84	0.002	0.002	84	0.004	0.001	84	0.007	0.001
112	0.012	0.003	112	0.003	0.003	112	0.009	0.001	112	0.003	0.001
140			140	0.007	0.003	140	0.010	0.002	140		
			15% MK235			**15% MK349**			**15% SF**		
			Age (Days)	Mean	Standard Deviation	Age (Days)	Mean	Standard Deviation	Age (Days)	Mean	Standard Deviation
			7	0.002	0.007	7	0.008	0.002	7	0.003	0.001
			14	0.012	0.003	14	0.008	0.002	12	0.004	0.001
			21	0.015	0.004	19	0.009	0.002	21	0.004	0.001
			28	0.013	0.003	28	0.011	0.003	28	0.006	0.000
			42	0.014	0.003	49	0.014	0.001	42	0.006	0.001
			63	0.016	0.003	65	0.017	0.002	63	0.001	0.000
			84	0.013	0.003	84	0.010	0.002	84	0.004	0.001
			112	0.013	0.005	112	0.013	0.002	112	0.004	0.000
			140	0.019	0.007	140	0.015	0.002	140		

References

China Clay Producers Association, http://www.kaolin.com/index.html, accessed October 2004.

DTA and TGA of Ball Clay and Kaolin, http://cems.alfred.edu/courses/ces101/firing/tc.html, accessed November 2004.

High Reactivity Metakaolin: Engineered Mineral Admixture for Use with Portland Cement, Advanced Cement Technologies, http://www.metakaolin.com/Operation%20Description.htm, accessed September 2004.

Humboldt Manufacturing - Vicat Consistency Testers, http://www.humboldtmfg.com; http://64.177.189.124/pdf1/46.pdf, accessed March 2005.

Ambroise, J., Maximilien, S. and Pera, J. (1994), Properties Of metakaolin blended cements, *Advanced Cement Based Materials*, 1(4): 161-168.

Ambroise, J., Murat, M., Pera, J. (1985), Hydration reaction and hardening of calcined clays and related minerals: V. Extension of the research and general conclusions, *Cement and Concrete Research*, 15: 261-268.

Aquino, W., Lange, D.A. and Olek, J. (2001), The influence of metakaolin and silica fume on the chemistry of alkali-silica reaction products, *Cement and Concrete Composites*, 23(6): 485-493.

Asbridge, A.H., Chadbourn, G.A. and Page, C.L. (2001), Effects of metakaolin and the interfacial transition zone on the diffusion of chloride ions through cement mortars, *Cement and Concrete Research*, 31(11): 1567-1572.

Bai, J. and Wild, S. (2002), Investigation of the temperature change and heat evolution of mortar incorporating PFA and metakaolin, *Cement and Concrete Composites*, 24(2): 201-209.

Bai, J., Wild, S., Sabir, B.B. and Kinuthia, J.M. (1999), Workability of concrete incorporating pulverized fuel ash and metakaolin, *Magazine of Concrete Research*, 51(3): 207-216.

Batis, G., Pantazopoulou, P., Tsivilis, S. and Badogiannis, E. (2004), The effect of metakaolin on the corrosion behavior of cement mortars, *Cement and Concrete Composites*, in press.

Bensted, J. and Barnes, P. (2002), *Structure and Performance of Cements, 2nd ed.*, New York: Spon Press.

Bentz, D.P., Garboczi, C.J., Haecker, C.J., Jensen, O.M. (1999), Effects of cement particle size distribution on performance properties of portland cement-based materials, *Cement and Concrete Research*, 29(10): 1663-1671.

Bérubé, M., Duchesne, J., Chouinard, D (1995), Why the accelerated mortar bar method ASTM C 1260 is reliable for evaluating the effectiveness of supplementary cementing materials in suppressing expansion due to alkali-silica reactivity, *Cement, Concrete, and Aggregates*, 17: 26-34.

Bhadeshia, H.K.D.H., An Introduction to Thermal Analysis Techniques, http://www.msm.cam.ac.uk/phase-trans/2002/thermal.analysis.html, accessed October 2004.

Boddy, A., Hooton, R.D. and Gruber, K.A. (2001), Long-term testing of the chloride-penetration resistance of concrete containing high-reactivity metakaolin, *Cement and Concrete Research*, 31(5): 759-765.

Brinkley, G.W. (1958), *Ceramic Fabrication Processes,* Cambridge & New York: Technology Press & John Wiley and Sons.

Brooks, J.J. and Johari, M.A.M. (2001), Effect of metakaolin on creep and shrinkage of concrete, *Cement and Concrete Composites*, 23(6): 495-502.

Brooks, J.J., Johari, M.A.M. and Mazloom, M. (2000), Effect of admixtures on the setting times of high-strength concrete, *Cement and Concrete Composites*, 22(1): 293-301.

Cabrera, J.G., Lee, R.E. (1985), A new method for for the measurement of workability of high-pulverised fuel ash concrete, *International Ash Utilization Symposium*, 347-360.

Caldarone, M.A., Gruber, K.A. and Burg, R.G. (1994), High reactivity metakaolin (HRM): a new generation mineral admixture for high performance concrete, *Concrete International*, 16(11): 37-40.

Courard, L., Darimont, A., Schouterden, M., Ferauche, F., Willem, X. and Degeimbre, R. (2003), Durability of mortars modified with metakaolin, *Cement and Concrete Research*, 33(9): 1473-1479.

Curcio, F., DeAngelis, B.A. and Pagliolico, S. (1998), Metakaolin as a pozzolanic microfiller for high-performance mortars, *Cement and Concrete Research*, 28(6): 803-809.

Diamond, S. (2000), Mercury porosimetry: an inappropriate method for the measurement of pore size distributions in cement-based materials, *Cement and Concrete Research*, 30: 1517-1525.

Ding, J.T. and Li, Z.J. (2002), Effects of metakaolin and silica fume on properties of concrete, *ACI Materials Journal*, 99(4): 393-398.

Dubey, A. and Banthia, N. (1998), Influence of high-reactivity metakaolin and silica fume on the flexural toughness of high-performance steel fiber-reinforced concrete, *ACI Materials Journal*, 95(3): 284-292.

Frías, M. and Cabrera, J. (2000), Pore size distribution and degree of hydration of metakaolin-cement pastes, *Cement and Concrete Research*, 30(4): 561-569.

Frías, M., de Rojas, M.I.S. and Cabrera, J. (2000), The effect that the pozzolanic reaction of metakaolin has on the heat evolution in metakaolin-cement mortars, *Cement and Concrete Research*, 30(2): 209-216.

Geiker, M., Knudsen, T. (1982), Chemical shrinkage of portland cement pastes, *Cement and Concrete Research*, 12: 603-610.

Gregg, S.J., Sing, K.S.W. (1982), *Adsorption, Surface Area, and Porosity, 2nd ed.*, London: Harcourt Brace Jovanovich.

Gruber, K.A., Ramlochan, T., Boddy, A., Hooton, R.D. and Thomas, M.D.A. (2001), Increasing concrete durability with high-reactivity metakaolin, *Cement and Concrete Composites*, 23(6): 479-484.

Jensen, O.M., Hansen, P.F. (1995), A dilatometer for measuring autogenous deformation in hardening cement paste, *Materials and Structures*, 28(181): 406-409.

Juenger, M.C.G. and Jennings, H.M. (2001), The use of nitrogen adsorption to assess the microstructure of cement paste, *Cement and Concrete Research*, 31: 883-892.

Khatib, J.M. and Clay, R.M. (2003), Absorption characteristics of metakaolin concrete, *Cement and Concrete Research*, in press.

Khatib, J.M., Hibbert, J.J. (2004), Selected engineering properties of concrete incorporating metakaolin and slag, *Construction and Building Materials*, in press.

Khatib, J.M. and Wild, S. (1996), Pore size distribution of metakaolin paste, *Cement and Concrete Research*, 26(10): 1545-1553.

Khatib, J.M. and Wild, S. (1998), Sulphate resistance of metakaolin mortar, *Cement and Concrete Research*, 28(1): 83-92.

Kingery, W.D., Uhlmann, D.R., Bowen, H.K. (1976), *Introduction to Ceramics, 2nd ed.*, New York: John Wiley and Sons.

Kinuthia, J.M., Wild, S., Sabir, B.B. and Bai, J. (2000), Self-compensating autogenous shrinkage in Portland cement-metakaolin-fly ash pastes, *Advances in Cement Research*, 12(1): 35-43.

Knudsen, T., Geiker, M. (1985), Obtaining hydration data by measurement of chemical shrinkage with an archimeter, *Cement and Concrete Research*, 15: 381-382.

Kurtis, K.E., Monteiro, P.J.M, and Madanat, S.M. (2000), Empirical models to predict concrete expansion caused by sulfate attack, *ACI Materials Journal*, 97(2): 156-162.

Li, S., Roy, D.M., Kumer, A. (1985), Quantitative determination of pozzolanas in hydrated system of cement or Ca(OH)2 with fly ash or silica fume, *Cement and Concrete Research*, 15(6): 1079-1086.

Li, Z.J. and Ding, Z. (2003), Property improvement of Portland cement by incorporating with metakaolin and slag, *Cement and Concrete Research*, 33(4): 579-584.

Mindess, S., Young, F.J. and Darwin, D. (2003), *Concrete, 2nd ed.*, Upper Saddle River: Prentice Hall.

Moulin, E., Blanc, P. and Sorrentino, D. (2001), Influence of key cement chemical parameters on the properties of metakaolin blended cements, *Cement and Concrete Composites*, 23(6): 463-469.

Oriol, M. and Pera, J. (1995), Pozzolanic activity Of metakaolin under microwave treatment, *Cement and Concrete Research*, 25(2): 265-270.

Oshawa, S., Asaga, K., Goto, S., Daimon, M. (1985), Quantitative determination of fly ash in the hydrated fly ash-CaSO4-Ca(OH)2 system, *Cement and Concrete Research*, 15(2): 357-366.

Palomo, A., Blanco-Varela, M.T., Granizo, M.L., Puertas, F., Vazquez, T. and Grutzeck, M.W. (1999), Chemical stability of cementitious materials based on metakaolin, *Cement and Concrete Research*, 29(7): 997-1004.

Poon, C.S., Kou, S.C. and Lam, L. (2002), Pore size distribution of high performance metakaolin concrete, *Journal Of Wuhan University Of Technology-Materials Science Edition*, 17(1): 42-46.

Poon, C.S., Lam, L., Kou, S.C., Wong, Y.L. and Wong, R. (2001), Rate of pozzolanic reaction of metakaolin in high-performance cement pastes, *Cement and Concrete Research*, 31(9): 1301-1306.

Qian, X.Q. and Li, Z.J. (2001), The relationships between stress and strain for high-performance concrete with metakaolin, *Cement and Concrete Research*, 31(11): 1607-1611.

Ramlochan, T., Thomas, M. and Gruber, K.A. (2000), The effect of metakaolin on alkali-silica reaction in concrete, *Cement and Concrete Research*, 30(3): 339-344.

Roy, D.M., Arjunan, P. and Silsbee, M.R. (2001), Effect of silica fume, metakaolin, and low-calcium fly ash on chemical resistance of concrete, *Cement and Concrete Research*, 31(12): 1809-1813.

Sabir, B.B., Wild, S. and Bai, J. (2001), Metakaolin and calcined clays as pozzolans for concrete: a review, *Cement and Concrete Composites*, 23(6): 441-454.

Salvador, S. (1995), Pozzolanic properties of flash-calcined kaolinite: a comparative study with soak-calcined products, *Cement and Concrete Research*, 25(1): 102-112.

Schroeder, P.A., Kaolin, New Georgia Encyclopedia, http://www.georgiaencyclopedia.org/nge/Article.jsp?path=/ScienceMedicine/EarthSciences/GeologicalResources&id=h-1178, accessed September 2004.

Sha, W. and Pereira, G.B. (2001), Differential scanning calorimetry study of ordinary portland cement paste containing metakaolin and theoretical approach of metakaolin activity, *Cement and Concrete Composites*, (23): 455-461.

Taylor, H.F.W. (1997), *Cement Chemistry, 2nd ed.,* London: Thomas Telford.

Vu, D.D., Stroeven, P. and Bui, V.B. (2001), Strength and durability aspects of calcined kaolin-blended Portland cement mortar and concrete, *Cement and Concrete Composites*, 23(6): 471-478.

Wee, T.H., Suryavanshi, A.K., and Tin, S.S. (2000), Evaluation of rapid chloride permeability test (RCPT) results for concrete containing mineral admixtures, *ACI Materials Journal*, 97(2): 221-232.

Wild, S. and Khatib, J.M. (1997), Portlandite consumption in metakaolin cement pastes and mortars, *Cement and Concrete Research*, 27(1): 137-146.

Wild, S., Khatib, J.M. and Jones, A. (1996), Relative strength, pozzolanic activity and cement hydration in superplasticised metakaolin concrete, *Cement and Concrete Research*, 26(10): 1537-1544.

Wild, S., Khatib, J.M. and Roose, L.J. (1998), Chemical shrinkage and autogenous shrinkage of Portland cement metakaolin pastes, *Advances in Cement Research*, 10(3): 109-119.

Wolfe, J.E., personal communications with K.E. Kurtis, April-June 2004.

Zhang, M.H. and Malhotra, V.M. (1995), Characteristics of a thermally activated alumino-silicate pozzolanic material and its use in concrete, *Cement and Concrete Research*, 25(8): 1713-1725.

Zhang, Z.Z., personal communication with J.M. Justice, September 2004.